



**University of
Zurich**^{UZH}

Estimating the impact of climate change on maize cultivation in Switzerland based on agricultural climate indicators

GEO 511 Master's Thesis

Author

Geraldine Zollinger
15-737-216

Supervised by

Dr. Sibylle Stöckli (sibylle.stoeckli@agroscope.admin.ch)
Dr. Sven Kotlarski (sven.kotlarski@meteoswiss.ch)

Faculty representative

Dr. Ilja van Meerveld

29.04.2024

Department of Geography, University of Zurich

Acknowledgements

Firstly, I would like to express my gratitude to my supervisors Dr. Sibylle Stöckli and Dr. Sven Kotlarski, who supported me throughout the whole thesis and whose advice was a big help and very appreciated. I also would like to thank Dr. Ilja van Meerveld for sharing her interesting thoughts and ideas for this study. I am grateful for Flavian Tschurr providing me his R scripts of his case study about agricultural climate indicators, which were a great inspiration in programming. Additionally, I would like to thank Daniel Erdin from Agristat for allowing me to use their maize yield data. I am thankful for Marc Vis creating virtual machines in ScienceCloud for my calculations and always finding time to help out in case of technical problems. I also thank Dr. Maria Staudinger for extracting the local time series of the observational climate data for me.

Finally, I would like to express my gratitude for my loved ones who have always supported me and whose encouragement and help throughout the entire thesis was deeply appreciated.

Abstract

Without climate mitigation measures, summers are expected to become drier and temperature extremes as well as heavy precipitation events to become more frequent and intense in the future. This poses a challenge for farmers, as weather events such as high temperatures, heavy precipitation events and droughts can negatively impact crop development and potentially lead to yield reduction. To mitigate the impact of climate change on crop cultivation, information about what climate-related challenges for individual crop cultivars lie ahead of us is required. Such information can be provided by using so-called agricultural climate indicators (ACIs) which link the response of plants to climate. There are studies about the impact of climate change on different agricultural sectors based on ACIs. However, an estimation of climate change impact using ACIs specified for maize and based on the CH2018 grid-data is yet to be done. Moreover, the ACIs in said studies often represent single stress factors. However, it has been shown that concurrent stress factors can be more harmful to the plants than individual stresses. Furthermore, a stronger focus on climate variability is needed, as this is an important factor influencing the year-to-year variability of maize yield. This thesis has two main goals: (1) to analyse how well the chosen ACIs can explain maize yield variation in the present Swiss climate, and (2) to estimate the impact of climate change on maize cultivation in Switzerland based on average occurrence and variability of ACIs and based on CH2018 grid-data for mid-century (2045–2074).

The used ACIs have been reported in literature and are specified for maize cultivation or are of importance for the agricultural sector in Switzerland. ACIs representing heat stress, low temperature stress, potential waterlogging and drought have been included. Moreover, these ACIs represent single stress factors as well as concurrent stress factors. The first goal of this thesis was achieved by comparing ACI occurrence with maize yield variation by using Spearman's correlation coefficient and fitting multiple linear regression models. For the second goal, it first had to be assessed how well the ACI occurrence is represented by the CH2018 grid-data by comparing the simulated ACI occurrence with the observed ACI occurrence during the reference period 1981–2010. The ACIs that were well represented by the CH2018 grid-data were then included in the climate impact analysis for 2045–2074 based on the RCP 2.6 and RCP 8.5 scenario.

This thesis indicates that, for some sites in Switzerland, heat stress related ACIs show a moderate but significant negative correlation with maize yield variation. However, for several other ACIs and sites there is in many cases no significant relationship with maize yield visible. Regarding the climate change impact analysis, for most ACIs a change in the average and variability of the yearly occurrence is expected until mid-century, especially based on the RCP 8.5 scenario. While the number of heat stress related ACIs during the defined maize growing season is expected to increase, the number of low temperature stress related ACIs is expected to decrease in the future. The number of days with drought is expected to increase. For potential waterlogging on the other hand, the change is uncertain.

By showing how ACI occurrence and variability is expected to change in the future, this thesis can provide a basis for adaptation measures for maize cultivation in Switzerland. With the new CH2025 climate scenarios to be published by the end of 2025, an updated climate impact analysis will be necessary. As the adaptability of farmers is an important factor in determining climate impact on agriculture, it is worth including this aspect in the updated climate impact analysis.

Table of Contents

Acknowledgements	i
Abstract	ii
Table of Contents	iii
List of Figures	vi
List of Tables	xi
List of Equations	xiv
List of Abbreviations	xv
List of used Agricultural Climate Indicators (ACIs)	xvi
1 Introduction	1
1.1 Estimating the impact of climate on maize cultivation	1
1.2 Related work about climate change impact on the agricultural sector	2
1.3 Research questions and hypotheses	3
2 Elaboration of maize development	5
3 Data	7
3.1 Maize yield data	7
3.2 Climate data	7
3.2.1 Observational climate data	7
3.2.2 CH2018 data	8
4 Method	10
4.1 Defining maize growing season	10
4.2 Choosing agricultural climate indicators	11
4.2.1 Heat stress	13
4.2.2 Low temperature stress	13
4.2.3 Potential waterlogging	14
4.2.4 Drought	14
4.2.5 Concurrent stress factors	16
4.3 Validating ACIs with maize yield data	16
4.4 Technical validation of ACI representation by the CH2018 grid-data	17

4.5	Implementation of climate change impact analysis	18
5	Results.....	19
5.1	Results of ACI validation with yield data.....	19
5.2	Results of technical validation of ACI representation by the CH2018 grid-data	21
5.3	Results of the climate impact analysis	24
5.3.1	Change in growing degree days.....	25
5.3.2	Change in heat stress.....	26
5.3.3	Change in low temperature stress	30
5.3.4	Change in potential waterlogging.....	34
5.3.5	Change in drought	35
5.3.6	Change in concurrent stress	36
5.3.6.1	Drought & heat stress.....	36
5.3.6.2	Drought & low temperature stress.....	38
5.3.6.3	Potential waterlogging & low temperature stress.....	40
6	Discussion.....	42
6.1	Relationship between maize yield and ACI occurrence.....	42
6.2	Impact of climate change on maize cultivation	43
6.2.1	Estimated change in heat stress.....	44
6.2.2	Estimated change in low temperature stress.....	44
6.2.3	Estimated change in potential waterlogging.....	45
6.2.4	Estimated change in drought.....	46
6.2.5	Estimated change in concurrent stress	46
7	Conclusion	48
7.1	Main Findings.....	48
7.2	Future Research	49
8	References.....	51
8.1	Literature	51
8.2	Used illustrations in Figures.....	57
Appendices		58
A	Supplemental results of ACI validation with yield data	58
A.1	Correlation between maize yield and individual ACIs	58
A.2	Multiple linear regression models.....	61
A.3	Relative importance models.....	62

B	Enlarged maps showing ACI occurrence and change signals	68
B.1	Heat stress	68
B.2	Low temperature stress.....	71
B.3	Potential waterlogging	74
B.4	Drought.....	75
B.5	Concurrent stress.....	76
C	Used R packages.....	79
C.1	Packages to work with NetCDF data or excel files	79
C.2	Packages used for data analysis and manipulation	79
C.3	Packages used for the calculation of the SPI.....	79
C.4	Packages for plotting	79
	Personal declaration.....	80

List of Figures

Figure 1: Maize physiology and anatomical terms based on Zhang et al. (2014) and Kaur et al. (2023). Sources of the illustrations of a maize plant: Pixabay (2013, 2014). 6

Figure 2: Overview of the municipalities from which the used maize yield data originated. Source of Swiss map: Federal Office of Topography swisstopo (2024). 19

Figure 3: Relative importance of univariate ACIs for maize yield variation in Moehlin from 2003–2022 21

Figure 4: Left: Deviation in number of days of the simulated average yearly number of SPIm & Frost Days from the observed average yearly number of SPIm & Frost Days during the reference period. The standardised RMSE is 0.37. Right: Same deviation as on the left, but only for the regions with GDD < 1430 °C (GDD estimation based on observational data). Regions with GDD ≥ 1430°C are coloured dark grey. The standardised RMSE in this case is 0.5. 24

Figure 5: Overview of the main findings using selected ACIs as examples. The range of the change signal for a listed ACI represents the interquartile range of the change signal for the whole of Switzerland in the climate model ensemble. Source of the illustration of a maize plant: Pixabay (2013) 25

Figure 6: Top left: Percentage of years with GDD ≥ 1600 °C based on observational data during the reference period (1981–2010). Bottom: Same as top left but in mid-century for RCP 2.6 scenario (left) and RCP 8.5 scenario (bottom right). Top right: Average percentage of years with GDD ≥ 1600 °C for the whole of Switzerland during the reference period (black) and mid-century (blue & red). The boxplots show the range of the climate model ensemble. The box represents the interquartile range, the line the median and the point the average of the climate model ensemble. 26

Figure 7: Top left: Average yearly number of HS30 based on observational data during the reference period (1981-2010). Bottom: Average of the change signal in number of days between the reference period and mid-century (2045-2074) for RCP 2.6 (left) and RCP 8.5 (right). Top right: Average yearly number of HS30 for the whole of Switzerland during the reference period (black) and mid-century (blue & red). The boxplots show the range of the climate model ensemble. The box represents the interquartile range, the line the median and the point the average of the climate model ensemble. 28

Figure 8: Top left: Standard deviation of the yearly number of HS30 based on observational data during the reference period (1981-2010). Bottom: Average of the change signal in number of days between the reference period and mid-century (2045-2074) for RCP 2.6 (left) and RCP 8.5 (right). Top right: Standard deviation of the yearly number of HS30 for the whole of Switzerland during the reference period (black) and mid-century (blue & red). The boxplots show the range of the climate model ensemble. The box represents the interquartile range, the line the median and the point the average of the climate model ensemble. 28

Figure 9: Top left: Average yearly number of HS35 based on observational data during the reference period (1981-2010). Bottom: Average of the change signal in number of days between the reference period and mid-century (2045-2074) for RCP 2.6 (left) and RCP 8.5 (right). Top right: Average yearly number of HS35 for the whole of Switzerland during the reference period (black) and mid-century (blue & red). The boxplots show the range of the climate model ensemble. The box represents the interquartile range, the line the median and the point the average of the climate model ensemble. 29

Figure 10: Top left: Average yearly HS35sum based on observational data during the reference period (1981-2010). Bottom: Average of the change signal in number of days between the reference period and mid-century (2045-2074) for RCP 2.6 (left) and RCP 8.5 (right). Top right: Average yearly HS35sum for the whole of Switzerland during the reference period (black) and mid-century (blue & red). The boxplots show the range of the climate model ensemble. The box represents the interquartile range, the line the median and the point the average of the climate model ensemble. 29

Figure 11: Top left: Standard deviation of the yearly HS35sum based on observational data during the reference period (1981-2010). Bottom: Average of the change signal in number of days between the reference period and mid-century (2045-2074) for RCP 2.6 (left) and RCP 8.5 (right). Top right: Standard deviation of the yearly HS35sum for the whole of Switzerland during the reference period (black) and mid-century (blue & red). The boxplots show the range of the climate model ensemble. The box represents the interquartile range, the line the median and the point the average of the climate model ensemble. 30

Figure 12: Top left: Average yearly number of Frost Days based on observational data during the reference period (1981-2010). Bottom: Average of the change signal in number of days between the reference period and mid-century (2045-2074) for RCP 2.6 (left) and RCP 8.5 (right). Top right: Average yearly number of Frost Days for the whole of Switzerland during the reference period (black) and mid-century (blue & red). The boxplots show the range of the climate model ensemble. The box represents the interquartile range, the line the median and the point the average of the climate model ensemble. 31

Figure 13: Top left: Standard deviation of the yearly number of Frost Days based on observational data during the reference period (1981-2010). Bottom: Average of the change signal in number of days between the reference period and mid-century (2045-2074) for RCP 2.6 (left) and RCP 8.5 (right). Top right: Standard deviation of the yearly number of Frost Days for the whole of Switzerland during the reference period (black) and mid-century (blue & red). The boxplots show the range of the climate model ensemble. The box represents the interquartile range, the line the median and the point the average of the climate model ensemble. 32

Figure 14: Top left: Average yearly Frostsum based on observational data during the reference period (1981-2010). Bottom: Average of the change signal in number of days between the reference period and mid-century (2045-2074) for RCP 2.6 (left) and RCP 8.5 (right). Top right: Average yearly Frostsum for the whole of Switzerland during the reference period (black) and mid-century (blue & red). The boxplots show the range of the climate model ensemble. The box represents the interquartile range, the line the median and the point the average of the climate model ensemble. 32

Figure 15: Top left: Standard deviation of the yearly Frostsum based on observational data during the reference period (1981-2010). Bottom: Average of the change signal in number of days between the reference period and mid-century (2045-2074) for RCP 2.6 (left) and RCP 8.5 (right). Top right: Standard deviation of the yearly Frostsum for the whole of Switzerland during the reference period (black) and mid-century (blue & red). The boxplots show the range of the climate model ensemble. The box represents the interquartile range, the line the median and the point the average of the climate model ensemble. 33

Figure 16: Top left: Average yearly number of LT6 based on observational data during the reference period (1981-2010). Bottom: Average of the change signal in number of days between the reference period and mid-century (2045-2074) for RCP 2.6 (left) and RCP 8.5 (right). Top right: Average yearly number of LT6 for the whole of Switzerland during the reference period (black) and mid-century (blue & red). The boxplots show the range of the climate model ensemble. The box represents the interquartile range, the line the median and the point the average of the climate model ensemble. 33

Figure 17: Top left: Average yearly number of HPE based on observational data during the reference period (1981-2010). Bottom: Average of the change signal in number of days between the reference period and mid-century (2045-2074) for RCP 2.6 (left) and RCP 8.5 (right). Top right: Average yearly number of HPE for the whole of Switzerland during the reference period (black) and mid-century (blue & red). The boxplots show the range of the climate model ensemble. The box represents the interquartile range, the line the median and the point the average of the climate model ensemble. 34

Figure 18: Top left: Standard deviation of the yearly number of HPE based on observational data during the reference period (1981-2010). Bottom: Average of the change signal in number of days between the reference period and mid-century (2045-2074) for RCP 2.6 (left) and RCP 8.5 (right). Top right: Standard deviation of the yearly number of HPE for the whole of Switzerland during the reference period (black) and mid-century (blue & red). The boxplots show the range of the climate model ensemble. The box represents the interquartile range, the line the median and the point the average of the climate model ensemble..... 35

Figure 19: Top left: Average yearly number of SPI_m based on observational data during the reference period (1981-2010). Bottom: Average of the change signal in number of days between the reference period and mid-century (2045-2074) for RCP 2.6 (left) and RCP 8.5 (right). Top right: Average yearly number of SPI_m for the whole of Switzerland during the reference period (black) and mid-century (blue & red). The boxplots show the range of the climate model ensemble. The box represents the interquartile range, the line the median and the point the average of the climate model ensemble. 36

Figure 20: Top left: Average yearly number of SPI_m & HS30 based on observational data during the reference period (1981-2010). Bottom: Average of the change signal in number of days between the reference period and mid-century (2045-2074) for RCP 2.6 (left) and RCP 8.5 (right). Top right: Average yearly number of SPI_m & HS30 for the whole of Switzerland during the reference period (black) and mid-century (blue & red). The boxplots show the range of the climate model ensemble. The box represents the interquartile range, the line the median and the point the average of the climate model ensemble. 37

Figure 21: Top left: Standard deviation of the yearly number of SPI_m & HS30 based on observational data during the reference period (1981-2010). Bottom: Average of the change signal in number of days between the reference period and mid-century (2045-2074) for RCP 2.6 (left) and RCP 8.5 (right). Top right: Standard deviation of the yearly number of SPI_m & HS30 for the whole of Switzerland during the reference period (black) and mid-century (blue & red). The boxplots show the range of the climate model ensemble. The box represents the interquartile range, the line the median and the point the average of the climate model ensemble..... 38

Figure 22: Top left: Average yearly number of SPI_m & Frost Days based on observational data during the reference period (1981-2010). Bottom: Average of the change signal in number of days between the reference period and mid-century (2045-2074) for RCP 2.6 (left) and RCP 8.5 (right). Top right: Average yearly number of SPI_m & Frost Days for the whole of Switzerland during the reference period (black) and mid-century (blue & red). The boxplots show the range of the climate model ensemble. The box represents the interquartile range, the line the median and the point the average of the climate model ensemble..... 39

Figure 23: Top left: Standard deviation of the yearly number of SPI_m & Frost Days based on observational data during the reference period (1981-2010). Bottom: Average of the change signal in number of days between the reference period and mid-century (2045-2074) for RCP 2.6 (left) and RCP 8.5 (right). Top right: Standard deviation of the yearly number of SPI_m & Frost Days for the whole of Switzerland during the reference period (black) and mid-century (blue & red). The boxplots show the range of the climate model ensemble. The box represents the interquartile range, the line the median and the point the average of the climate model ensemble..... 40

Figure 24: Top left: Average yearly number of HPE & Frost Days based on observational data during the reference period (1981-2010). Bottom: Average of the change signal in number of days between the reference period and mid-century (2045-2074) for RCP 2.6 (left) and RCP 8.5 (right). Top right: Average yearly number of HPE & Frost Days for the whole of Switzerland during the reference period (black) and mid-century (blue & red). The boxplots show the range of the climate model ensemble. The box represents the interquartile range, the line the median and the point the average of the climate model ensemble..... 41

Figure 25: Left column: Average yearly number of HS30 based on observational data during the reference period (top) and based on the RCP 2.6 scenario (middle) and the RCP 8.5 scenario (bottom) during mid-century. Right column: Same as on the left but for the standard deviation of the yearly number of HS30..... 68

Figure 26: Average yearly number of HS35 based on observational data during the reference period (top) and based on the RCP 2.6 scenario (middle) and the RCP 8.5 scenario (bottom) during mid-century. 69

Figure 27: Left column: Average yearly HS35sum based on observational data during the reference period (top) and based on the RCP 2.6 scenario (middle) and the RCP 8.5 scenario (bottom) during mid-century. Right column: Same as on the left but for the standard deviation of the yearly HS35sum. ... 70

Figure 28: Left column: Average yearly number of Frost Days based on observational data during the reference period (top) and based on the RCP 2.6 scenario (middle) and the RCP 8.5 scenario (bottom) during mid-century. Right column: Same as on the left but for the standard deviation of the yearly number of Frost Days. 71

Figure 29: Left column: Average yearly Frostsum based on observational data during the reference period (top) and based on the RCP 2.6 scenario (middle) and the RCP 8.5 scenario (bottom) during mid-century. Right column: Same as on the left but for the standard deviation of the yearly Frostsum. .. 72

Figure 30: Average yearly number of LT6 based on observational data during the reference period (top) and based on the RCP 2.6 scenario (middle) and the RCP 8.5 scenario (bottom) during mid-century.73

Figure 31: Left column: Average yearly number of HPE based on observational data during the reference period (top) and based on the RCP 2.6 scenario (middle) and the RCP 8.5 scenario (bottom) during mid-century. Right column: Same as on the left but for the standard deviation of the yearly number of HPE. 74

Figure 32: Average yearly number of SPIm based on observational data during the reference period (top) and based on the RCP 2.6 scenario (middle) and the RCP 8.5 scenario (bottom) during mid-century. 75

Figure 33: Left column: Average yearly number of SPIm & HS30 based on observational data during the reference period (top) and based on the RCP 2.6 scenario (middle) and the RCP 8.5 scenario (bottom) during mid-century. Right column: Same as on the left but for the standard deviation of the yearly number of SPIm & HS30. 76

Figure 34: Left column: Average yearly number of SPIm & Frost Days based on observational data during the reference period (top) and based on the RCP 2.6 scenario (middle) and the RCP 8.5 scenario (bottom) during mid-century. Right column: Same as on the left but for the standard deviation of the yearly number of SPIm & Frost Days..... 77

Figure 35: Average yearly number of HPE & Frost Days based on observational data during the reference period (top) and based on the RCP 2.6 scenario (middle) and the RCP 8.5 scenario (bottom) during mid-century..... 78

List of Tables

Table 1: List of the municipalities from which the used maize yield data originated and the respective number of years with available maize yield data..... 7

Table 2: Overview of the used ACIs and their respective source sorted by the categories heat stress, low temperature stress, potential waterlogging, drought and concurrent stress..... 11

Table 3: Overview of Spearman's correlation coefficients ρ . Listed are the number of positive linear relationships ($\rho > 0$) and the respective number of correlation coefficients with a p-value < 0.1 and < 0.05 , and the number of negative linear relationships ($\rho < 0$) and the respective number of correlation coefficients with a p-value < 0.1 and < 0.05 20

Table 4: Results of the technical validation of the representation of ACIs by CH2018 data. This table includes all statistical parameters of an ACI with a standardised RMSE < 0.5 and Spearman's correlation coefficient $\rho > 0.8$. These ACIs are rated as well represented by the CH2018 data with respect to the listed statistical parameter..... 22

Table 5: Results of the technical validation of the representation of ACIs by CH2018 data. This table includes all statistical parameters of an ACI with a standardised RMSE ≥ 0.5 and their respective Spearman's correlation coefficient ρ . For these ACIs, the representation by the CH2018 data is defined as biased with respect to the listed statistical parameter. 23

Table 6: Spearman's rank correlation ρ between ACI occurrence and maize yield and the corresponding p-value for the municipalities Aristau, Dietwil and Islisberg. For each municipality, the number of years with available maize yield data is listed. 58

Table 7: Spearman's rank correlation ρ between ACI occurrence and maize yield and the corresponding p-value for the municipalities Moehlin, Zetzwil and Hohenrain. For each municipality, the nr. of years with available maize yield data is listed. 59

Table 8: Spearman's rank correlation ρ between ACI occurrence and maize yield and the corresponding p-value for the municipalities Ramsen, Schlatt and Thundorf. For each municipality, the nr. of years with available maize yield data is listed. 59

Table 9: Spearman's rank correlation ρ between ACI occurrence and maize yield and the corresponding p-value for the municipalities Yvorne, Schwerzenbach and Thalheim an der Thur. For each municipality, the nr. of years with available maize yield data is listed..... 60

Table 10: Output of the multiple linear regression model for maize yield and all univariate ACIs and the corresponding p-value for individual municipalities. For each municipality, the number of years with available maize yield data is listed. 61

Table 11: Relative importance of each individual ACI listed below for maize yield variation in Aristau (nr. of years with maize yield data = 18 years). The metrics are normalised sum to 100%. The occurrence of the ACIs not included in this list was too low for the ACI to be included in this estimation. The output of the relative importance model shows the portion of maize yield variation explained by the listed univariate ACIs..... 62

Table 12: Relative importance of each individual ACI listed below for maize yield variation in Dietwil (nr. of years with maize yield data = 20 years). The metrics are normalised sum to 100%. The occurrence of the ACIs not included in this list was too low for the ACI to be included in this estimation. The output of the relative importance model shows the portion of maize yield variation explained by the listed univariate ACIs..... 62

Table 13: Relative importance of each individual ACI listed below for maize yield variation in Islisberg (nr. of years with maize yield data = 17 years). The metrics are normalised sum to 100%. The occurrence of the ACIs not included in this list was too low for the ACI to be included in this estimation. The output of the relative importance model shows the portion of maize yield variation explained by the listed univariate ACIs..... 63

Table 14: Relative importance of each individual ACI listed below for maize yield variation in Moehlin (nr. of years with maize yield data = 19 years). The metrics are normalised sum to 100%. The occurrence of the ACIs not included in this list was too low for the ACI to be included in this estimation. The output of the relative importance model shows the portion of maize yield variation explained by the listed univariate ACIs..... 63

Table 15: Relative importance of each individual ACI listed below for maize yield variation in Zetzwil (nr. of years with maize yield data = 19 years). The metrics are normalised sum to 100%. The occurrence of the ACIs not included in this list was too low for the ACI to be included in this estimation. The output of the relative importance model shows the portion of maize yield variation explained by the listed univariate ACIs..... 64

Table 16: Relative importance of each individual ACI listed below for maize yield variation in Hohenrain (nr. of years with maize yield data = 18 years). The metrics are normalised sum to 100%. The occurrence of the ACIs not included in this list was too low for the ACI to be included in this estimation. The output of the relative importance model shows the portion of maize yield variation explained by the listed univariate ACIs..... 64

Table 17: Relative importance of each individual ACI listed below for maize yield variation in Ramsen (nr. of years with maize yield data = 19 years). The metrics are normalised sum to 100%. The occurrence of the ACIs not included in this list was too low for the ACI to be included in this estimation. The output of the relative importance model shows the portion of maize yield variation explained by the listed univariate ACIs..... 64

Table 18: Relative importance of each individual ACI listed below for maize yield variation in Schlatt (nr. of years with maize yield data = 18 years). The metrics are normalised sum to 100%. The occurrence of the ACIs not included in this list was too low for the ACI to be included in this estimation. The output of the relative importance model shows the portion of maize yield variation explained by the listed univariate ACIs..... 65

Table 19: Relative importance of each individual ACI listed below for maize yield variation in Thundorf (nr. of years with maize yield data = 17 years). The metrics are normalised sum to 100%. The occurrence of the ACIs not included in this list was too low for the ACI to be included in this estimation. The output of the relative importance model shows the portion of maize yield variation explained by the listed univariate ACIs..... 65

Table 20: Relative importance of each individual ACI listed below for maize yield variation in Yvorne (nr. of years with maize yield data = 17 years). The metrics are normalised sum to 100%. The occurrence of the ACIs not included in this list was too low for the ACI to be included in this estimation. The output of the relative importance model shows the portion of maize yield variation explained by the listed univariate ACIs..... 66

Table 21: Relative importance of each individual ACI listed below for maize yield variation in Schwerzenbach (nr. of years with maize yield data = 17 years). The metrics are normalised sum to 100%. The occurrence of the ACIs not included in this list was too low for the ACI to be included in this estimation. The output of the relative importance model shows the portion of maize yield variation explained by the listed univariate ACIs. 66

Table 22: Relative importance of each individual ACI listed below for maize yield variation in Thalheim an der Thur (nr. of years with maize yield data = 17 years). The metrics are normalised sum to 100%. The occurrence of the ACIs not included in this list was too low for the ACI to be included in this estimation. The output of the relative importance model shows the portion of maize yield variation explained by the listed univariate ACIs. 67

List of Equations

Equation 1: Calculation of temperature sum S_T based on Buzzi et al. (2021), which corresponds to the sum of growing degree days (McMaster and Wilhelm, 1997)..... 10

Equation 2: Calculation of the standardised root-mean-square-error. Adapted from Tschurr et al. (2020). 17

List of Abbreviations

ACI	Agricultural Climate Indicator
GCM	Global Climate Model
GDD	Growing Degree Days
GEV distribution	Generalised Extreme Value distribution
RCM	Regional Climate Model
RCP	Representative Concentration Pathway
RMSE	Root-Mean-Square Error
SD	Standard Deviation
SPI	Standardised Precipitation Index

List of used Agricultural Climate Indicators (ACIs)

Category	ACI	Description
Heat stress	HS30 [Days]	Days with maximum temperatures above 30 °C.
	HS35 [Days]	Days with maximum temperatures above 35 °C.
	HS35sum [°C]	Sum of maximum temperature exceedance of 35 °C over the whole growing season.
Low temperature stress	Frost Day [Days]	Days with minimum temperatures below 0 °C.
	Frostsum [°C]	Sum of absolute minimum temperatures below 0 °C over the whole growing season.
	LT6 [Days]	Days with minimum temperatures below 6 °C.
Potential waterlogging	HPE [Days]	Days with at least 50 mm precipitation.
Drought	SPI _m [Days]	Days with an SPI below -1.
	SPI _e [# Events]	Number of events with an SPI below -1.6 for at least seven consecutive days.
Concurrent stress	SPI _m & HS30 [Days]	Days with maximum temperatures above 30 °C and an SPI below -1.
	SPI _e & HS35 [Days]	Number of days with maximum temperatures above 35 °C and an SPI that has been below -1.6 for at least seven consecutive days.
	HPE & HS30 [Days]	Days with maximum temperatures above 30 °C and at least 50 mm precipitation.
	HPE & HS35 [Days]	Days with maximum temperatures above 35 °C and at least 50 mm precipitation.
	SPI _m & Frost Day [Days]	Days with minimum temperatures below 0 °C and an SPI below -1.
	SPI _e & Frost Day [Days]	Number of days with minimum temperatures below 0 °C and an SPI that has been below -1.6 for at least seven consecutive days.
	HPE & Frost Day	Days with minimum temperatures below 0 °C and at least 50 mm precipitation.

1 Introduction

1.1 Estimating the impact of climate on maize cultivation

Climate is a fundamental determinant of maize quality and yield (Zscheischler *et al.*, 1984; Waqas *et al.*, 2021). Temperature extremes can negatively affect water use efficiency as well as photosynthetic activity and may cause metabolic alterations (Waqas *et al.*, 2021). Drought is associated with restrained growth and, especially when occurring around flowering, yield loss (Anami *et al.*, 2009; Dierauer and Gelencsér, 2019). Moreover, heavy precipitation events can lead to waterlogging, which in turn can cause a lack of oxygen in the root zone, reduced photosynthetic rate and finally to reduced yield (Kozłowski, 1997; Tian *et al.*, 2019; Huang *et al.*, 2022).

There have been indications that climate change has, in some cases, already led to a negative response of maize yield within the past decades (Lobell and Field, 2007; Hawkins *et al.*, 2013). With further global warming the frequency and intensity of weather extremes such as heat waves and in some regions agricultural droughts are expected to increase in the future (IPCC, 2021), potentially leading to reduced crop yield depending on the climate zone (Olesen and Bindi, 2002). To mitigate the impact of climate change on crop cultivation, farmers need to adapt their production practices (Reidsma *et al.*, 2010). For this purpose, information about climate-related challenges in the future, specified for individual crop cultivars, are necessary to provide a basis for the adaptation process (NCCS, 2023, 2024).

In order to estimate the impact of climate change on a specific sector, so-called climate impact models can be used, which combine climate change information with knowledge about the influence of climate on specific indicators relevant to the respective sector (NCCS, 2021). A widespread method to analyse climate impact on crop is the use of process based crop models, or, in short, crop models (Reidsma *et al.*, 2010; Webber *et al.*, 2022). These models allow to simulate the complex interactions between plants and several environmental factors, such as climate, soil and management (Eitzinger *et al.*, 2012; Pasley *et al.*, 2022). As Eitzinger *et al.* (2012) elaborate, crop models are useful to analyse the physiological response of crop to climate change. However, the same authors also state that the results of these models are usually associated with uncertainties and limitations. Examples of such are the simplified representation of reality, low quality of input data and the lack of long-term data for crop model validation and calibration (Eitzinger *et al.*, 2012). The potential influence of farmer decisions on the impact of climate change is another uncertainty in crop modelling (Eitzinger *et al.*, 2012; Arnell and Freeman, 2021).

Another possibility to analyse the impact of climate on crop is the use of agricultural climate indicators (Eitzinger *et al.*, 2012). An agricultural climate indicator (ACI) is based on meteorological variables and represents the interactions between crop and climate (Nobakht *et al.*, 2019, 2024). An example for an ACI is the number of consecutive dry days (days with less than 1 mm precipitation), which provides information about possible drought damage in agriculture (Nobakht *et al.*, 2019). ACIs are in comparison to crop models simpler to calculate, making them a valuable tool for operational purposes such as drought or frost monitoring (Eitzinger *et al.*, 2012). ACIs can also be used for yield forecasting

(Mathieu and Aires, 2018). Furthermore, ACIs are a useful method to estimate which aspects of climate change pose a risk to crop yield (Eitzinger *et al.*, 2012). They are thus also used to evaluate the impact of climate change on crop cultivation and are a helpful tool for decision support in the adaptation process (Holzkämper and Fuhrer, 2015; Arnell and Freeman, 2021).

Such climate impact analyses are also very important for Switzerland (NCCS, 2021). In Switzerland, heavy precipitation events as well as heat waves have become more frequent and intense and the summers have become drier in the past decades (CH2018, 2018; Scherrer *et al.*, 2022). Moreover, according to the CH2018 climate scenarios, without climate mitigation it is likely that these trends will continue (CH2018, 2018). Thus, climate change also poses a challenge to maize cultivation in Switzerland (Holzkämper and Fuhrer, 2015). Maize is an important crop for Switzerland. It is one of the most used crops for feeding livestock in Switzerland (Schweizer Bauernverband, 2021). In 2020, grain maize accounted for over 20% of cereal production (Bundesamt für Statistik, 2022). Information about future climate-related challenges specified for maize cultivation in Switzerland can provide a basis for the adaptation process to mitigate the impact of climate change (NCCS, 2023, 2024).

1.2 Related work about climate change impact on the agricultural sector

Holzkämper and Fuhrer (2015) estimated the future climatological suitability for maize cultivation in Switzerland based on ACIs. However, the climate data used in their study is older than the current CH2018 climate data. Since 2018, new climate scenarios for Switzerland are available, namely the CH2018 climate scenarios (CH2018 Project Team, 2018). The CH2018 scenarios are, at the time of this thesis, the most up-to-date climate information available for climate change impact estimations (CH2018, 2018). Tschurr *et al.* (2020) evaluated how well the CH2018 data can simulate the occurrence of ACIs. However, the used ACI in their study were chosen based on their relevance for several sectors in agriculture and were not specified for maize. Moreover, the study by Tschurr *et al.* (2020) was based on station data. An ACI-based climate impact analysis with the current CH2018 grid-data, covering the whole of Switzerland, is yet to be done.

Another important aspect of climatological limitations for maize cultivation is the simulation of concurrent stress factors (Webber *et al.*, 2022). There are several studies investigating the effect of single stress factors on maize (e.g. Waqas *et al.*, 2021; Githui *et al.*, 2022; Zhou *et al.*, 2022). However, in the field plants often experience more than one abiotic stress factor at the same time, and the impact of concurrent stress can be more harmful for plants than an individual stress factor (Suzuki *et al.*, 2014; Shabbir *et al.*, 2022; Webber *et al.*, 2022). Tschurr *et al.* (2020) did not include ACIs that specifically represent two or more simultaneous stress factors. The same counts for the study by Holzkämper and Fuhrer (2015). There are studies that investigate the impact of concurrent stress factors for maize (Suzuki *et al.*, 2014; Hussain *et al.*, 2020; Shabbir *et al.*, 2022; Hu *et al.*, 2023). However, no studies were found investigating climate change impact on maize cultivation in Switzerland with respect to concurrent stress factors.

Finally, the focus in climate impact studies for the agricultural sectors often lies on the average climatological limitations (e.g. Holzkämper and Fuhrer, 2015; Holzkämper *et al.*, 2015; Tschurr *et al.*, 2020). However, the year-to-year fluctuations in maize yield also depend on temporal climate

variability – i.e. the interannual variation of climatological parameters – and poses a challenge in maize cultivation (Southworth *et al.*, 2000; Lobell and Field, 2007; Buzzi *et al.*, 2021). Zscheischler *et al.* (1984) also suggest cultivating more than one maize variety with differing growing length to ensure that in spite of interannual climate variability at least one of the varieties can take full advantage of the growing season. For end-users it may thus be useful to also receive information about the temporal variability of stress factors.

1.3 Research questions and hypotheses

This thesis aims to address these research gaps and is embedded in the ecosystem services project by the NCCS-impacts programme, which focuses on the development of user-oriented climate services (NCCS, 2023). The impact of climate change on maize cultivation in Switzerland is analysed by evaluating the occurrence of ACIs and their temporal variability based on the CH2018 grid-data. The used ACIs are mostly specified for maize cultivation in Switzerland or Europe and represent single stress factors as well as simultaneous stress factors. Regarding variability, the focus lies on temporal variability, i.e. the year-to-year variability of ACI occurrence at a specific site, while the spatial variability of ACIs, i.e. the difference in ACI occurrence between different sites in Switzerland, is discussed marginally. In this thesis, the following research questions are investigated:

1. *How well do agricultural climate indicators explain maize yield variation in the present Swiss climate?*

Hypothesis 1: There is a significant negative relationship between maize yield and the occurrence of agricultural climate indicators in the present Swiss climate.

2. *Will the average occurrence of agricultural climate indicators in Switzerland change with climate change?*

Hypothesis 2: The average occurrence of agricultural climate indicators will be different in the future Swiss climate.

3. *Will the variability of agricultural climate indicators in Switzerland change with climate change?*

Hypothesis 3: The variability of the agricultural climate indicators will be different in the future Swiss climate.

In order to answer the first research question, yearly maize yield data from 2003–2022 for several sites in Switzerland were compared to the yearly ACI occurrence. By using Spearman’s correlation coefficient and multiple linear regression model it was estimated whether there exists a relationship between maize yield variation and ACI occurrence.

To answer the second and the third question, the CH2018 grid-data was used to estimate the ACI occurrence and its temporal variability in 2045–2075 (also referred to as mid-century (CH2018, 2018)) for the RCP 2.6 and RCP 8.5 scenario. The temporal variability of an ACI was calculated by estimating

the temporal standard deviation of the yearly number of the respective ACI. The results were then illustrated in change signal maps and boxplots in order to estimate whether there is a potential change in the average occurrence and temporal variability ACI until mid-century.

2 Elaboration of maize development

In order to understand how climatological stress is related to maize growth, knowledge about maize development may be advantageous. Thus, in this segment, maize development and maize susceptibility to climatological stress is elaborated.

In the present Swiss climate, maize is sown between April and May depending – among other factors – on meteorological conditions (Holzkämper, Calanca and Fuhrer, 2013; Dierauer and Gelencsér, 2019; Strickhof, 2023). After sowing, the seedling emerges and the development of leaves begins within the following weeks (Zscheischler *et al.*, 1984). Note that in phenology, growth stages that are clearly identifiable, such as leaf unfolding and flowering, are also called phenological phases (MeteoSwiss, no date b).

At early development stages, maize is very sensitive to low temperature stress as this limits germination as well as the seedling growth and can also damage plant tissue (Waqas *et al.*, 2021; Webber *et al.*, 2022; Zhou *et al.*, 2022). Moreover, it has been shown that the impact of waterlogging on maize is higher in earlier growing stages (Ren *et al.*, 2016; Huang *et al.*, 2022).

Around July, flowering starts (Holzkämper, Calanca and Fuhrer, 2013). During flowering, the formed anthers at the top of the maize plant (Figure 1, based on Zhang *et al.* (2014) and Kaur *et al.* (2023)) start to shed pollen (also called anthesis) (Elmore, 2012). Pollination occurs when the shed pollen are caught by the silks (Fonseca *et al.*, 2003). Flowering belongs to one of the development stages that are the most susceptible to heat stress with regards to yield reduction due to the loss of kernel number and shortening grain filling duration (Waqas *et al.*, 2021; Webber *et al.*, 2022). Additionally, while drought impacts maize in all growing phases (Anami *et al.*, 2009; Shabbir *et al.*, 2022), it is the development stages right before, during and after flowering that are most sensible to drought, as about half of the total water required by this plant is taken up about three weeks before and after flowering (Anami *et al.*, 2009; Dierauer and Gelencsér, 2019).

After flowering, the process of grain filling begins (Holzkämper, Calanca and Fuhrer, 2013). The moment the plant has enough dry matter, maize is harvested, which is usually around September to November, depending on maize variety and climatological conditions (Dierauer and Gelencsér, 2019; Hiltbrunner *et al.*, 2023; Strickhof, 2023).

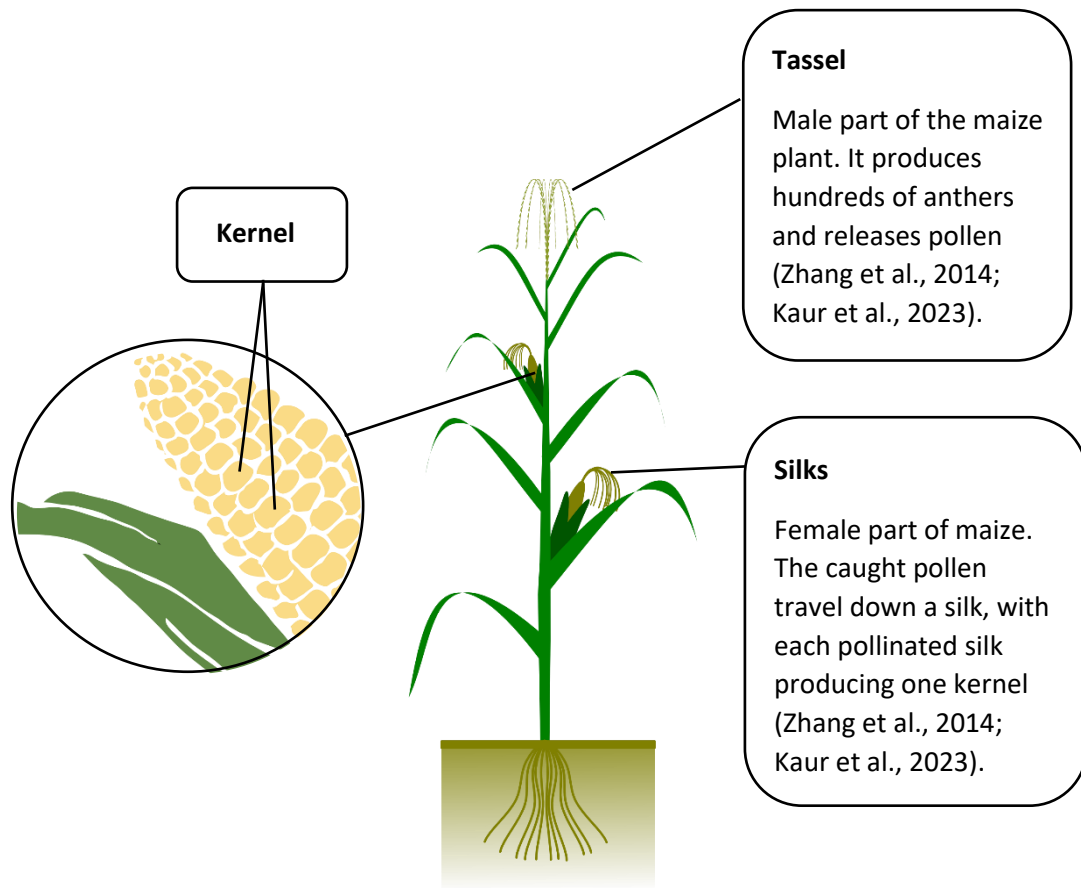


Figure 1: Maize physiology and anatomical terms based on Zhang et al. (2014) and Kaur et al. (2023). Sources of the illustrations of a maize plant: Pixabay (2013, 2014).

3 Data

3.1 Maize yield data

The used yield data was provided by Agristat, the Swiss farmer association (unpublished data). The data included yearly maize yield separated by grain, silage, green maize and whole maize plant as well as by municipality from 2003–2022. However, only one municipality includes yield data for all 20 years. The other municipalities showed data gaps for sometimes several years. Thus, in order to include time series as long as possible, only maize yield data from municipalities that included data for at least 17 out of 20 years have been included, which are 12 municipalities in total (Table 1). The number of reported maize yield varied per municipality from year to year, and the exact farm of a report is kept anonymous. In order to handle the differing number of maize yield reports, for each year the maize yield data was averaged over the respective number of reports for each included municipality.

Table 1: List of the municipalities from which the used maize yield data originated and the respective number of years with available maize yield data.

Canton	Municipality	Number of years
Aargau	Aristau	18
Aargau	Dietwil	20
Aargau	Islisberg	17
Aargau	Möhlin	19
Aargau	Zetzwil	19
Lucerne	Hohenrain	18
Schaffhausen	Ramsen	19
Thurgau	Schlatt (TG)	18
Thurgau	Thundorf	17
Vaud	Yvorne	19
Zurich	Schwerzenbach	17
Zurich	Thalheim an der Thur	17

3.2 Climate data

3.2.1 Observational climate data

The used observational climate data is provided by MeteoSwiss. They provide spatial climate analyses for several parameters and time aggregations for the past decades as grid-data based on a spatial analysis of near-surface measurements (MeteoSwiss and Federal Department of Home Affairs, 2021c). The grid-data is available in the format NetCDF and on different grid structures. In this thesis, the 'ch02.lonlat' grid structure with longitude and latitude increments and a spatial resolution of approximately 2 km has been used (MeteoSwiss and Federal Department of Home Affairs, 2021c). The

R packages used to work with NetCDF data are listed in Appendix C. In general, all programming for this thesis was conducted in R studio (R Core Team, 2023), using OpenAI's GPT-3.5 (OpenAI, no date) to help with the programming.

The used grid-data include daily precipitation, daily maximum, minimum and average temperature for the period 1981–2010 for the whole of Switzerland. While the daily temperature grid-data covers Switzerland within its national borders, the daily precipitation data was only available for hydrological Switzerland, which also contains regions outside the Swiss borders. Thus, for reasons of consistency, the precipitation grid-points that were not part of the temperature grid were excluded. Moreover, local time series of the mentioned four parameters for the period 2003–2022 for the municipalities listed in Table 1 were used, which are based on the same grid-data products (MeteoSwiss and Federal Department of Home Affairs, 2015).

Since about 1990, temperature data is mainly derived from the mean of 10-minute measurement intervals from midnight to midnight UTC. In the years beforehand, temperature data was derived from manual readings. Uncertainties regarding temperature data are associated with the limited capability to resolve several small-scale effects such as urban heat islands or cold air pools (MeteoSwiss and Federal Department of Home Affairs, 2021a).

The daily precipitation data is derived from rain-gauge measurements and is based on accumulated precipitation and snow water equivalent from 6 UTC to 6 UTC of the following day in hydrological Switzerland. Uncertainties arise by measurement errors, especially during snowfall and at wind-exposed locations. Moreover, single grid-point values are expected to potentially show substantial interpolation errors – especially in summer – with a tendency to underestimate intense precipitation. In case of convective rainfalls, interpolation uncertainty is relatively higher due to its high spatial variation (MeteoSwiss and Federal Department of Home Affairs, 2021b).

In general, uncertainties in the used grid-data are connected to the fact that the resolution of the data is higher than the spacing of the measurement station networks, leading to potential deviation of statistical properties from reality with a general underestimation of the frequency of extremes (MeteoSwiss and Federal Department of Home Affairs, 2021c).

3.2.2 CH2018 data

As mentioned in the introduction, the CH2018 scenarios provide information about how the climate in Switzerland can change in the future, including useful data e.g. for climate impact analysis (CH2018, 2018). Three different Representative Concentration Pathways are used in the CH2018 report. The Representative Concentration Pathways (RCP) represent possible scenario of long-lived greenhouse gas concentrations and are used to explore how climate changes depending on greenhouse gas emissions. The RCP 2.6 scenario assumes strong climate mitigation with substantial reductions in global emissions. The RCP 4.5 scenario assumes a decline in emissions after 2050. The RCP 8.5 scenario assumes no climate mitigation and further growing greenhouse gas emissions (CH2018, 2018). In this thesis, the localized CH2018 datasets based on the RCP 2.6 scenario and the RCP 8.5 scenario were used.

The following information about the CH2018 data are derived from CH2018 (2018). In this thesis, the data product 'DAILY-GRIDDED' was used. It contains daily time series for precipitation sum, maximum, minimum and average temperature 2 meters above the surface on a grid with spatial resolution of approximately 2 km. The format of the data is NetCDF. Each time series is based on the output of a EURO-CORDEX model chain, which refers to a combination of a global climate model (GCM) and a regional climate model (RCM), and simulates the climate from 1981–2099. The CH2018 project team then applied quantile mapping on the output of each EURO-CORDEX simulation, a method involving statistical downscaling and bias correction based on observational grid-data as reference. More details about the technical background of the CH2018 dataset is available in CH2018 (2018).

In this thesis, the localized dataset for 1981–2010 (referred to as reference period) and for 2045–2075 (also referred to as mid-century) based on the RCP 8.5 scenario and for the latter time period also based on the RCP 2.6 scenario have been used. This dataset includes 31 different simulations for the RCP 8.5 scenario and 12 simulations for the RCP 2.6 scenario. As stated by Kotlarski and Rajczak (2018), the simulations are based on free running GCMs, meaning that the temporal evolution of weather patterns does neither coincide with other simulations nor with the observations, and thus for example do not necessarily represent a warm summer in 2003, as it was observed.

The CH2018 dataset also involves other limitations and potential remaining biases. For example, temporal climate variability is not corrected by quantile mapping, which is a highly relevant limitation for this thesis, as the temporal variability of ACIs is investigated. Thus, a validation of the simulated standard deviation by the climate models is extremely important. The validation process is also especially necessary for multivariate ACI, as quantile mapping has been applied in a univariate manner, i.e. without correcting for potential biases in inter-variable relationships. Additionally, spatial variability at daily scale may not be represented properly as the raw climate model output has a lower spatial resolution than the high-resolution grid of the 'DAILY-GRIDDED' product. It is also noteworthy that uncertainties in the observational reference grid-data are replicated in the CH2018 data. Information about further limitations of the CH2018 data are available in CH2018 (2018).

All computations involving the CH2018 data were done on the ScienceCloud of the University of Zurich.

4 Method

4.1 Defining maize growing season

In this thesis, the occurrence of ACIs during the maize growing season is calculated with the sowing date being defined as the 5th of May and the harvesting date as the 11th of October. Those dates are based on the median of the sowing and maturity dates estimated by Holzkämper, Calanca and Fuhrer (2013), who investigated the climatic limitations to grain maize yield in Switzerland. In the same study, the harvesting date is estimated with the sum of so-called growing degree days (GDD). This model allows to set the phenological development rate in relation to temperature with regards to the cardinal temperature of the respective plant (Yin *et al.*, 1995; Buzzi *et al.*, 2021; Hiltbrunner *et al.*, 2023). Cardinal temperature describes the base, optimal and maximum temperature at which plant growth occurs (Yin *et al.*, 1995).

In this thesis, the base temperature is defined as 6 °C and the maximum temperature as 30 °C according to Buzzi *et al.* (2021), who developed temperature sum maps for maize cultivation in Switzerland. Thus, below 6 °C and above 30 °C, no plant growth is expected (Eder, Ziegler and Eiblmeier, no date; Buzzi *et al.*, 2021). Buzzi *et al.* (2021) calculated in their study the temperature sum S_T , which corresponds to the sum of growing degree days (GDD) (McMaster and Wilhelm, 1997). The calculation is done as followed:

$$T_e = \begin{cases} \frac{1}{2}(T_{min} + T_{max}) & \text{if } T_{max} < 30 \text{ }^\circ\text{C} \\ \frac{1}{2}(T_{min} + 30) & \text{if } T_{max} \geq 30 \text{ }^\circ\text{C} \end{cases}$$

$$S_T = \sum_{\text{Sowing date}}^{\text{Harvesting date}} \max(T_e - 6, 0)$$

*Equation 1: Calculation of temperature sum S_T based on Buzzi *et al.* (2021), which corresponds to the sum of growing degree days (McMaster and Wilhelm, 1997).*

T_{min} is the daily minimum air temperature and T_{max} the daily maximum air temperature. Note that if the maximum air temperature exceeds the maximum cardinal temperature of 30 °C, the respective value is instead set to 30 °C. T_e is the effective temperature. From each daily effective temperature, the base temperature of 6 °C is subtracted and afterwards accumulated over the whole growing season, leading to the temperature sum S_T , which corresponds to the sum of growing degree days (McMaster and Wilhelm, 1997). Note that if the subtraction of the base temperature from the effective temperature leads to a negative value, the value 0 °C is used for the accumulation instead.

In this thesis, the growing degree day model is used to illustrate in which regions of Switzerland the necessary growing degree days of 1600 °C for early grain maize to mature (Holzkämper, Calanca and

Fuhrer, 2013; Buzzi *et al.*, 2021) can be reached. This allows to compare the maps showing ACI occurrence in Switzerland to a map showing which sites are potentially suitable for grain maize cultivation based on GDD threshold exceedance.

4.2 Choosing agricultural climate indicators

The used ACIs are based on literature research and are summarised in Table 2. If possible, literature about maize cultivation in Switzerland has been used. In some cases, literature about crop cultivation or about the general agricultural sector in Switzerland or Europe as well as some reviews about climate impact on maize that are not specified for Europe had to be included. The reason for this is limited availability of climatological parameters or of literature on maize cultivation in Switzerland and Europe. The categories heat stress, low temperature stress, potential waterlogging and drought are represented by different ACIs, as well as the combination drought & heat, potential waterlogging & heat, drought & low temperature as well as potential waterlogging & low temperature. In the following, the selection process is elaborated.

Table 2: Overview of the used ACIs and their respective source sorted by the categories heat stress, low temperature stress, potential waterlogging, drought and concurrent stress.

Category	ACI	Description	Source
Heat stress	HS30 [Days]	Days with maximum temperatures above 30 °C.	Buzzi <i>et al.</i> (2021), Waqas <i>et al.</i> (2021)
	HS35 [Days]	Days with maximum temperatures above 35 °C.	Adapted from Holzkämper, Calanca and Fuhrer (2013)
	HS35sum [°C]	Sum of maximum temperature exceedance of 35 °C over the whole growing season.	Adapted from Holzkämper, Calanca and Fuhrer (2013)
Low temperature stress	Frost Day [Days]	Days with minimum temperatures below 0 °C.	Adapted from Holzkämper, Calanca and Fuhrer (2013) and Tschurr <i>et al.</i> (2020)
	Frostsum [°C]	Sum of absolute minimum temperatures below 0 °C over the whole growing season.	Holzkämper, Calanca and Fuhrer (2013)
	LT6 [Days]	Days with minimum temperatures below 6 °C.	Sánchez, Rasmussen and Porter (2014), Buzzi <i>et al.</i> (2021), Waqas <i>et al.</i> (2021)

Table 2 (continued)

Category	ACI	Description	Source
Potential waterlogging	HPE [Days]	Days with at least 50 mm precipitation.	Tschurr <i>et al.</i> (2020)
Drought	SPI _m [Days]	Days with an SPI below -1.	Tschurr <i>et al.</i> (2020)
	SPI _e [# Events]	Number of events with an SPI below -1.6 for at least seven consecutive days.	
Concurrent stress	SPI _m & HS30 [Days]	Days with maximum temperatures above 30 °C and an SPI below -1.	Several multivariate ACIs are a combination of univariate ACIs of which the respective sources are listed above.
	SPI _e & HS35 [Days]	Number of days with maximum temperatures above 35 °C and an SPI that has been below -1.6 for at least seven consecutive days.	
	HPE & HS30 [Days]	Days with maximum temperatures above 30 °C and at least 50 mm precipitation.	
	HPE & HS35 [Days]	Days with maximum temperatures above 35 °C and at least 50 mm precipitation.	
	SPI _m & Frost Day [Days]	Days with minimum temperatures below 0 °C and an SPI below -1.	
	SPI _e & Frost Day [Days]	Number of days with minimum temperatures below 0 °C and an SPI that has been below -1.6 for at least seven consecutive days.	
	HPE & Frost Day [Days]	Days with minimum temperatures below 0 °C and at least 50 mm precipitation.	

4.2.1 Heat stress

As elaborated in chapter 2, heat stress is a highly relevant stress factor for maize (Waqas *et al.*, 2021). Note that in CH2018 (2018), 'heat stress' is defined as days with high temperature and humidity (CH2018, 2018). In this thesis, heat stress is defined as high maximum temperatures potentially harming maize. The ACIs representing heat stress are HS30 and HS35 which are defined as days with maximum temperatures above 30 °C and 35 °C respectively, as well as HS35sum defined as the sum of maximum temperature excess of 35 °C over the whole growing season.

The value of 30 °C is based on the study from Buzzi *et al.* (2021), who use this threshold as maximum cardinal temperature. The use of this value is not only motivated by the fact, that in Switzerland no further growth is expected above that threshold (Eder, Ziegler and Eiblmeier, no date; Buzzi *et al.*, 2021), but also because in the project AgriAdapt (2019) the number of days with maximum temperatures above 28 °C has been used as a heat stress related ACI for maize in a pilot project in Germany, underlining the relevance of temperatures above 30 °C. In a review about the impact of temperature extremes on maize it is elaborated that optimal temperature for maize varies from 25 °C to 33 °C, and that the exposure of maize to temperatures above 30 °C for a prolonged period can lead to yield loss (Waqas *et al.*, 2021). Note that the latter review does not focus on Switzerland or Europe and includes literature from several regions around the world.

The ACI HS35sum, defined as the sum of maximum temperature excess of 35 °C over the whole growing season, is an adapted version of an ACI from the study by Holzkämper, Calanca and Fuhrer (2013), where the authors calculated the average daily maximum temperature exceedance of 35 °C. As HS35sum may not be as intuitive for end-users, another adapted version was included, which is the ACI HS35, defined as days with maximum temperatures above 35 °C.

4.2.2 Low temperature stress

Temperatures below the temperature optimum window may negatively affect crop through delayed development, reduced photosynthetic rate and water use efficiency, and can also lead to yield reduction (Foyer *et al.*, 2002; Hussain *et al.*, 2018, 2020; Shabbir *et al.*, 2022; Zhou *et al.*, 2022). The used ACIs for low temperature stress are LT6 defined as days with minimum temperatures below 6 °C, Frost Days defined as days with minimum temperatures below 0 °C as well as Frostsum defined as the sum of absolute minimum temperature below 0 °C over the whole growing season.

The threshold of 6 °C for the ACI LT6 is based on Buzzi *et al.* (2021) who used this threshold as base temperature, indicating that in Switzerland no plant growth below this temperature is expected. The reviews of Sánchez, Rasmussen and Porter (2014) and Waqas *et al.* (2021) about the relation between temperature and maize development also includes information about potential damage on maize caused by temperatures below 6 °C.

The ACI Frostsum, defined as the sum of absolute minimum temperatures below 0 °C over the whole growing season, is an adapted version of an ACI from the study by Holzkämper, Calanca and Fuhrer

(2013), where the authors calculated the average daily minimum temperature below 0 °C in absolute values.

Moreover, an adapted version of Frostsum has been included defined as the number of days with minimum temperatures below 0 °C, which is according to CH2018 (2018) also a climate indicator named Frost Day. Thus, this ACI is named accordingly. Tschurr *et al.* (2020) used the threshold of 0 °C in their case study about ACIs for agricultural sectors in Switzerland as well, with the difference that their used ACI was defined as the number of Frost Days within the growing season but before the 1st of August.

4.2.3 Potential waterlogging

Waterlogging is an important abiotic stress factor for maize, as the saturated soil pores can lead to anoxia of crop roots, decrease maize growth and potentially lead to yield loss, depending on the phenological phase and duration of soil saturation (Yanar, Lipps and Deep, 1997; Ren *et al.*, 2016; Githui *et al.*, 2022; Huang *et al.*, 2022).

Heavy precipitation events can lead to waterlogging, this, however, depends on factors like soil structure and soil drainage (Ren *et al.*, 2016; Huang *et al.*, 2022). Possibly due to such dependencies, no clear precipitation threshold for potential waterlogging in arable lands in Switzerland was found. In general, waterlogging is compared to e.g. drought and heat stress a much less investigated stress factor for maize (Rötter *et al.*, 2018). The case study of Tschurr *et al.* (2020) included an ACI representing heavy precipitation events defined as the yearly number of days with a total precipitation sum of at least 50 mm, a threshold that is also in accordance with the rain hazard category three for the north of the Alps and in the Alps by MeteoSwiss (MeteoSwiss, no date c). Because Tschurr *et al.* (2020) denote this as an indicator relevant for agricultural sectors in Switzerland, and because it is stated in literature that that excessive precipitation can lead to waterlogging (Ren *et al.*, 2016; Githui *et al.*, 2022; Huang *et al.*, 2022), it is included in this thesis and used as an approximation for potential waterlogging.

4.2.4 Drought

The chosen ACIs representing drought are based on the daily Standardised Precipitation Index (SPI), an index developed by McKee, Doesken and Kleist (1993). The SPI is useful to monitor and warn about droughts, is simpler to calculate compared to other drought indicators, and is also flexible in its application, as it can be applied to different timescales and thus different types of droughts (World Meteorological Organization, 2012).

The World Meteorological Organization (2012) explains the calculation of the SPI as followed: The SPI is calculated by ideally using a monthly precipitation record of at least 30 years. Next, a probability distribution is fitted to this precipitation record. For many regions in Europe, the gamma distribution is suitable (Stagge *et al.*, 2015; Copernicus European Drought Observatory (EDO), 2020). Another

possibility is to use the Generalised Extreme Value (GEV) distribution (see e.g. Zhang and Li, 2020). As further explained by the World Meteorological Organization (2012), this probability distribution is then transformed into a normal distribution, so that the mean SPI takes the value zero. Thus, the SPI value for a given moment shows the standardised precipitation anomaly based on precipitation sum over a defined time scale. When using e.g. a time scale for three months – as done in this thesis – the precipitation accumulation within three months is compared to the mean precipitation for the same time period within the precipitation record. For example: if a precipitation record from 1981–2010 is used for the probability distribution, and the SPI value for the end of March 2005 should be calculated, the precipitation sum from January to March 2005 is compared to the precipitation sum from January to March during 1981–2010. If, based on this comparison, a negative precipitation deviation is detected in 2005, the SPI value takes a negative value, indicating a drier situation than normal. If a positive precipitation deviation is detected, the SPI value is positive, indicating a wetter situation than normal.

For this thesis, the SPI is used according to the study of Tschurr *et al.* (2020). As mentioned, a time scale of three months is used for a 30 year-long daily precipitation record from 1981–2010 and for the climate impact analysis for 2045–2074 respectively. A timescale of three months allows for the SPI to indicate more immediate impacts by reduced precipitation such as reduced soil moisture (World Meteorological Organization, 2012; Copernicus European Drought Observatory (ED0), 2020).

For the comparison of the SPI and maize yield data, the precipitation record has been fitted to a GEV distribution with the help of the ‘evd’ package (Stephenson, 2002). The SPI was then calculated with the ‘SCI’ package (Stagge *et al.*, 2015, 2016; Gudmundsson and Stagge, 2016). Unfortunately, the ‘SCI’ package only worked with the local time series. When calculating the SPI based on grid-data, the estimation of the maximum likelihood failed partially. Thus, for the SPI calculations based on grid-data, the gamma distribution was used with the help of the R package ‘SPEI’ (Beguería and Vicente-Serrano, 2023). The resulting SPI values based on the ‘SCI’ package with the GEV distribution, and the ‘SPEI’ package with the gamma distribution, were compared for randomly chosen grid-points, namely Lucerne, Zurich Kloten, Locarno Magadino and Pizol. Based on Spearman’s correlation coefficient ρ , the respective SPI values showed a very high similarity ($\rho > 0.98$). As the SPI values based on the different probability distributions were so similar, the SPI values for the comparison of ACI occurrence and maize yield data were not recalculated with a gamma distribution. It is nonetheless important to acknowledge this inconsistency, as it may still lead to small differences in the respective results.

The ACI SPI_m is defined as days with an SPI value below -1 , the ACI SPI_e indicates events with an SPI below -1.6 over at least seven consecutive days. These definitions are taken from the study of Tschurr *et al.* (2020). An SPI value below -1 indicates moderate dryness, SPI values of -1.5 to -1.99 indicate severe dryness (World Meteorological Organization, 2012). A small difference between the study of Tschurr *et al.* (2020) and this thesis is, that Tschurr *et al.* (2020) represent the number of days with an SPI below -1 as the percentage of days of the year or the vegetation period with an SPI value undergoing this threshold. In this thesis, the absolute number of days with an SPI value undergoing this threshold is illustrated instead.

4.2.5 Concurrent stress factors

Maize is often exposed to simultaneous or sequential abiotic stress factors in the field (Mittler, 2006; Rossini, Maddonni and Otegui, 2016; Hussain *et al.*, 2020; Shabbir *et al.*, 2022; Webber *et al.*, 2022). Concurrent stress can have a more drastic impact on the plant than the respective individual stress factors (Shabbir *et al.*, 2022; Webber *et al.*, 2022).

In this thesis, univariate ACIs of different stress categories are combined, leading to ACIs representing the number of days with concurrent drought and heat stress (SPIm & HS30, SPle & HS35), potential waterlogging and heat stress (HPE & HS30, HPE & HS35), drought and low temperature stress (SPIm & Frost Day, SPle & Frost Day) as well as potential waterlogging and low temperature stress (HPE & Frost Day). High temperature stress and low temperature stress was not combined due to the rarity of days with simultaneous maximum temperatures above 30 °C (HS30) and minimum temperatures below freezing point (Frost Day), as confirmed by the observational grid-data from 1981–2010.

4.3 Validating ACIs with maize yield data

In order to investigate how well ACIs can explain maize yield variation, the yearly number of ACIs between the 5th of May and 11th of October from 2003–2022 was estimated for each of the 12 included municipalities with the use of local time series by MeteoSwiss (MeteoSwiss and Federal Department of Home Affairs, 2015). Note that due to technical reasons, if a municipality included a lake, the lake area was also included in the respective local time series. For each of the 12 included municipalities the maize yield data was averaged as elaborated in chapter 3.1.

Next, Spearman's rank correlation coefficient between the yearly number of a single ACI and maize yield was calculated for each municipality. Some ACIs did not occur within the investigated time period, thus no correlation could be estimated for these ACIs.

Afterwards, a multiple linear regression model was fitted to all univariate ACIs and maize yield data in order to analyse how well variation in the yield data can be explained by the combination of all univariate ACIs. The multivariate ACIs were excluded in the latter calculation, since the multivariate ACIs are defined as a combination of univariate ACIs. If e.g. the multivariate ACI SPIm & HS30 was included in the multiple linear regression model, the occurrence of days with maximum temperatures above 30 °C could be overrepresented in the regression model as this is already included in the univariate ACI HS30. The calculation of Spearman's correlation coefficient and the fitting of the multiple linear regression model was both conducted with the help of packages that are part of R (R Core Team, 2023).

Finally, the relative importance of each univariate ACI for the variation of yield data was estimated by using the R package 'relaimpo' (Grömping, 2006). This function could however only be applied if there was enough data, meaning that ACIs that occurred in only one of the 20 years or less had to be excluded from this step. For this new selection of ACIs, another multiple linear regression model was fitted. For reasons of simplicity, this alternate regression model shall be referred to as 'relative importance model'.

4.4 Technical validation of ACI representation by the CH2018 grid-data

Before calculating the change in the average yearly number of ACIs and temporal standard deviation of yearly ACIs until mid-century respectively, a technical validation of the representation of ACIs by the CH2018 grid-data was necessary. This means, in essence, that it had to be assessed whether the simulation of the average as well as the standard deviation of the yearly number of ACIs by the climate models is realistic. This step is important, as it allows to quantify the influence of the limitations of the CH2018 data on the climate impact analysis (Kotlarski and Rajczak, 2018) and to sort out the ACIs that are not well enough represented by the CH2018 data. As mentioned in chapter 3.2.2, this step is especially important for the standard deviation of the yearly number of ACIs as well as the multivariate ACIs.

For this validation, the average yearly number of the ACIs as well as the standard deviation of their yearly occurrence during the fixed maize growing season during the reference period (1981–2010) was calculated. The same was done for the calculation of the growing degree days (GDD), which were elaborated in chapter 4.1. These calculations were first done based on the observational grid-data, and secondly based on each individual model chain of the CH2018 data based on the RCP 8.5 scenario. The RCP 8.5 scenario was chosen because it contains more model chains than the RCP 2.6 scenario. Moreover, as projections of an emission scenario start in 2005, the respective RCP 8.5 scenario and RCP 2.6 scenario of a given individual model chain coincide with each other for the time period between 1981–2004 (CH2018, 2018). Thus, the validation process was not repeated with the RCP 2.6 based model chains.

After these calculations, the average of the model chain simulations was calculated in order to get a mean estimate of ACI occurrence based on the CH2018 grid-data. Note that this is a small inconsistency to the CH2018 scenarios where the central estimate is based on the median of the model chains and also an upper and lower estimate is included (CH2018, 2018).

For the quantification of deviations between the CH2018 data and the observational data, the standardised root-mean-square error (RMSE) was used as a primary skill score in accordance with Tschurr *et al.* (2020). As explained in their study, the standardisation of the RMSE allows to compare this skill score between different ACIs of different units. The calculation of the standardised RMSE was done as followed:

$$RMSE = \sqrt{\frac{\sum((model(ACI)_{(i)} - obs(ACI)_{(i)})^2)}{Number\ of\ grid\ cells}}$$

$$Standardised\ RMSE = \frac{RMSE}{SD_{obs}}$$

Equation 2: Calculation of the standardised root-mean-square-error. Adapted from Tschurr et al. (2020).

Where $model(ACI)_{(i)}$ is the average or temporal standard deviation of the yearly number of a given ACI at a given grid-cell (i) based on CH2018 data and $obs(ACI)_{(i)}$ is the same but based on observational data. SD_{obs} is the spatial standard deviation of the respective ACI occurrence over Switzerland based

on observational data from the reference period 1981–2010. In accordance with the study of Tschurr *et al.* (2020), an ACI is defined as well represented by the CH2018 data if the standardised RMSE lies below 0.5. If the standardised RMSE is 0.5 or higher, the representation by the CH2018 data is defined as biased.

As a second skill score, Spearman’s correlation coefficient ρ was used to estimate the spatial correlation, i.e. the spatial similarity, between the observed and simulated average and standard deviation of the yearly number of ACIs. This coefficient is treated as a complementary skill score in order to evaluate whether ACIs with a standardised RMSE below 0.5 also show good results with a different skill score. If the correlation coefficient ρ has a value of at least 0.8, the relationship is defined as very strong (based on Akoglu, 2018).

If the standardised RMSE lies below 0.5 and Spearman’s correlation coefficient above 0.8, the ACI and the respective statistical parameter (here the average or the standard deviation) was included in the calculation for the time period 2045–2074.

4.5 Implementation of climate change impact analysis

To estimate the change in the occurrence of an ACI until mid-century – in other words the change signal of an ACI (CH2018, 2018) – the average of the yearly number of this ACI was calculated for mid-century based on the CH2018 grid-data for the RCP 2.6 scenario and for the RCP 8.5 scenario. For some ACI, this step was repeated for the standard deviation of the yearly number of that ACI, depending on the results of the technical validation elaborated in chapter 4.4. This leads to grid maps showing the average and, for some ACIs, the standard deviation of the yearly number of an ACI in mid-century respectively. The CH2018 data-based grid maps showing the occurrence of the respective ACI during the reference period was then subtracted from the grid-map for mid-century. This resulting grid map then showed the difference – or the change signal – of the average or standard deviation of the yearly number of a specific ACI between the reference period and mid-century. The climate impact analysis in this thesis was based on these estimated change signals. The R packages used to create these maps are listed in Appendix C.

In order to quantify the uncertainty of the climate impact analysis, a boxplot for each ACI was included showing the range of the climate model ensemble. Based on the change signal maps and the boxplots, it was estimated if and to what extent the occurrence of an ACI is expected to change until mid-century.

5 Results

5.1 Results of ACI validation with yield data

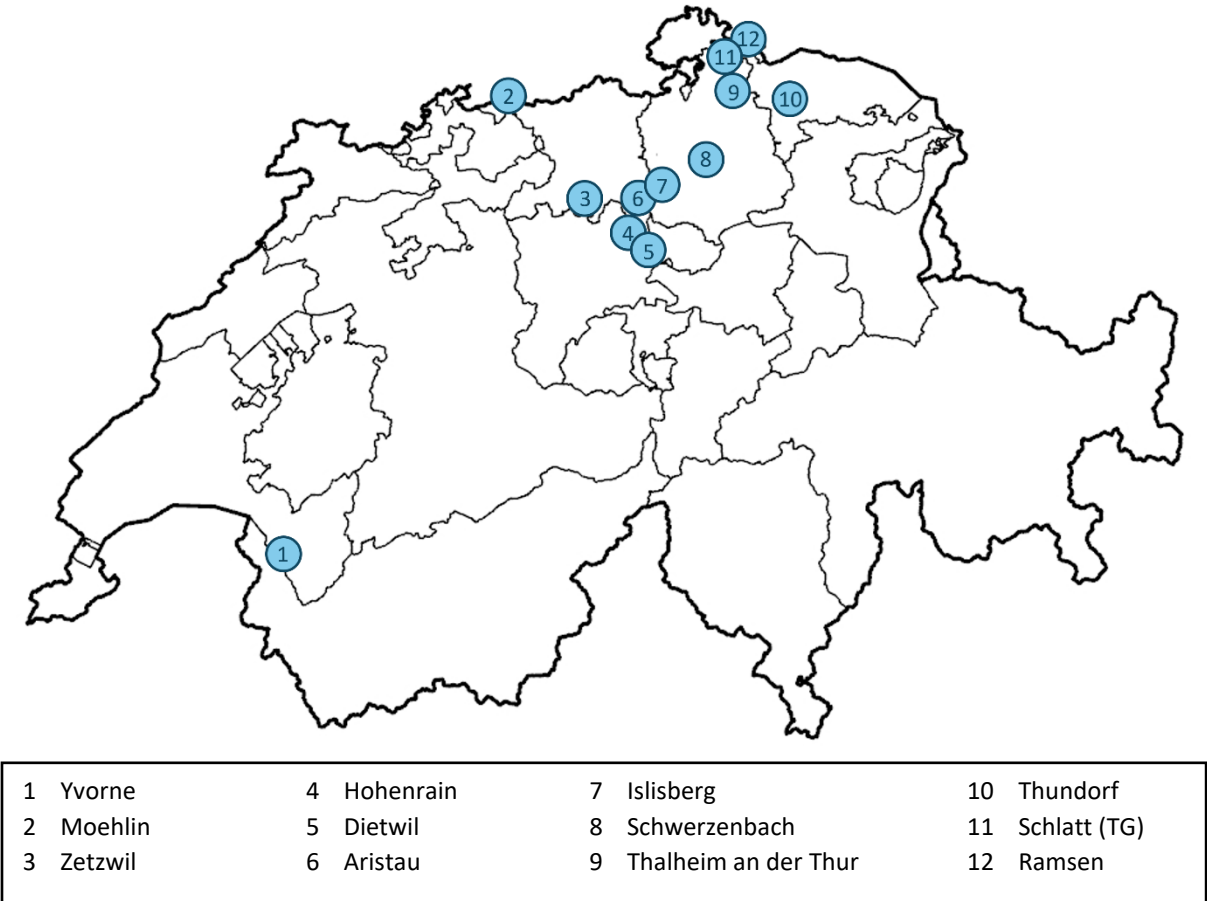


Figure 2: Overview of the municipalities from which the used maize yield data originated. Source of Swiss map: Federal Office of Topography swisstopo (2024)

In order to investigate to what extent ACIs can explain maize yield variation, the relationship between maize yield and the occurrence of ACIs was investigated based on Spearman’s correlation coefficient ρ and multiple linear regression models. An overview of the results for each individual municipality is available in Appendix A. Table 3 shows a summary of the correlation coefficients. Note that no correlation coefficients are available for ACIs that did not occur during the investigated time period, thus, the respective ACIs are not listed in Table 3. For a more detailed overview of the results, two significance levels are included, namely 0.05 and 0.1. Correlation coefficients with a p-value below 0.1 are defined as statistically significant.

Overall, the results include negative as well as positive relationships between maize yield and individual univariate ACIs. Negative correlations exist mainly between maize yield and the heat stress related ACIs HS30, HS35 and HS35sum, but also between the multivariate ACI SPI_m & HS30 and maize yield. For Schlatt (Nr. 11 in Figure 2, 18 yrs. with yield data) and Thalheim an der Thur (Nr. 9, 17 yrs.

with yield data), all three univariate heat stress related ACIs show a significant negative correlation with ρ between -0.41 and -0.61 (see also Appendix A.1), indicating a moderate correlation. Aristau (Nr. 6) is the only municipality showing a significant correlation between maize yield and the multivariate ACI SPI_m & HS30 with a correlation coefficient of -0.49 (p -value = 0.04 , 18 yrs. with yield data). While Schlatt (Nr. 11) and Thalheim an der Thur (Nr. 9) do show in comparison to the other municipalities a higher occurrence of HS30, HS35 and HS35sum (not listed in this thesis), there are also other municipalities with a high occurrence of these three ACIs. Moehlin (Nr. 2, 19 yrs. with yield data) for example, shows an even higher number of heat stress related ACIs. For this site however, only weak negative correlations with no statistical significance are visible.

For the drought-related ACIs SPI_m and SPI_e, no clear tendency towards positive or negative correlation is visible. The only statistically significant correlation is a positive correlation between SPI_m and maize yield in Dietwil (Nr. 5) with a correlation coefficient of 0.57 (p -value = 0.01 , 20 yrs. with yield data).

The potential waterlogging related ACI HPE as well as the low temperature stress related ACIs Frost Day, Frostsum and LT6 show no clear tendency towards positive or negative correlation either. While Yvorne (Nr. 1, 19 yrs. with yield data) shows a moderate but significant positive correlation between maize yield and Frost Days ($\rho = 0.43$, p -value = 0.07) and Frostsum ($\rho = 0.43$, p -value = 0.06) respectively, Schwerzenbach (Nr. 8) indicates a moderate but significant negative correlation between LT6 and maize yield ($\rho = -0.55$, p -value = 0.02 , 17 yrs. of yield data). For many municipalities, Frost Days were extremely rare and thus Frostsum very small between the 5th of May and the 11th of October. In some cases, these two ACIs did not occur at all within the investigated period. Moreover, the only multivariate ACIs that occurred in some of the municipalities during the defined growing season from 2003–2022 were the ACIs SPI_m & HS30 and SPI_m & Frost Day.

Table 3: Overview of Spearman's correlation coefficients ρ . Listed are the number of positive linear relationships ($\rho > 0$) and the respective number of correlation coefficients with a p -value < 0.1 and < 0.05 , and the number of negative linear relationships ($\rho < 0$) and the respective number of correlation coefficients with a p -value < 0.1 and < 0.05 .

ACI	$\rho > 0$	p-value		$\rho < 0$	p-value	
		< 0.1	< 0.05		< 0.1	< 0.05
HS30	4	–	–	8	2	1
HS35	1	–	–	9	3	2
HS35sum	1	–	–	9	2	2
Frost Day	3	1	–	4	–	–
Frostsum	3	1	–	4	–	–
LT6	7	–	–	5	1	1
HPE	5	–	–	7	1	–
SPI _m	7	1	1	5	–	–
SPI _e	5	–	–	6	–	–
SPI _m & HS30	3	–	–	9	1	1
SPI _m & Frost Day	3	–	–	3	–	–

Regarding the multiple linear regression models, for Moehlin (Nr. 2) the results indicate that the univariate ACIs can explain a significant amount of the variability in maize yield with an R^2 of 0.62 and an adjusted R^2 of 0.37 (p-value = 0.08, 19 yrs. with yield data). In the same municipality, the univariate ACIs that showed the highest relative importance for maize yield variation were the heat stress related ACIs (Figure 3). For Schlatt (Nr. 11), the multiple linear regression model shows an R^2 of 0.68 and an adjusted R^2 of 0.4 with a p-value of 0.104 (18 yrs. with yield data), which lies very slightly above the significance level of 0.1. The relative importance model on the other hand indicates an R^2 of 0.66 and an adjusted R^2 of 0.42 with a p-value of 0.07. In contrast to the multiple linear regression model, the relative importance model for Schlatt does not include the ACIs Frost Day and Frostsum, as the occurrence of these two ACIs was too low for them to be included in the relative importance model. For the remaining municipalities, neither the multiple linear regression models nor the relative importance models showed significant results (see Appendix A.2 and A.3).

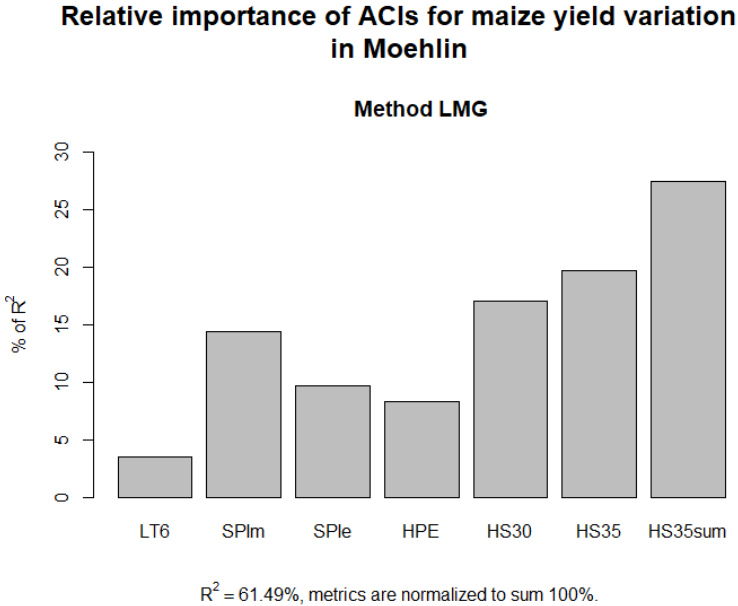


Figure 3: Relative importance of univariate ACIs for maize yield variation in Moehlin from 2003–2022

5.2 Results of technical validation of ACI representation by the CH2018 grid-data

The technical validation of the representation of the ACIs by the CH2018 data revealed that overall, the simulation of the average occurrence of univariate ACIs such as HS30, Frost Day and HPE is mostly similar to the observation. For these ACIs, the standardised RMSE lies below 0.5 and the correlation coefficient ρ mostly above 0.9 (Table 4). The same counts for the GDD with a standardised RMSE of 0.23 and a correlation coefficient of 0.97 (not listed in Table 4). However, for some ACIs, the simulation of the standard deviation (SD) of the yearly occurrence showed a standardised RMSE higher than 0.5 and thus, this statistical parameter for the respective ACI had to be excluded from the climate change impact analysis. This was for example the case for the ACIs HS35 and LT6 (Table 5). Moreover, while the average occurrence of the ACI SPIm is simulated well by the climate models, the validation shows a poorer result for the average as well as the standard deviation of the ACI SPle with a standardised RMSE of 0.6 and 0.67 respectively.

Multivariate ACIs partially showed a standardised RMSE above 0.5 and thus were excluded from further calculations. This concerns multivariate ACIs that include SPIe (e.g. the ACI SPIe & HS35), as well ACIs that occur very rarely, like the ACI HPE & HS30. According to the observations, the ACI HPE & HS35 has not occurred during the reference period, thus no correlation coefficient and RMSE value are available for this indicator, leading to an exclusion from the climate change impact analysis. However, the climate models are capable of simulating the occurrence of the multivariate ACIs SPIm & Frost Day and SPIm & HS30 realistically enough as well as the average occurrence of the ACI HPE & Frost Day.

Table 4: Results of the technical validation of the representation of ACIs by CH2018 data. This table includes all statistical parameters of an ACI with a standardised RMSE < 0.5 and Spearman's correlation coefficient $\rho > 0.8$. These ACIs are rated as well represented by the CH2018 data with respect to the listed statistical parameter.

ACI	Statistical parameter	Standardised RMSE	ρ
HS30	Average	0.10	0.99
	SD	0.17	0.98
HS35	Average	0.34	0.90
HS35sum	Average	0.43	0.90
	SD	0.44	0.89
Frost Day	Average	0.07	0.99
	SD	0.29	0.98
Frostsum	Average	0.07	0.98
	SD	0.25	0.98
LT6	Average	0.05	0.997
HPE	Average	0.21	0.95
	SD	0.32	0.93
SPIm	Average	0.36	0.94
SPIm & HS30	Average	0.39	0.93
	SD	0.48	0.92
SPIm & Frost Day	Average	0.37	0.97
	SD	0.37	0.97
HPE & Frost Day	Average	0.46	0.91

Table 5: Results of the technical validation of the representation of ACIs by CH2018 data. This table includes all statistical parameters of an ACI with a standardised RMSE ≥ 0.5 and their respective Spearman's correlation coefficient ρ . For these ACIs, the representation by the CH2018 data is defined as biased with respect to the listed statistical parameter.

ACI	Statistical parameter	Standardised RMSE	ρ
HS35	SD	0.51	0.90
LT6	SD	0.53	0.93
SPI_m	SD	0.53	0.89
SPI_e	Average	0.60	0.84
	SD	0.67	0.83
SPI_e & HS35	Average	0.86	0.39
	SD	0.87	0.39
HPE & HS30	Average	24.46	0.15
	SD	8.86	0.15
HPE & HS35	Average	-	-
	SD	-	-
SPI_e & Frost Day	Average	0.64	0.84
	SD	0.53	0.84
HPE & Frost Day	SD	0.52	0.91

It is important to emphasize that the calculation of the standardised RMSE and Spearman's correlation coefficient ρ is based on grid-data covering the entirety of Switzerland. If, however, one was to include only certain regions in the validation process, the results of the technical validation would differ, leading to a slightly different set of ACIs to be included in the climate change impact analysis. For example, the ACI SPI_m & Frost Day mainly occurs in elevated regions and occurs very rarely in low-lying regions during the defined growing season. When comparing the observational data with the CH2018 data, there are thus many regions in lower altitudes that push the skill scores to a good validation result (Figure 4, left). During the validation process, those low-lying regions were included, leading to a standardised RMSE of 0.37 for the average yearly number of this multivariate ACI. However, if only regions were included where this ACI occurs more often – for example regions that are too cold to cultivate early silage maize based on observational data (indicated by GDD < 1430 °C (Buzzi *et al.*, 2021)) (Figure 4, right) – the standardised RMSE would be 0.5, which would lead to an exclusion of this ACI. In this thesis, the validation is based on grid-data covering the entirety of Switzerland. In future research, it would be a possibility to include calculations for several regions in Switzerland and then consider the different results during the technical validation process.

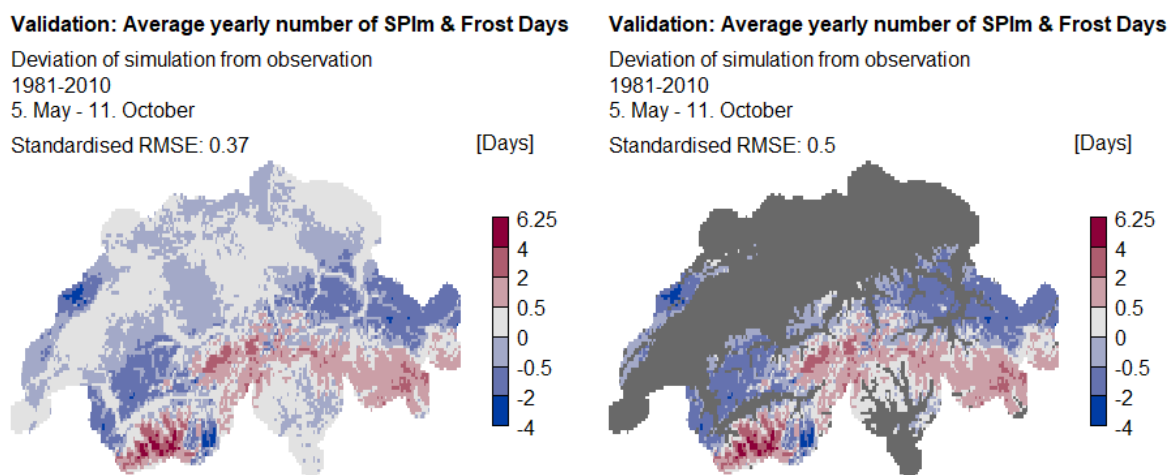


Figure 4: Left: Deviation in number of days of the simulated average yearly number of SPIm & Frost Days from the observed average yearly number of SPIm & Frost Days during the reference period. The standardised RMSE is 0.37. Right: Same deviation as on the left, but only for the regions with GDD < 1430 °C (GDD estimation based on observational data). Regions with GDD ≥ 1430 °C are coloured dark grey. The standardised RMSE in this case is 0.5.

5.3 Results of the climate impact analysis

Overall, the results of the climate impact analysis indicate that until mid-century heat stress as well as drought stress are expected to increase for maize, while low temperature stress is expected to decrease during the defined maize growing season (Figure 5). Heat stress (HS30, HS35, HS35sum) is expected to increase strongest in low altitudes, whereas low temperature stress (Frost Days, Frostsum, LT6) is expected to decrease strongest in higher altitudes. The number of days with an SPI below -1 (SPI_m), a threshold indicating moderate drought (World Meteorological Organization, 2012), is expected to increase for most regions based on the RCP 2.6 scenario. The RCP 8.5 scenario suggests an increase for all regions with a maximum increase mainly in western and northwestern Switzerland as well as in the central parts of the Plateau. For heavy precipitation events and thus for potential waterlogging (HPE), there is partially a very slight increase possible. However, the change signal is associated with large uncertainties, making it unclear whether the occurrence of this ACI is expected to change during the defined growing season until mid-century.

The change in the temporal standard deviation and thus in temporal variability often aligns with the change in the average occurrence of an ACI. This means if an ACI occurs on average more often in mid-century, the standard deviation often increases as well. The same counts vice versa for the cases where the occurrence of an ACI decreases until mid-century. However, there are some regional exceptions for the ACI Frost Day and the ACI SPI_m & Frost Day.

Regarding spatial variability, the change signal of temperature related ACIs is often more pronounced in the respective regions where the ACI already occurs most frequently during the reference period. Hence, the contrast of the spatial differences in the number of heat stress related ACIs is amplified to a certain extent. For the low temperature stress related ACIs Frost Day and Frostsum on the other hand the contrast is rather reduced.

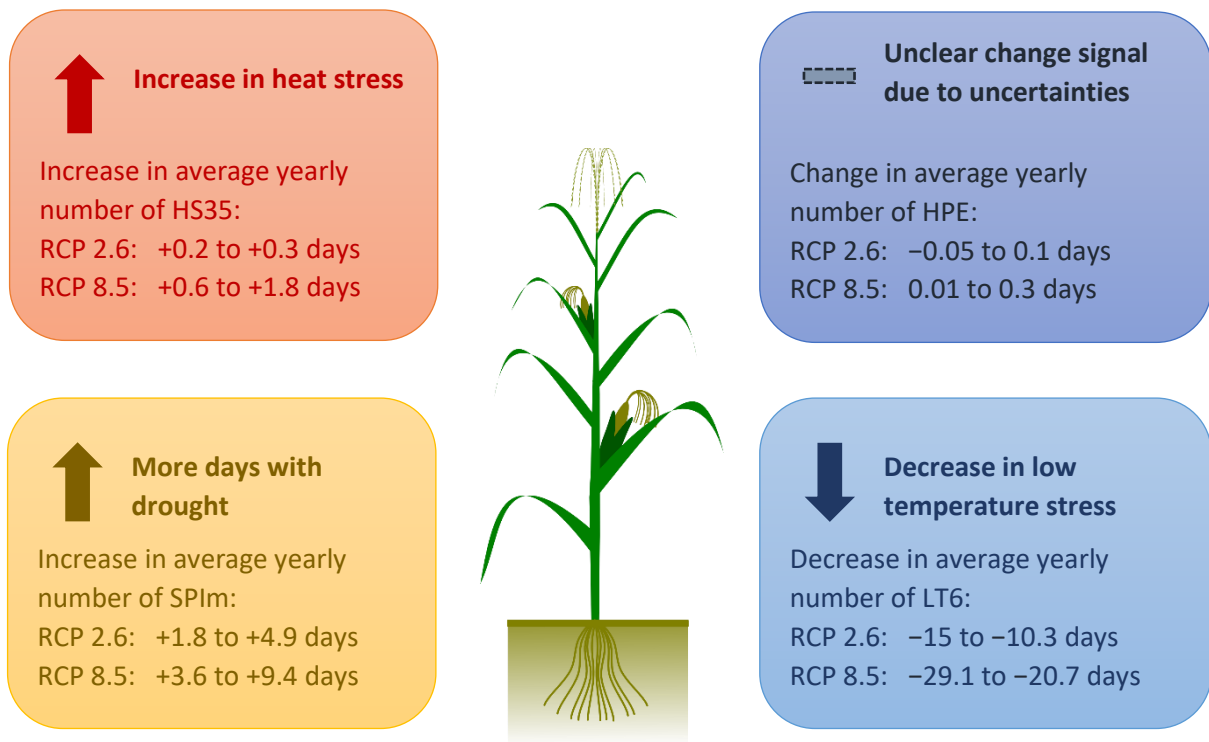


Figure 5: Overview of the main findings using selected ACIs as examples. The range of the change signal for a listed ACI represents the interquartile range of the change signal for the whole of Switzerland in the climate model ensemble. Source of the illustration of a maize plant: Pixabay (2013)

5.3.1 Change in growing degree days

Before elaborating the results of the climate impact analysis based on the individual ACIs, it is first shown in which regions the necessary growing degree days (GDD) for maize cultivation is reached in the present and in the future Swiss climate. This allows to consider in which regions maize cultivation could potentially occur based on GDD threshold exceedance (Buzzi *et al.*, 2021) when examining the maps showing the change signal of an ACI.

In the present Swiss climate, maize is usually cultivated below 500 to 900 m MSL (Buzzi *et al.*, 2021; Strickhof, 2023). Until mid-century, the RCP 2.6 as well as the RCP 8.5 scenario suggests, that the necessary GDD for maize cultivation – or more specifically for early grain maize (Buzzi *et al.*, 2021) – will be reached in more and in comparatively higher elevated regions, especially based on the RCP 8.5 scenario (Figure 6, bottom). The boxplots in Figure 6, representing the range of the climate model ensemble, underline the clear increase in the number of years with a GDD of at least 1600 °C until mid-century. Note that besides temperature, factors such as soil quality and restrictions in land use also determines whether maize can be cultivated (Holzkämper, Calanca and Fuhrer, 2013; Bundesamt für Landwirtschaft BLW, 2024). Nevertheless, these maps can give a first impression, in which regions maize could potentially be cultivated in mid-century, based on the GDD threshold exceedance.

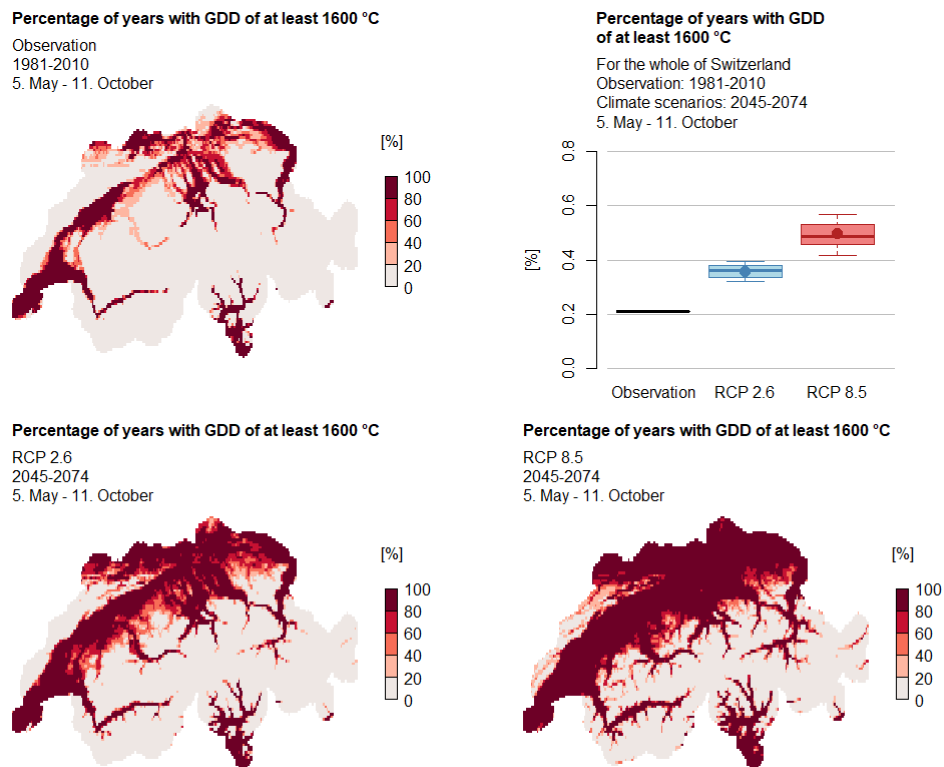


Figure 6: Top left: Percentage of years with GDD ≥ 1600 °C based on observational data during the reference period (1981–2010). Bottom: Same as top left but in mid-century for RCP 2.6 scenario (left) and RCP 8.5 scenario (bottom right). Top right: Average percentage of years with GDD ≥ 1600 °C for the whole of Switzerland during the reference period (black) and mid-century (blue & red). The boxplots show the range of the climate model ensemble. The box represents the interquartile range, the line the median and the point the average of the climate model ensemble.

In the following, the results for each individual ACI are discussed. Enlarged versions of the maps showing the occurrence of ACIs and the respective change signal is available in Appendix B.

5.3.2 Change in heat stress

Compared to the reference period 1981–2010, the average occurrence of all heat stress related ACIs show an increase until mid-century, especially based on the RCP 8.5 scenario (Figures 7 to 11). The RCP 2.6 scenario, however, shows only a slight increase for HS35 and HS35sum, with the boxplot indicating that the minimum of the range of the climate model ensemble exhibits almost the same value as the average of the observations. This indicates, that, based on the RCP 2.6 scenario, a slight increase in days with maximum temperatures above 35 °C is possible until mid-century compared to the reference period. However, the change signal may be trivial overall. As mentioned, the RCP 8.5 scenario shows a much clearer increase of all three ACIs. Note however, that the range of the change signal in the climate model ensemble for RCP 8.5 is also drastically bigger compared to the RCP 2.6 scenario, leading to higher uncertainty regarding the exact change signal.

According to the average estimate of the RCP 8.5 simulations, in low altitudes a widespread increase of 15 to over 35 days with maximum temperatures above 30 °C (HS30) (Figure 7, bottom right) and an increase of 1 to over 10 days with maximum temperatures above 35 °C (HS35) (Figure 9, bottom right)

is to be expected, depending on the region. Moreover, the sum of maximum temperature exceedance of 35 °C over the whole growing season (HS35sum) is expected to increase by about 5 to 24 °C in the lowest altitudes (Figure 10, bottom right). The change signal is usually strongest where the number of these three ACIs is already highest during the reference period, namely in low-lying regions in the Plateau, the Rhone Valley, Ticino and the Rhine Valley. It is interesting to note that while Ticino is one of the regions with the highest occurrence of HS30, the number of HS35 and HS35sum show a higher occurrence in the north of the Alps.

Unfortunately, the representation of the standard deviation of the yearly number of HS35 by the CH2018 data is biased (see chapter 5.2). This statistical parameter of HS35 is thus not included in the calculations for mid-century. The standard deviation of the yearly HS35sum on the other hand is well represented. Not only does the standard deviation indicate that in northwestern Switzerland the exceedance of 35 °C varies by several degrees Celsius during the reference period (Figure 11, top left), the standard deviation also increases even further until mid-century (Figure 11, bottom). In general, a widespread increase in standard deviation of HS35sum between 5 to 10 °C, locally even up to over 20 °C based on the RCP 8.5 scenario is expected in Switzerland (Figure 11, bottom right). Regarding the standard deviation of the yearly number of HS30, in the reference period, the values in the lower altitudes in the northern part of the Plateau often lie between 6 to 10 days (Figure 8, top left). In Ticino, standard deviations reach up to almost 14 days. Until mid-century, a widespread increase by about 2 to 4 days based on the RCP 2.6 scenario and about 4 to 10 days based on the RCP 8.5 scenario is expected (Figure 8, bottom). Note that according to the boxplot for RCP 8.5 the calculated average of the climate model ensemble showing the standard deviation of the yearly number of HS30 in mid-century is slightly higher than the calculated median (Figure 8, top right), and that the change signal maps are based on the average of the climate model ensemble.

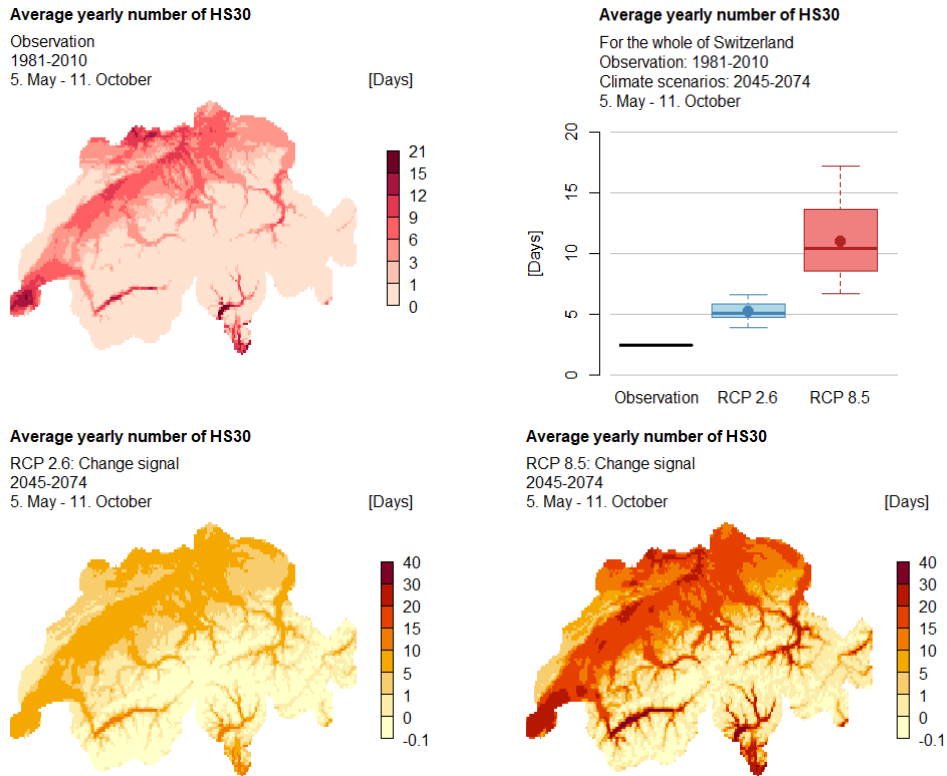


Figure 7: Top left: Average yearly number of HS30 based on observational data during the reference period (1981-2010). Bottom: Average of the change signal in number of days between the reference period and mid-century (2045-2074) for RCP 2.6 (left) and RCP 8.5 (right). Top right: Average yearly number of HS30 for the whole of Switzerland during the reference period (black) and mid-century (blue & red). The boxplots show the range of the climate model ensemble. The box represents the interquartile range, the line the median and the point the average of the climate model ensemble.

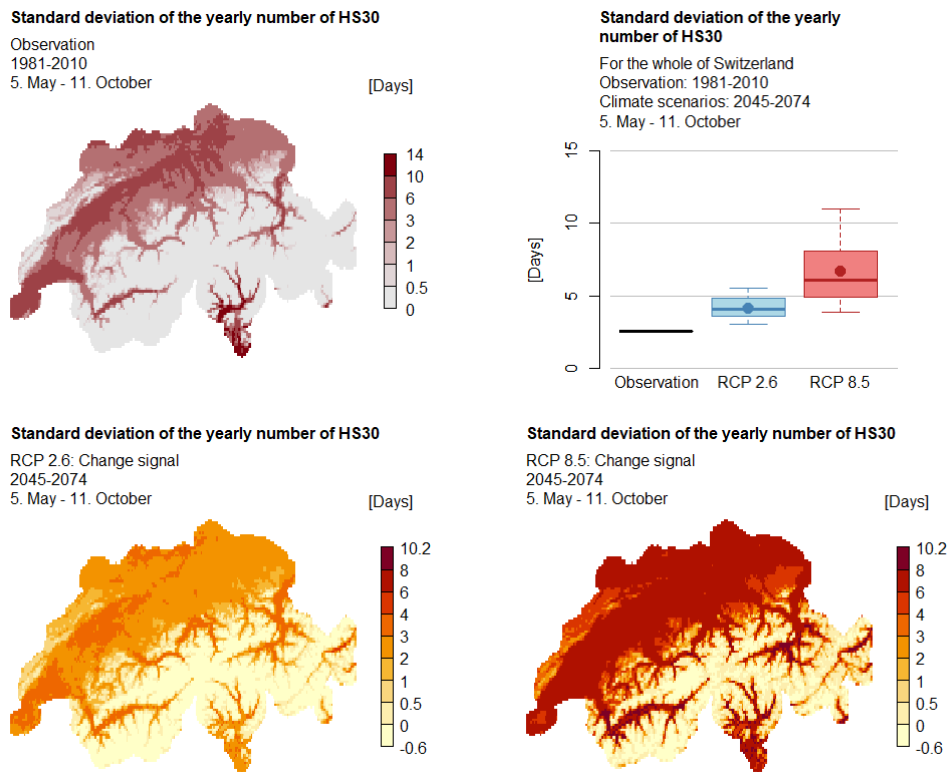


Figure 8: Top left: Standard deviation of the yearly number of HS30 based on observational data during the reference period (1981-2010). Bottom: Average of the change signal in number of days between the reference period and mid-century (2045-2074) for RCP 2.6 (left) and RCP 8.5 (right). Top right: Standard deviation of the yearly number of HS30 for the whole of Switzerland during the reference period (black) and mid-century (blue & red). The boxplots show the range of the climate model ensemble. The box represents the interquartile range, the line the median and the point the average of the climate model ensemble.

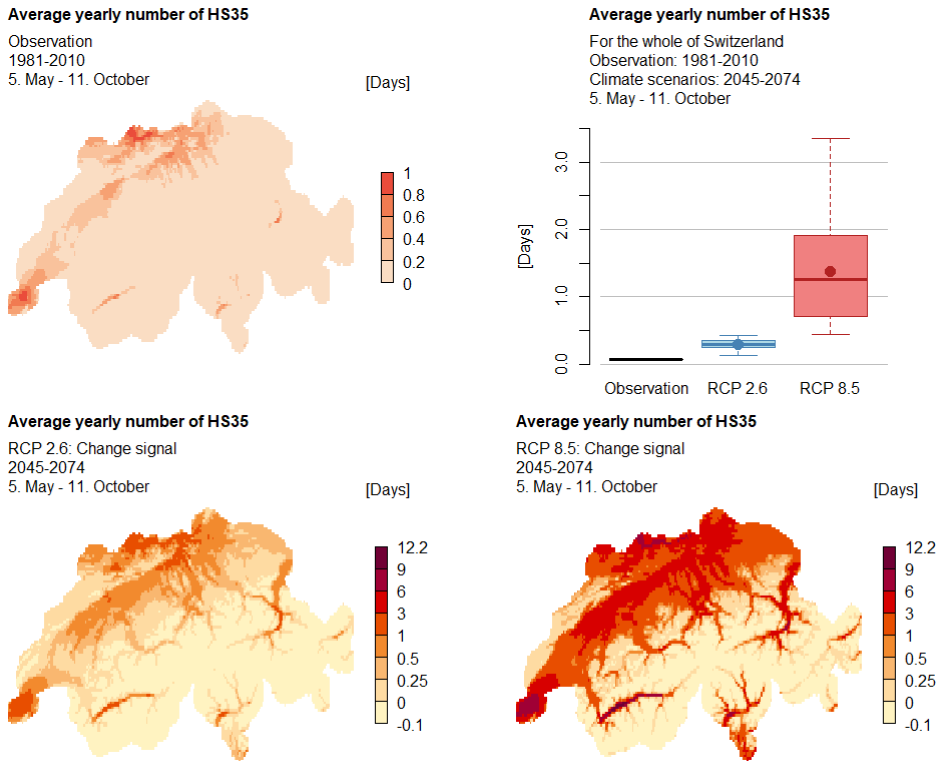


Figure 9: Top left: Average yearly number of HS35 based on observational data during the reference period (1981-2010). Bottom: Average of the change signal in number of days between the reference period and mid-century (2045-2074) for RCP 2.6 (left) and RCP 8.5 (right). Top right: Average yearly number of HS35 for the whole of Switzerland during the reference period (black) and mid-century (blue & red). The boxplots show the range of the climate model ensemble. The box represents the interquartile range, the line the median and the point the average of the climate model ensemble.

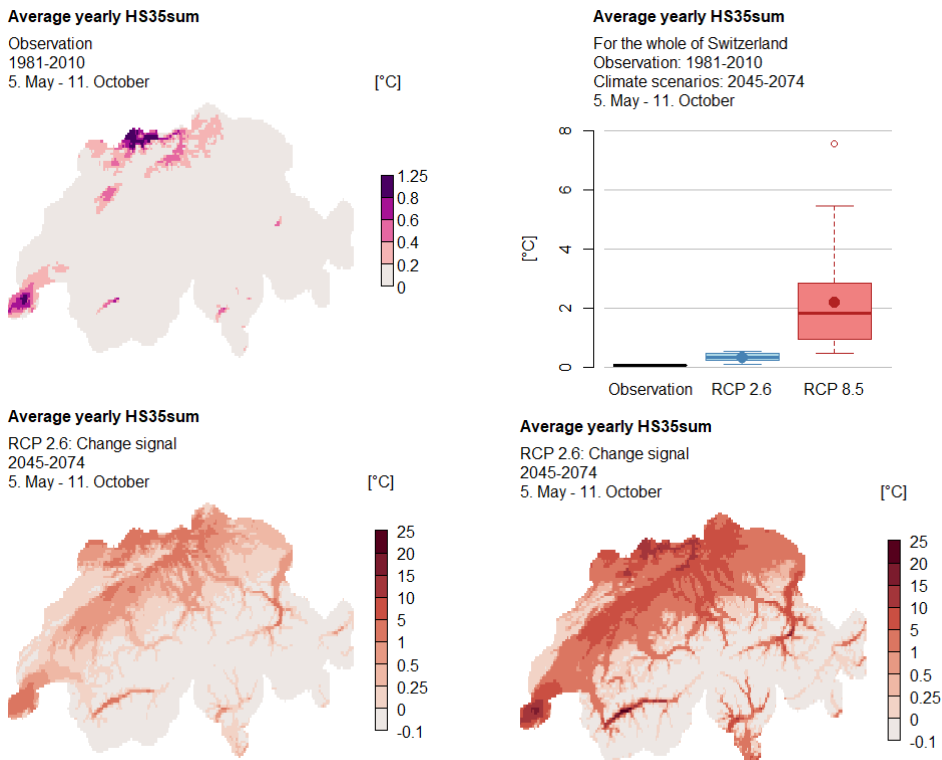


Figure 10: Top left: Average yearly HS35sum based on observational data during the reference period (1981-2010). Bottom: Average of the change signal in number of days between the reference period and mid-century (2045-2074) for RCP 2.6 (left) and RCP 8.5 (right). Top right: Average yearly HS35sum for the whole of Switzerland during the reference period (black) and mid-century (blue & red). The boxplots show the range of the climate model ensemble. The box represents the interquartile range, the line the median and the point the average of the climate model ensemble.

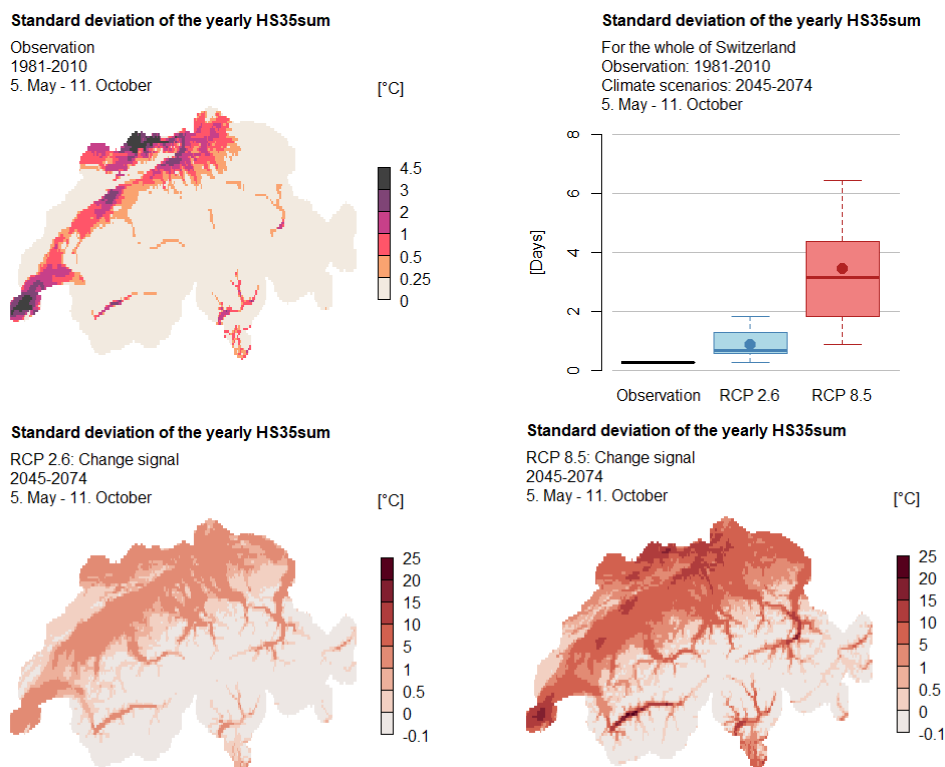


Figure 11: Top left: Standard deviation of the yearly HS35sum based on observational data during the reference period (1981–2010). Bottom: Average of the change signal in number of days between the reference period and mid-century (2045–2074) for RCP 2.6 (left) and RCP 8.5 (right). Top right: Standard deviation of the yearly HS35sum for the whole of Switzerland during the reference period (black) and mid-century (blue & red). The boxplots show the range of the climate model ensemble. The box represents the interquartile range, the line the median and the point the average of the climate model ensemble.

5.3.3 Change in low temperature stress

Compared to the reference period 1981–2010, the average number of all three low temperature stress related ACIs is expected to decrease until mid-century based on both scenarios – RCP 2.6 and RCP 8.5 (Figures 12 to 16). The negative change signal is strongest in high altitudes and especially in case of the ACIs Frost Day and Frostsum only very small in low altitudes.

The maximum range of the RCP 2.6 climate model ensemble for the standard deviation of the yearly number of Frost Days clearly exceeds the observation during the reference period (Figure 13, top right). This indicates uncertainties regarding the question if and to what extent the standard deviation of the yearly number of Frost Days for the whole of Switzerland decreases until mid-century based on the RCP 2.6 scenario. This is also the case for the simulated standard deviation of the yearly Frostsum based on the RCP 2.6 scenario (Figure 15, top right).

While overall the change signal for all three low temperature stress related ACIs is usually strongest in high altitudes, the climate models simulate only a very weak decrease in the average yearly number of LT6 until mid-century for parts of the Jungfrau region, southern Valais and for local sites in the upper Engadin (Figure 16, bottom). This is especially visible in the RCP 2.6 scenario. Moreover, the same sites show an increase of the standard deviation of the yearly number of Frost Days until mid-century (Figure 13, bottom).

Otherwise, with a decrease in average occurrence of the ACIs the standard deviation decreases as well, with the strongest decrease usually being where the standard deviation is highest during the reference period (Figures 13 and 15). For the regions of interest regarding potential maize cultivation (see chapter 5.3.1, Figure 6), the change signal for the ACIs Frost Days and Frostsum between the 5th of May and the 11th of October is mostly very small, as the number of days with minimum temperatures below 0 °C are often rare during the defined maize growing season (Figure 12 to 15). The change signal for the ACI LT6 is more pronounced in low altitudes as this ACI also occurs more often during the defined growing season (Figure 16). Thus, low temperature stress is expected to affect maize in low altitudes less during the here defined growing season in mid-century compared to the reference period.

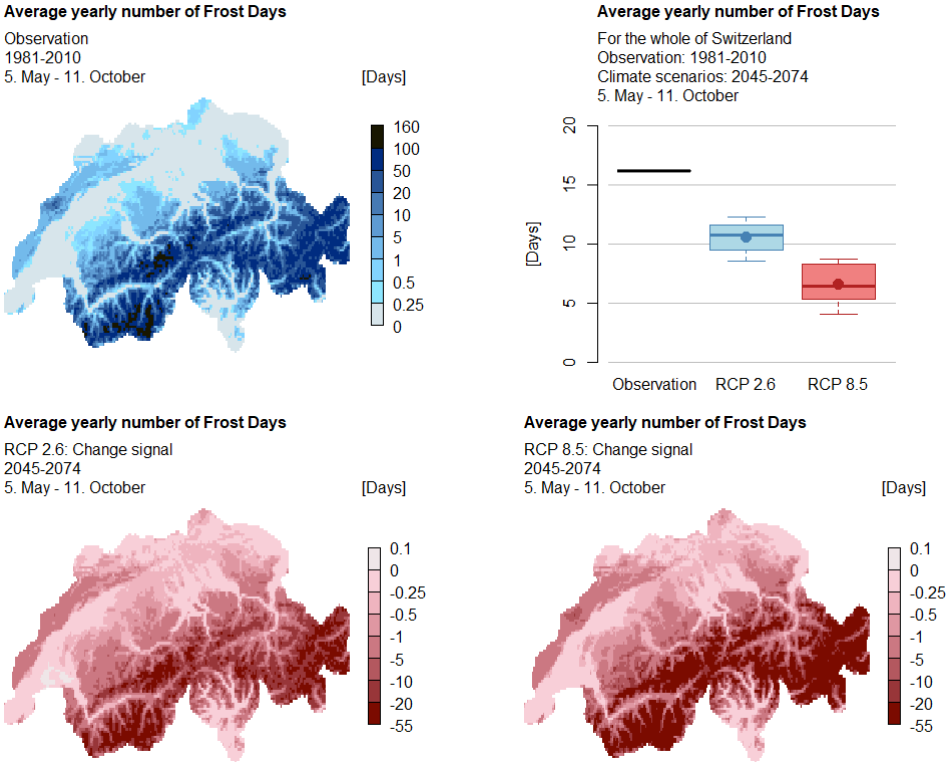
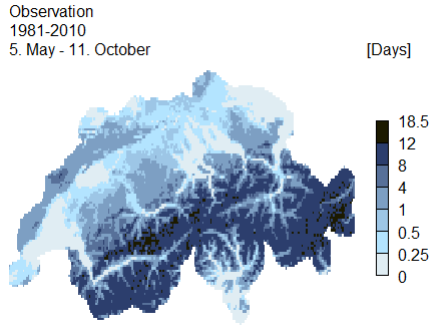
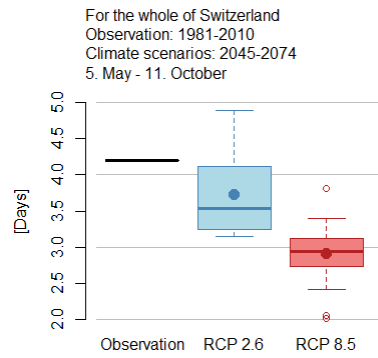


Figure 12: Top left: Average yearly number of Frost Days based on observational data during the reference period (1981-2010). Bottom: Average of the change signal in number of days between the reference period and mid-century (2045-2074) for RCP 2.6 (left) and RCP 8.5 (right). Top right: Average yearly number of Frost Days for the whole of Switzerland during the reference period (black) and mid-century (blue & red). The boxplots show the range of the climate model ensemble. The box represents the interquartile range, the line the median and the point the average of the climate model ensemble.

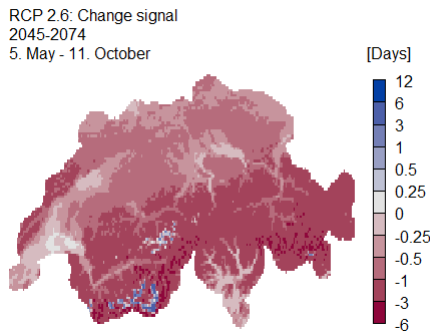
Standard deviation of the yearly number of Frost Days



Standard deviation of the yearly number of Frost Days



Standard deviation of the yearly number of Frost Days



Standard deviation of the yearly number of Frost Days

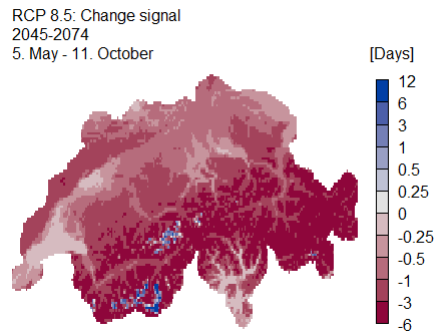
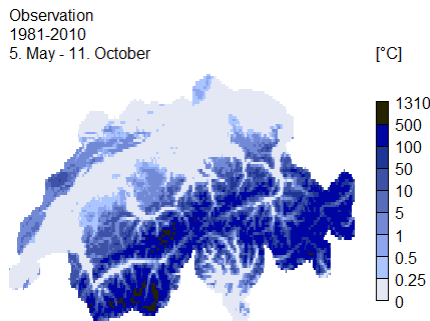
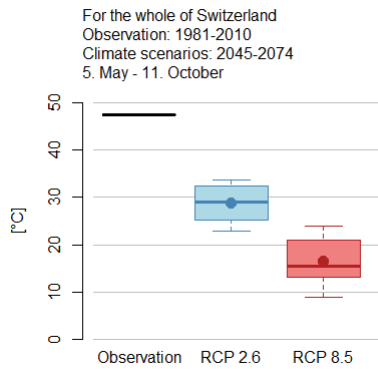


Figure 13: Top left: Standard deviation of the yearly number of Frost Days based on observational data during the reference period (1981-2010). Bottom: Average of the change signal in number of days between the reference period and mid-century (2045-2074) for RCP 2.6 (left) and RCP 8.5 (right). Top right: Standard deviation of the yearly number of Frost Days for the whole of Switzerland during the reference period (black) and mid-century (blue & red). The boxplots show the range of the climate model ensemble. The box represents the interquartile range, the line the median and the point the average of the climate model ensemble.

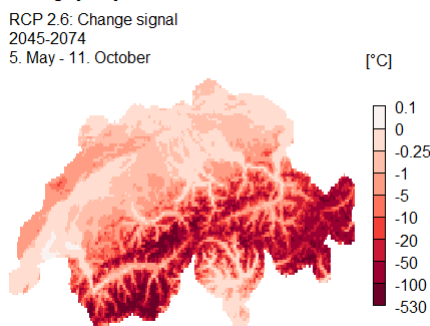
Average yearly Frostsum



Average yearly Frostsum



Average yearly Frostsum



Average yearly Frostsum

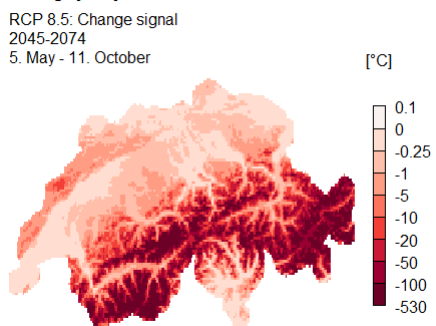
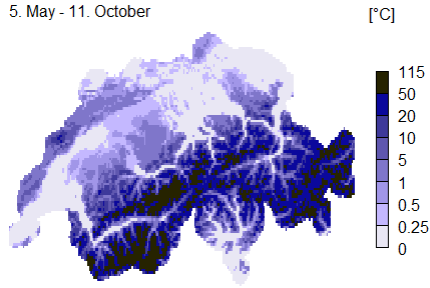


Figure 14: Top left: Average yearly Frostsum based on observational data during the reference period (1981-2010). Bottom: Average of the change signal in number of days between the reference period and mid-century (2045-2074) for RCP 2.6 (left) and RCP 8.5 (right). Top right: Average yearly Frostsum for the whole of Switzerland during the reference period (black) and mid-century (blue & red). The boxplots show the range of the climate model ensemble. The box represents the interquartile range, the line the median and the point the average of the climate model ensemble.

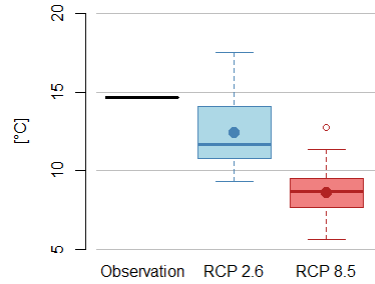
Standard deviation of the yearly Frostsum

Observation
1981-2010
5. May - 11. October



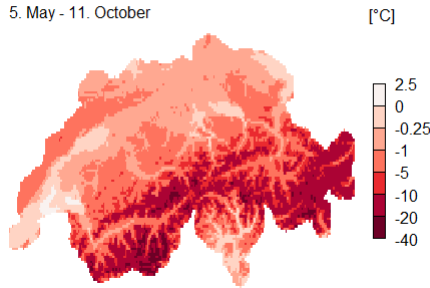
Standard deviation of the yearly Frostsum

For the whole of Switzerland
Observation: 1981-2010
Climate scenarios: 2045-2074
5. May - 11. October



Standard deviation of the yearly Frostsum

RCP 2.6: Change signal
2045-2074
5. May - 11. October



Standard deviation of the yearly Frostsum

RCP 8.5: Change signal
2045-2074
5. May - 11. October

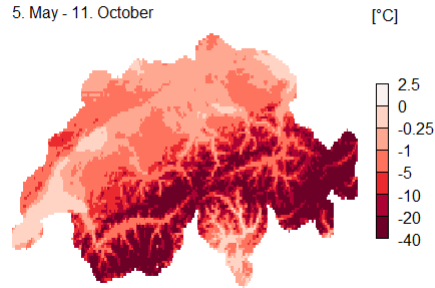
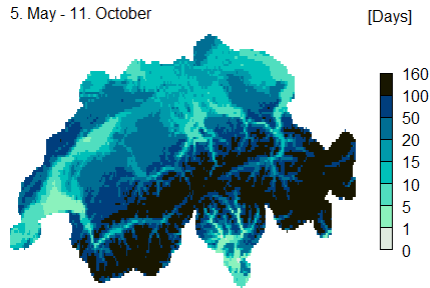


Figure 15: Top left: Standard deviation of the yearly Frostsum based on observational data during the reference period (1981-2010). Bottom: Average of the change signal in number of days between the reference period and mid-century (2045-2074) for RCP 2.6 (left) and RCP 8.5 (right). Top right: Standard deviation of the yearly Frostsum for the whole of Switzerland during the reference period (black) and mid-century (blue & red). The boxplots show the range of the climate model ensemble. The box represents the interquartile range, the line the median and the point the average of the climate model ensemble.

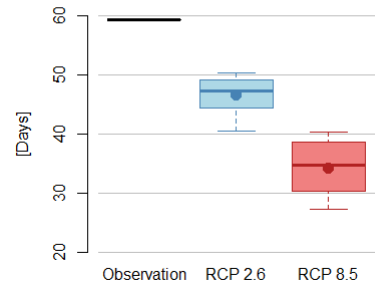
Average yearly number of LT6

Observation
1981-2010
5. May - 11. October



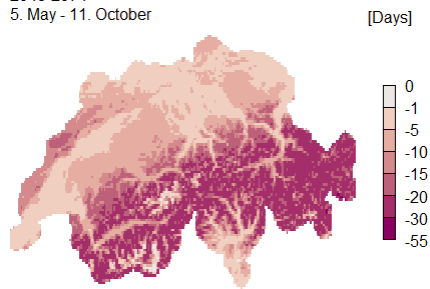
Average yearly number of LT6

For the whole of Switzerland
Observation: 1981-2010
Climate scenarios: 2045-2074
5. May - 11. October



Average yearly number of LT6

RCP 2.6: Change signal
2045-2074
5. May - 11. October



Average yearly number of LT6

RCP 8.5: Change signal
2045-2074
5. May - 11. October

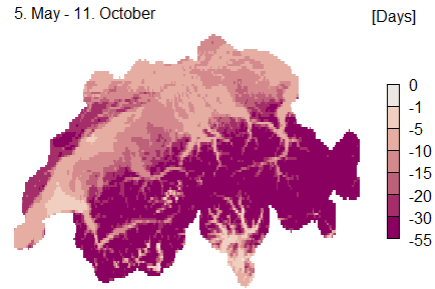


Figure 16: Top left: Average yearly number of LT6 based on observational data during the reference period (1981-2010). Bottom: Average of the change signal in number of days between the reference period and mid-century (2045-2074) for RCP 2.6 (left) and RCP 8.5 (right). Top right: Average yearly number of LT6 for the whole of Switzerland during the reference period (black) and mid-century (blue & red). The boxplots show the range of the climate model ensemble. The box represents the interquartile range, the line the median and the point the average of the climate model ensemble.

5.3.4 Change in potential waterlogging

During the reference period 1981–2010, the average number of HPE is quite low in most regions of the Plateau (Figure 17, top left). With an average around 0.25 to 0.75 days and sometimes even less, such an event occurs on average in a few years within a decade during the defined maize growing season. However, along the Alps this event occurs on average each year. This is especially the case for the central, southern and eastern Alps. The maximum average occurrence is in Ticino.

The change signal for the average yearly number of HPE until mid-century is quite uncertain. The average of the climate models suggests for most regions a very small increase, mainly in the central, southern and eastern Alps (Figure 17, bottom). However, not only is the change signal small, but according to the range of the climate model ensembles (Figure 17, top right) it is also uncertain whether there actually is an increase in the average yearly number of HPE to expect.

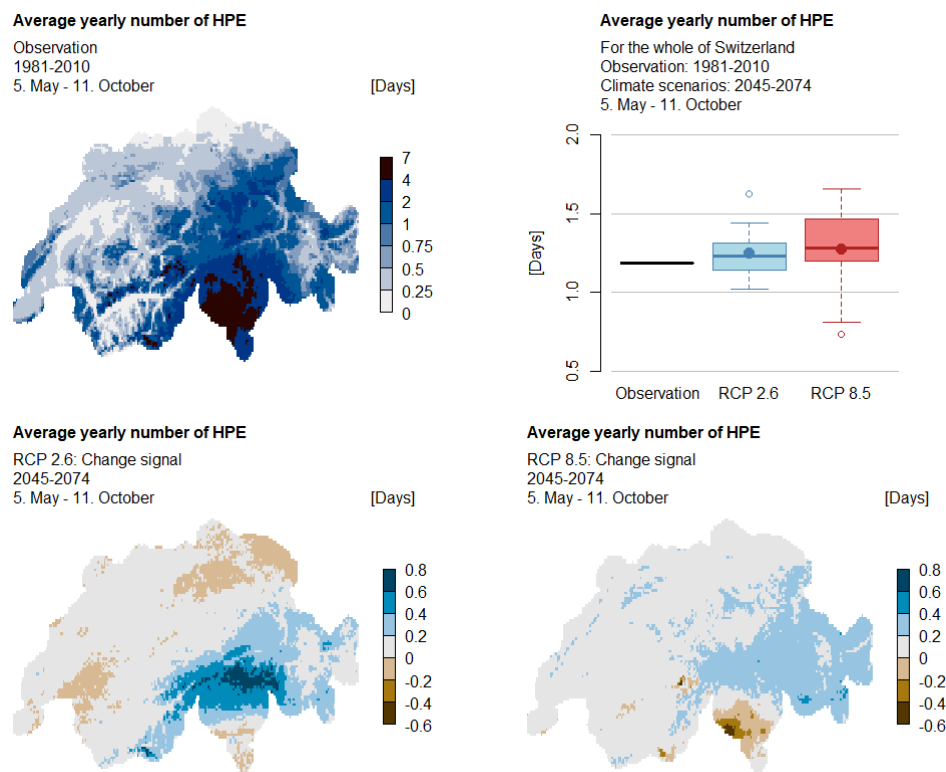


Figure 17: Top left: Average yearly number of HPE based on observational data during the reference period (1981-2010). Bottom: Average of the change signal in number of days between the reference period and mid-century (2045-2074) for RCP 2.6 (left) and RCP 8.5 (right). Top right: Average yearly number of HPE for the whole of Switzerland during the reference period (black) and mid-century (blue & red). The boxplots show the range of the climate model ensemble. The box represents the interquartile range, the line the median and the point the average of the climate model ensemble.

The standard deviation of the yearly number of HPE during the reference period is again highest in Ticino (Figure 18, top left). The change signal is once more associated with large uncertainties. The RCP 2.6 scenario suggests a very small increase mainly along the central, southern and eastern Alps, while indicating a very small decrease in parts of the Plateau and Prealps (Figure 18, bottom left). The RCP 8.5 scenario on the other hand shows the possibility of mainly increases in the Plateau and the eastern Alps (Figure 18, bottom right). However, the range of the standard deviation for a single grid cell in the climate model ensemble often exceeds 0.75 days (not illustrated), which is a rather high

range in relation to the small change signals, indicating relatively high uncertainties in the change signal. Moreover, the first quartiles of the climate model ensemble for RCP 2.6 and for RCP 8.5 lie below the observations during 1981–2010, while the third quartiles lie above the observations (Figure 18, top right). Hence, it is uncertain, whether and to what extent the standard deviation of the yearly number of HPE for the whole of Switzerland changes until mid-century.

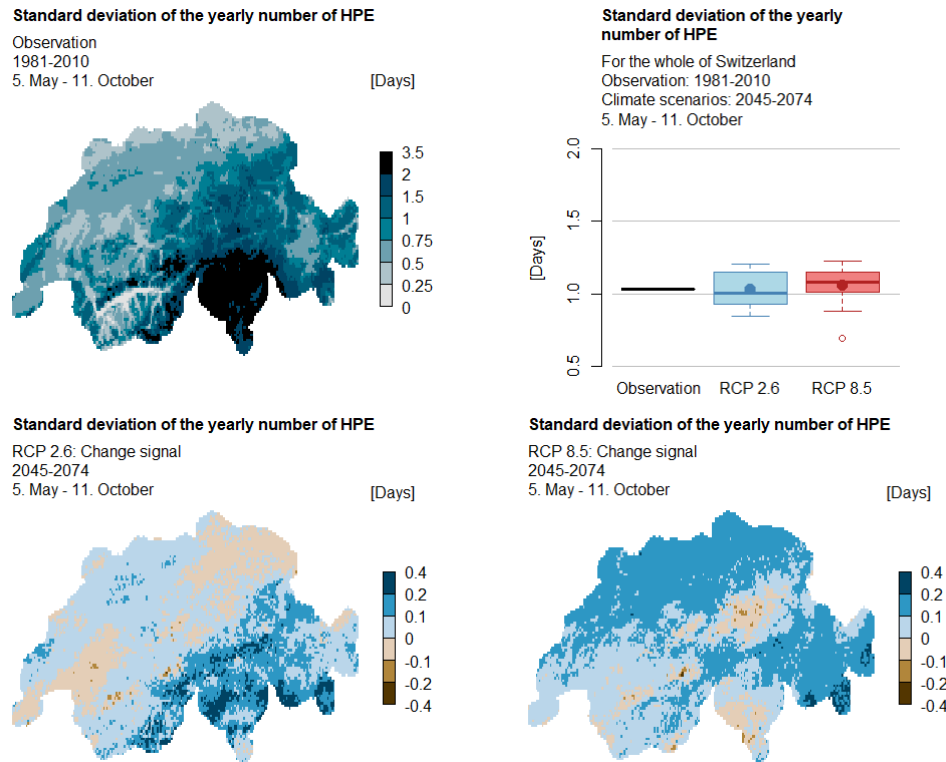


Figure 18: Top left: Standard deviation of the yearly number of HPE based on observational data during the reference period (1981-2010). Bottom: Average of the change signal in number of days between the reference period and mid-century (2045-2074) for RCP 2.6 (left) and RCP 8.5 (right). Top right: Standard deviation of the yearly number of HPE for the whole of Switzerland during the reference period (black) and mid-century (blue & red). The boxplots show the range of the climate model ensemble. The box represents the interquartile range, the line the median and the point the average of the climate model ensemble.

5.3.5 Change in drought

During the reference period, the maximum of the number of days with an SPI below -1 (SPI_m) is along the Jura, parts of the northern Plateau as well as in the Rhone Valley (Figure 19, top left). This means that in those sites a negative precipitation anomaly occurs more often. Along the Prealps for example, an SPI of smaller than -1 occurs less often.

Until mid-century, based on both climate scenarios an increase in the average yearly number of SPI_m is expected (Figure 19, bottom). The RCP 2.6 scenario shows a widespread increase by several days with a maximum positive change signal mainly along the Prealps, northeastern Switzerland and parts of the Engadin. Based on the RCP 8.5 scenario, for most parts of Switzerland an increase of about 3 to 9 days is expected. In the canton Grisons the increase is less pronounced. However, the climate model ensemble based on the RCP 8.5 scenario once more show a rather big range (Figure 19, top right),

indicating that the exact increase in the average yearly number of SPI_m for the whole of Switzerland is comparatively uncertain.

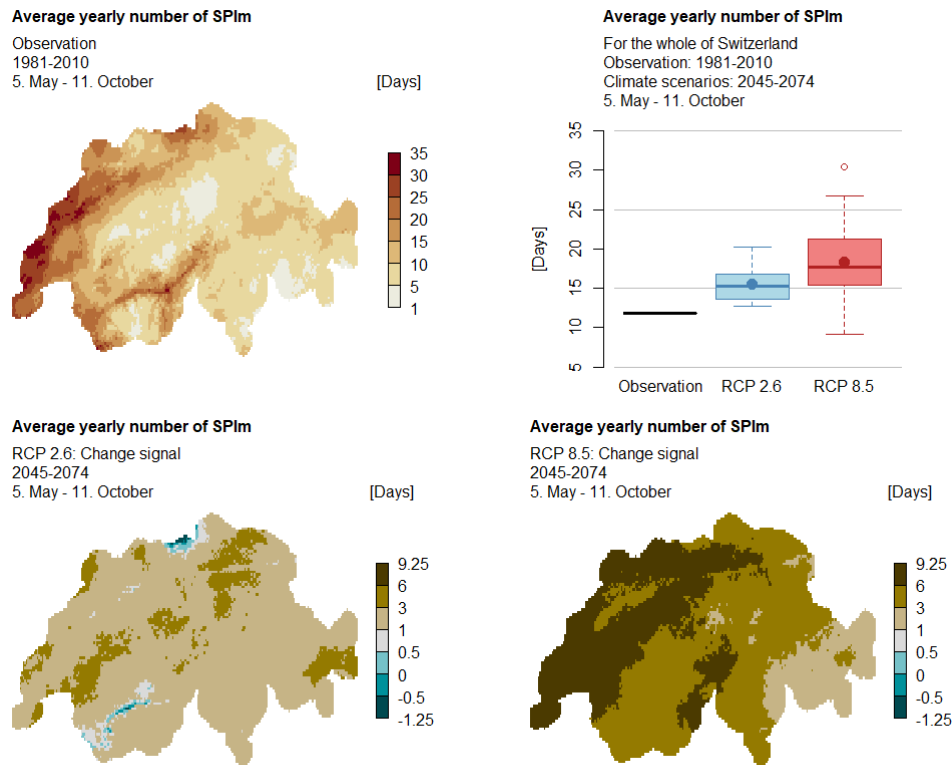


Figure 19: Top left: Average yearly number of SPI_m based on observational data during the reference period (1981-2010). Bottom: Average of the change signal in number of days between the reference period and mid-century (2045-2074) for RCP 2.6 (left) and RCP 8.5 (right). Top right: Average yearly number of SPI_m for the whole of Switzerland during the reference period (black) and mid-century (blue & red). The boxplots show the range of the climate model ensemble. The box represents the interquartile range, the line the median and the point the average of the climate model ensemble.

5.3.6 Change in concurrent stress

5.3.6.1 Drought & heat stress

Even though the individual average yearly number of the univariate ACI HS30 and the ACI SPI_m show an occurrence of several days during the growing season during the reference period (see chapters 5.3.2 and 5.3.5), the number of days for the multivariate ACI SPI_m & HS30 is quite small in comparison (Figure 20, top left). The maximum occurrence during the reference period is found in the northern, central and western part of the Plateau, as well as in the Rhone Valley and Ticino.

Until mid-century, an increase in the average yearly number of SPI_m based on both climate scenarios is expected. The RCP 2.6 scenario shows the highest increase in the average yearly number of SPI_m & HS30 in western Switzerland and in the Rhone Valley (Figure 20, bottom left). Ticino, however, showcases a lower occurrence of this ACI compared to the other regions with high occurrence of this ACI. The northern part of the Plateau does not show such a strong increase either. However, there a higher occurrence in absolute numbers (not illustrated) than in Ticino is still expected. Note that the increase is still only small and often lies between 0.5 and 1.5 days, depending on the region. Based on

the RCP 8.5 scenario, it is possible that until mid-century the average yearly number of SPI_m & HS30 increases by around 6 to locally over 12 days (Figure 20, bottom right). However, due to the large range of the climate model ensemble based on the RCP 8.5 scenario, those exact numbers need to be handled with care (Figure 20, top right).

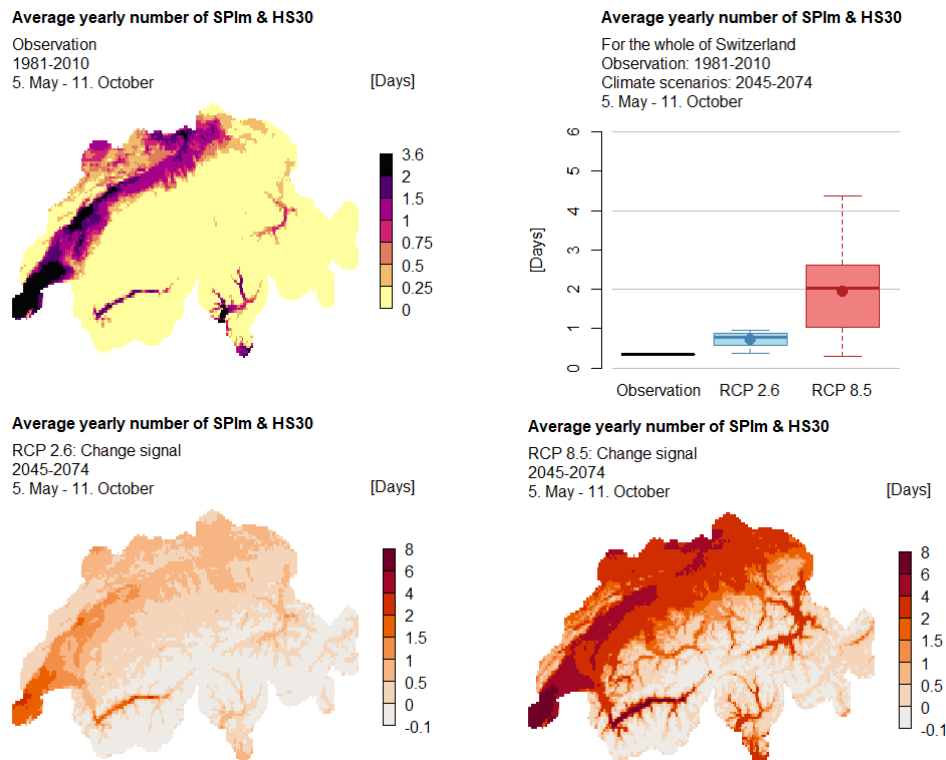


Figure 20: Top left: Average yearly number of SPI_m & HS30 based on observational data during the reference period (1981-2010). Bottom: Average of the change signal in number of days between the reference period and mid-century (2045-2074) for RCP 2.6 (left) and RCP 8.5 (right). Top right: Average yearly number of SPI_m & HS30 for the whole of Switzerland during the reference period (black) and mid-century (blue & red). The boxplots show the range of the climate model ensemble. The box represents the interquartile range, the line the median and the point the average of the climate model ensemble.

While the ACI SPI_m & HS30 shows a low occurrence during the reference period on average, the standard deviation shows values up to several days indicating a noticeable year-to-year variability (Figure 21, top left). During the reference period, the regions with the highest average occurrence also show the highest standard deviation with values around 6 to over 13 days. With an increase in the average occurrence, the temporal variability is expected to increase until mid-century as well (Figure 21, bottom). However, the RCP 8.5 scenario-based climate model ensemble once more shows a large range (Figure 21, top right).

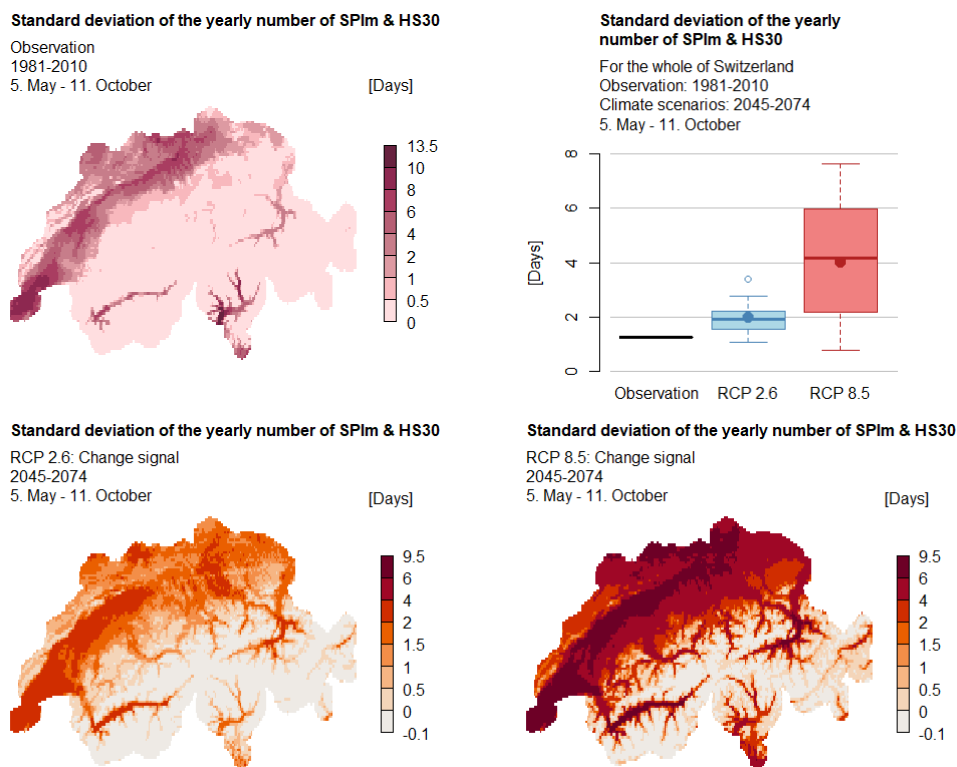


Figure 21: Top left: Standard deviation of the yearly number of SPIm & HS30 based on observational data during the reference period (1981-2010). Bottom: Average of the change signal in number of days between the reference period and mid-century (2045-2074) for RCP 2.6 (left) and RCP 8.5 (right). Top right: Standard deviation of the yearly number of SPIm & HS30 for the whole of Switzerland during the reference period (black) and mid-century (blue & red). The boxplots show the range of the climate model ensemble. The box represents the interquartile range, the line the median and the point the average of the climate model ensemble.

5.3.6.2 Drought & low temperature stress

During the reference period, the regions where the necessary GDD for grain maize is mostly reached (see chapter 5.3.1, Figure 6) experience on average very rarely days with simultaneous moderate drought and minimum temperatures below 0 °C (SPIm & Frost Days) between the 5th of May and 11th of October (Figure 22, top left). Therefore, the change signal based on both climate scenarios is very weak in these regions (Figure 22, bottom). The RCP 8.5 scenario shows a clear change in the number of SPIm & Frost Day until mid-century in the Alps with a widespread decrease of –1 to –4 days, even more locally. Only some local sites in the southern Valais show a slight increase. The RCP 2.6 also shows in comparison to the RCP 8.5 scenario a smaller decrease until mid-century. However, for some regions in Grisons, in the Jungfrau region and southern Valais, a slight increase in the number of SPIm & Frost Days is indicated. The extent to which this ACI decreases based on this scenario is rather uncertain, as the third quartile of the climate model ensemble for the average for the whole of Switzerland is slightly higher even than the observed average during the reference period (Figure 22, top right).

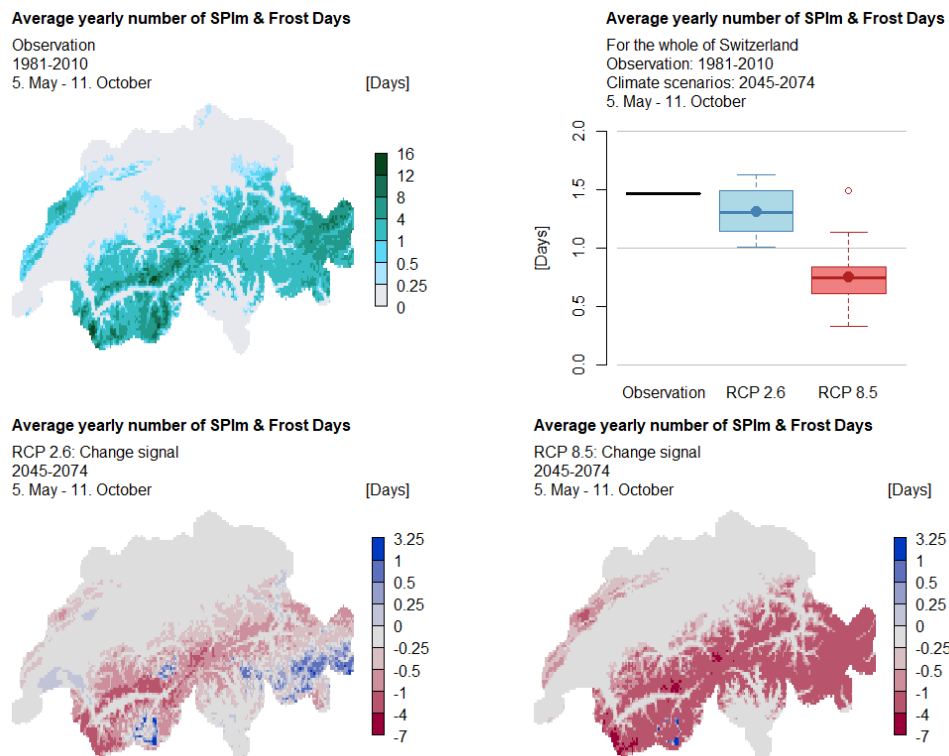


Figure 22: Top left: Average yearly number of SPIm & Frost Days based on observational data during the reference period (1981-2010). Bottom: Average of the change signal in number of days between the reference period and mid-century (2045-2074) for RCP 2.6 (left) and RCP 8.5 (right). Top right: Average yearly number of SPIm & Frost Days for the whole of Switzerland during the reference period (black) and mid-century (blue & red). The boxplots show the range of the climate model ensemble. The box represents the interquartile range, the line the median and the point the average of the climate model ensemble.

With the decrease in the average yearly number of SPIm & Frost Day, the standard deviation decreases as well (Figure 23, bottom and top right). Based on the RCP 2.6 scenario, the sites in southern Valais that show an increase in the average ACI occurrence also showcase an increase in the standard deviation. Other than that, based on both climate scenarios most regions show a decrease in the standard deviation of the yearly number of SPIm & Frost Day despite the potential increase in average occurrence, as is the case e.g. in Grisons (Figure 22, bottom). The RCP 8.5 scenario is clearer on a widespread decrease in temporal variability.

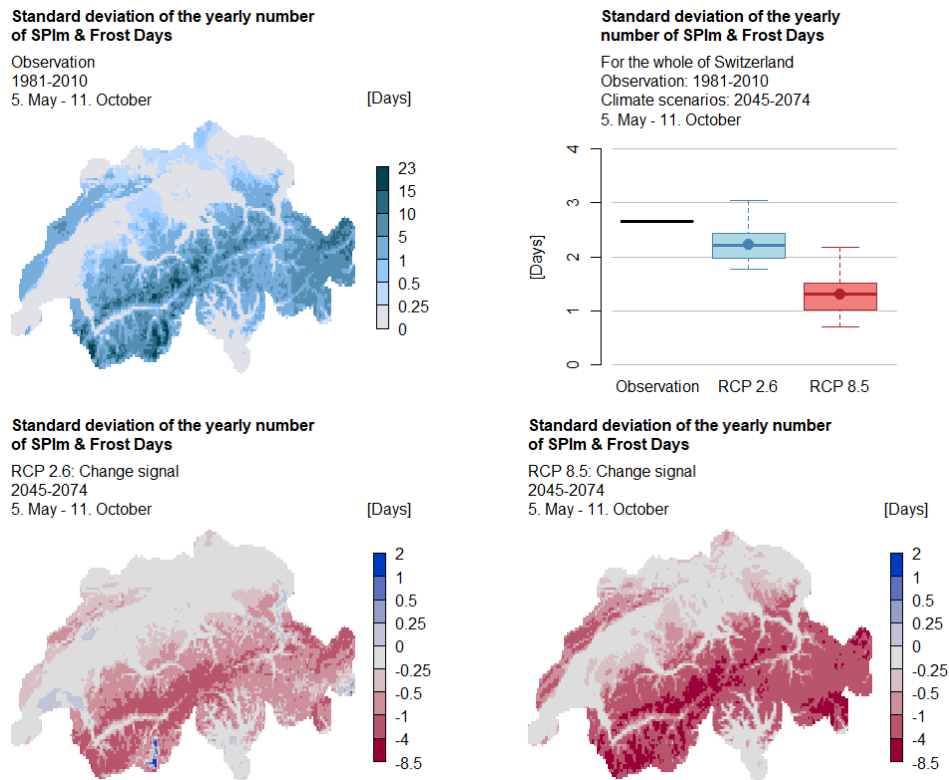


Figure 23: Top left: Standard deviation of the yearly number of SPIm & Frost Days based on observational data during the reference period (1981-2010). Bottom: Average of the change signal in number of days between the reference period and mid-century (2045-2074) for RCP 2.6 (left) and RCP 8.5 (right). Top right: Standard deviation of the yearly number of SPIm & Frost Days for the whole of Switzerland during the reference period (black) and mid-century (blue & red). The boxplots show the range of the climate model ensemble. The box represents the interquartile range, the line the median and the point the average of the climate model ensemble.

5.3.6.3 Potential waterlogging & low temperature stress

During the reference period, the ACI HPE & Frost Day mainly occurs in the Alps (Figure 24, top left) and in regions that are based on the small growing degree days sum not suitable for grain maize (Figure 6). In those sites, on average about 0.5 to locally almost 7 days per growing season with the ACI HPE & Frost Day occurred.

Since this ACI mainly occurs along the Alps, these are also the only regions that partially show a clear decrease until mid-century, with the change signal being a bit stronger and more widespread in the RCP 8.5 scenario compared to the RCP 2.6 scenario (Figure 24, bottom). Because there are many other regions in Switzerland where this ACI occurs rarely and thus can only show a small change signal until mid-century, the average occurrence for the whole of Switzerland during the reference period as well as in mid-century is very small, as illustrated by the boxplots in Figure 24.

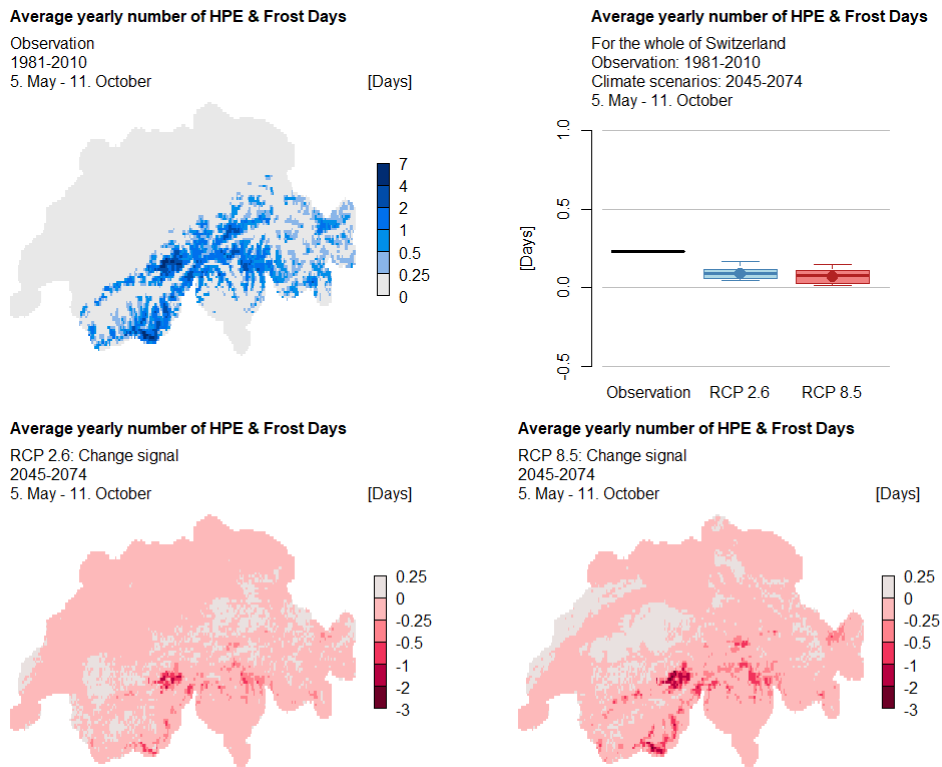


Figure 24: Top left: Average yearly number of HPE & Frost Days based on observational data during the reference period (1981-2010). Bottom: Average of the change signal in number of days between the reference period and mid-century (2045-2074) for RCP 2.6 (left) and RCP 8.5 (right). Top right: Average yearly number of HPE & Frost Days for the whole of Switzerland during the reference period (black) and mid-century (blue & red). The boxplots show the range of the climate model ensemble. The box represents the interquartile range, the line the median and the point the average of the climate model ensemble.

6 Discussion

6.1 Relationship between maize yield and ACI occurrence

This thesis shows that despite the small used maize yield data set there is often a negative relationship between heat stress related ACIs and maize yield visible. This indicates that the chosen heat stress related ACIs can, in some cases also to a significant extent, explain a part of maize yield variation. However, for some individual univariate ACIs, Spearman's correlation coefficient showed for some municipalities a positive relationship between them and maize yield, while showing a negative relationship for other municipalities. Moreover, only a few of these relationships were statistically significant.

A possible explanation for these partially quite different correlation coefficients is that within a municipality, sometimes different farms have reported their maize yield data for a different number of years, often leading to a relatively big variance in maize yield per municipality. Another potential reason is that some ACIs only occurred very rarely in the chosen municipalities, such as the ACI Frost Day and the multivariate ACI SPIm & Frost Day. Additionally, the calculated ACI occurrence is based on local time series, which are associated with uncertainties in the representation of small-scale climate effects like cold air pools (see chapter 3.2.1) (MeteoSwiss and Federal Department of Home Affairs, 2021a, 2021c). It is also important to acknowledge that the number of ACIs was estimated within a fixed growing season, whereas the effective growing season length may differ due to climatological conditions (Holzkämper, Calanca and Fuhrer, 2013). This means that in some cases, the estimated number of ACIs may differ to some extent from the number of ACIs that the maize plants actually experienced in those respective years. This is especially possible for low temperature stress related ACIs that occur more often in spring and autumn than in summer (MeteoSwiss, 2024a). However, the assumption of a fixed sowing and harvesting date made it possible to directly compare the number of ACI during the reference period to the number of ACI in mid-century without having to consider the influence of differences in the sowing date and length of the growing season. For reasons of continuity, the fixed growing season was also used for the validation process with maize yield data. Finally, a possible reason for the differences in the resulting correlation coefficients, and that only a few multiple linear regression models can explain maize yield variation to a significant extent, are mitigation measures by farmers. If, for example, there was a moderate drought indicated by the ACI SPIm, farmers can irrigate their fields in order to prevent yield loss (Meuli, 2020). Another possibility is that some farmers could have been cultivating more heat tolerant maize genotypes in comparison to others. This may explain the weak and statistically insignificant Spearman's correlation coefficient between heat stress related ACIs and maize yield from the municipality Moehlin (see Appendix A.1).

There are several different possible ways to compare the occurrence of indicators with maize yield data, with some methods being more refined, but also demanding much more capacity and investment. Mathieu and Aires (2018) for example aimed to evaluate which weather inputs are most suitable for their crop yield forecast model by evaluating the covariance between corn yield and two weather inputs with a 2-input linear model and repeating this step until they had enough suitable inputs for their yield forecast model. After collecting the suitable weather inputs, a cross validation

process based on several criteria, like correlation with yield anomalies and the Akaike Information Criterion, was applied to define what number of inputs is most suitable for the model. Another example is illustrated in the study by Holzkämper, Calanca and Fuhrer (2013), in which Willmott's index of agreement was used to validate how well their estimated climate indicators-based suitability score for maize corresponded with maize yield variability.

This thesis indicates that even with simpler methods, a moderate but significant relationship is visible between heat stress related ACIs and maize yield. It is thus possible, that the impact of heat stress on maize yield may be more difficult to mitigate in comparison to e.g. drought. In fact, Lobell and Field (2007) estimated the change in global crop production and concluded that there is a clear negative response of global maize yield to increasing temperature.

6.2 Impact of climate change on maize cultivation

Overall, the average occurrence of most ACIs is expected to change until mid-century, especially based on the RCP 8.5 scenario. Without climate mitigation, particularly heat stress is projected to increase strongly until mid-century. Without adaptation measures, like using more heat resistant maize genotypes, maize development is likely to be negatively affected by high maximum temperatures, which may lead to reduced maize yield. With the change in the average occurrence of ACIs, the temporal variability represented by standard deviation is expected to change as well. In most cases, an increase in average occurrence comes with an increase in standard deviation and vice versa. The contrast in the spatial differences of ACI occurrence is in the case of heat stress related ACIs to some extent amplified, and in the case of the ACIs Frost Day and Frostsum rather reduced.

It is important to note that the ideal threshold for an ACI representing stress for maize depends on the respective maize genotype (Sánchez, Rasmussen and Porter, 2014; Holzkämper and Fuhrer, 2015; Waqas *et al.*, 2021). In Switzerland alone, several different maize varieties are recommended for cultivation; in 2023, Agroscope recommended a total of over 60 maize varieties for Switzerland (Hiltbrunner *et al.*, 2023). Thus, this should be kept in mind when using those results to evaluate climatological challenges in maize cultivating in Switzerland. In fact, Parent *et al.* (2018) state that maize yield may even increase in Europe until 2050 if farmers keep adapting their maize cultivation by using different maize genotypes and adapting the sowing date. Smit and Skinner (2002) also emphasize that the vulnerability of farms to climate change related risks can be reduced by adaptation measures. The same authors elaborate that there are several adaptation options, including adaptation in production practices as well as adaptations on financial and technological levels, like buying more crop insurance or developing new maize varieties that are more resistant to climatological stress.

Furthermore, for this thesis the climatological variables temperature and precipitation have been used. However, factors such as solar radiation, CO₂ concentrations, wind, air moisture, soil moisture and nutrients influence maize development as well (Suzuki *et al.*, 2014; Shabbir *et al.*, 2022; Webber *et al.*, 2022). Moreover, concurrent stress factors are very relevant for maize cultivation, but the interaction between the multiple stress factors can be complicated and the impact of such are not necessarily additive (Webber *et al.*, 2022). While this thesis suggests an increase of concurrent heat and drought stress, estimating to what extent such an event would decrease the climate suitability for

maize as e.g. Holzkämper, Calanca and Fuhrer (2013) did in their study, would be a research topic for a different study. In the following, the results of each stress category are discussed in more detail.

6.2.1 *Estimated change in heat stress*

In general, especially in the regions where the GDD threshold of 1600 °C is most often reached, heat stress will occur on average more often between the 5th of May and the 11th of October. Especially in the lowest altitudes of the Plateau, as well as in the Rhone Valley, Ticino, and the Rhine Valley, heat stress is likely to be an increasingly limiting factor for maize cultivation without adaptation measures. This also corresponds to the results in the study by Holzkämper and Fuhrer (2015), who discuss that an increase in heat stress leads to a reduction in climate suitability for maize in low altitudes – partially also because due to the higher temperatures, maize development is accelerated and thus leads to reduced maize yield. However, the same authors also mention that in elevated regions on the other hand, climate suitability for maize increases until mid-century.

The change in standard deviation suggests an increase in temporal variability in heat stress until mid-century, again especially in the lowest altitudes. Even though the climate model ensemble for the RCP 8.5 scenario shows a high range for the calculated standard deviation of heat stress related ACIs, the median and average of the climate model ensemble still show a clear increase. For maize cultivation in low altitudes, a change to a more heat tolerant maize genotype may be helpful in mitigating the impact of climate change (Holzkämper and Fuhrer, 2015; Waqas *et al.*, 2021). Moreover, sowing earlier in the year may allow maize to grow under more favourable conditions (Torriani *et al.*, 2007; Waqas *et al.*, 2021).

6.2.2 *Estimated change in low temperature stress*

Low temperature stress is expected to decrease in most regions, whereby the decrease is strongest in high altitudes. Exceptions to this are parts of the Jungfrau region, southern Valais and for local sites in the upper Engadin, who show a smaller decrease in the average occurrence of LT6 in comparison to other mountainous regions (see chapter 5.3.3, Figure 16, bottom). These mountainous sites are likely regions with an altitude around 4000 m MSL. Therefore, a possible explanation is that these regions may still be high enough to not be affected as much by the rising temperatures. Similarly, the altitude may also explain the expected increase in standard deviation of the yearly number of Frost Days in these sites (see chapter 5.3.3, Figure 13, bottom). Due to rising temperatures (CH2018, 2018), these sites may on one hand experience warm summers with few Frost Days, but on the other hand also below-average warm summers where these locations are still high enough to experience several Frost Days.

Despite the rare occurrence of the ACI Frost Days and small values of the ACI Frostsum in low altitudes, low temperature stress is still relevant for maize cultivation in mid-century. Especially days with minimum temperatures below 6 °C are still expected to widely occur during the growing season as shown by the ACI LT6. The ACI Frost Day is expected to occur rather rarely, especially in the Plateau,

along the Prealps and in the Rhone Valley and Rhine Valley. Based on the GDD simulation driven by the RCP 8.5 scenario, in regions like the lower Engadin or the upper Rhone Valley the necessary GDD for grain maize cultivation is expected to be reached relatively often in mid-century, but those regions also show a higher occurrence of Frost Days in comparison to the Plateau. However, another factor to take into account is that the representation of small-scale effects such as cold air pools in the observational grid-data is limited (MeteoSwiss and Federal Department of Home Affairs, 2021a), and that such uncertainties are passed on to the CH2018 data (Kotlarski and Rajczak, 2018). Moreover, if maize was to be sown earlier in the year in order to adapt to climate change as suggested by several studies (Torriani *et al.*, 2007; Holzkämper and Fuhrer, 2015; Holzkämper, 2020; Waqas *et al.*, 2021), the risk of late frost may still be present or could even increase until 2050 depending on the site, which is illustrated in the study of Meier, Fuhrer and Holzkämper (2018), where the changing risk of spring frost damage in grapevines in the Rhone Valley is investigated.

6.2.3 Estimated change in potential waterlogging

Waterlogging is an important aspect for maize, as this may damage maize plants and lead to yield reduction, depending on the development stage of maize, the maize genotype and the duration of waterlogging (Ren *et al.*, 2016; Githui *et al.*, 2022; Huang *et al.*, 2022). However, modelling a future scenario for the frequency of waterlogging is rather difficult, as it is a complicated process (Githui *et al.*, 2022). Moreover, there are several possible reasons for waterlogging, such as excessive precipitation or irrigation, or poor soil drainage (Ren *et al.*, 2016; Githui *et al.*, 2022). Githui *et al.* (2022) for example used crop models in order to simulate crop growth and phenology under waterlogging. Holzkämper *et al.* (2015) used water availability, defined as the difference between precipitation and the calculated reference evapotranspiration, as an indicator for water shortage as well as for water excess. Their results showed a similar spatial distribution of excess water as the results of this thesis for the occurrence of heavy precipitation events.

In this thesis, potential waterlogging was indicated by the ACI HPE, defined as days with at least 50 mm of precipitation, a threshold taken from the study of Tschurr *et al.* (2020). It is however highly important to acknowledge that those numbers should not be directly translated into the number of waterlogging events but should instead rather be understood as an approximation to an indicator for potential waterlogging. Also, as mentioned in chapter 3.2.1, intense precipitation is rather underestimated in the observational grid-data and thus as well in the CH2018 data (Kotlarski and Rajczak, 2018; MeteoSwiss and Federal Department of Home Affairs, 2021b).

The results of this thesis suggest a very small increase in the average number of HPE for some parts of Switzerland – especially along the southern Alps and in parts of the southeastern Alps (see chapter 5.3.4, Figure 17, bottom). Despite that, the results for the whole of Switzerland, as shown in the boxplots in Figure 17, do not show a clear change and are associated with large uncertainties. Additionally, based on the boxplots in Figure 18, it is also uncertain whether the standard deviation in the yearly number of HPE changes until mid-century. The study of Tschurr *et al.* (2020) on the other hand shows a small but relatively widespread increase in the number of heavy precipitation events based on the RCP 8.5 scenario. However, the authors investigated the number of heavy precipitation events throughout the whole year, while in this thesis the number of HPE was analysed between the

5th of May and the 11th of October. Based on the CH2018 scenarios, frequency and intensity of heavy rainfall events is expected to increase particularly in winter (CH2018, 2018). Thus, this difference in the investigated time period may explain a part of the differences between the results in this thesis and the case study of Tschurr *et al.* (2020).

6.2.4 *Estimated change in drought*

While the climate impact model based on the RCP 2.6 scenario mainly suggests an increase in the average yearly number of SPI_m along the Prealps, northeastern Switzerland and parts of the Engadin, the RCP 8.5 scenario shows a clear widespread increase with a maximum change signal in western and northwestern Switzerland (see chapter 5.3.5, Figure 19, bottom). Those findings are similar to those of Tschurr *et al.* (2020). Holzkämper and Fuhrer (2015) show that water shortage increases for the maturation phase of maize, but due to accelerated maize development caused by higher temperatures it is possible that the phenological phase that is most sensitive to drought occurs earlier in the year and thus at a time when water stress is not as severe. However, as Anami *et al.* (2009) state, drought is relevant for the whole growth cycle of maize. Thus, based on the results of this thesis as well as on the mentioned studies, more irrigation may be necessary in some cases in order to mitigate the impact of drought, depending on the maize variety and the respective site (Holzkämper and Fuhrer, 2015; Holzkämper, 2020; Eisenring, Holzkämper and Calanca, 2021).

It must be acknowledged that the World Meteorological Organization (2012) states, that the SPI is not suitable for climate change analyses due to the fact that temperatures are not involved in this drought indicator. Temperature is an important factor when determining dryness as rising temperatures lead to increased evaporation (Seneviratne *et al.*, 2010; World Meteorological Organization, 2012; CH2018, 2018). However, the SPI is a useful tool in drought monitoring, simple to calculate and – when calculated for a shorter accumulation period as done in this thesis – can be used to indicate impacts such as reduced soil moisture (World Meteorological Organization, 2012; Copernicus European Drought Observatory (EDO), 2020). Thus, the SPI was used in this thesis.

6.2.5 *Estimated change in concurrent stress*

As in the CH2018 scenarios quantile mapping has been applied in a univariate manner (CH2018, 2018), it was very important that the representation of ACIs containing more than one climatological parameter by the CH2018 data was validated first. This thesis showed, that the CH2018 data are able to represent some multivariate ACIs realistically, like the ACI SPI_m & HS30. Thus, while the findings in this thesis and other studies (e.g. Holzkämper and Fuhrer, 2015; Tschurr *et al.*, 2020) suggest that heat stress and drought stress individually is expected to increase with climate change, this thesis also establishes that – without adaptation measures in maize cultivation – it is not just the individual stress factors that can potentially increasingly affect maize cultivation, but also their simultaneous occurrence.

On the other hand, as low temperature stress decreases until mid-century, the average yearly number of the ACI SPIm & Frost Day and the ACI HPE & Frost Day mostly show a decrease in average occurrence as well, as does the standard deviation of the yearly number of SPIm & Frost Day. The climate impact analysis based on the RCP 2.6 scenario shows an increase in the average occurrence and the standard deviation of the yearly number of SPIm & Frost Day for some sites in Grisons, Valais and Jungfrau region as well as some other few local sites (see chapter 5.3.6.2, Figure 22 bottom left and Figure 23, bottom left), which may be connected to the increase in the univariate ACI SPIm. Despite the results suggesting a decrease in the occurrence of the ACI SPIm & Frost Day and the ACI HPE & Frost Day, it is important to consider that since low temperature stress may still be relevant in mid-century, as elaborated in chapter 6.2.2, concurrent stress events involving such may also still be of importance in the future.

There are other methods to estimate the impact of concurrent stress on maize. Zhao *et al.* (2023) for example evaluated the vulnerability of maize in Songliao Plain to concurrent low temperature stress and drought by creating a model using the so-called vine copula method, which considers the intensity of the respective stress factors. In the study of Guo *et al.* (2023), a hazard assessment model for maize was created, which considers severity, duration and probability of the occurrence of drought and heat compound extreme events. This thesis shows that ACIs can also be a useful and, in comparison, simpler tool to estimate the impact of climate change with regard to simultaneous stress factors on maize.

7 Conclusion

7.1 Main Findings

In this thesis, the impact of climate change on maize cultivation in Switzerland was investigated by using agricultural climate indicators, which indicate (potential) climatological stress for maize. The research questions and respective hypotheses are:

1. *How well do agricultural climate indicators explain maize yield variation in the present Swiss climate?*

Hypothesis 1: There is a significant negative relationship between maize yield and the occurrence of agricultural climate indicators in the present Swiss climate.

2. *Will the average occurrence of agricultural climate indicators in Switzerland change with climate change?*

Hypothesis 2: The average occurrence of agricultural climate indicators will be different in the future Swiss climate.

3. *Will the variability of agricultural climate indicators in Switzerland change with climate change?*

Hypothesis 3: The variability of the agricultural climate indicators will be different in the future Swiss climate.

The used ACIs are based on literature (Holzkämper, Calanca and Fuhrer, 2013; Sánchez, Rasmussen and Porter, 2014; Tschurr *et al.*, 2020; Buzzi *et al.*, 2021; Waqas *et al.*, 2021) and have been compared to maize yield data from 2003–2022. The results show, depending on the site, a significant moderate negative relationship between heat stress related ACIs and maize yield, indicating that the respective ACIs (namely HS30, HS35 and HS35sum) can in some cases explain maize yield variation. For other ACIs, the results are more ambiguous. Depending on the municipality and the ACI, positive as well as negative correlations are visible, of which only very few are of statistical significance, with the significant relationships again being of moderate strength. These findings underline the complexity of the relationship between maize yield and ACIs, as the response of plants to stressors not only depends on whether they occur individually or simultaneously (Mittler, 2006; Suzuki *et al.*, 2014; Hussain *et al.*, 2018; Webber *et al.*, 2022; Hu *et al.*, 2023), but also on the farm characteristics and the capability of farmers to mitigate climatological stress (Torriani *et al.*, 2007; Reidsma *et al.*, 2010; Suzuki *et al.*, 2014). Overall, the first hypothesis can be accepted for some municipalities for heat stress related ACIs. For the other ACIs, due to the differing direction of the relationship between maize yield and the respective ACIs and the lack of significant results, the first hypothesis is rejected.

The analysis of the climate change impact on maize cultivation was done by using the high-resolution CH2018 grid-data (CH2018 Project Team, 2018), allowing an overview of the expected climatological

limitations over the whole of Switzerland based on the chosen ACIs. In order to estimate for which ACIs the second and third hypotheses can be accepted, the range of the climate model ensemble as illustrated in the boxplots (Figures 7 to 24, top right) have been considered in the climate impact analysis to take into account uncertainties in the change signal.

The results show that especially based on the RCP 8.5 scenario, the average occurrence of most ACIs is expected to change until mid-century with an increase in heat stress and drought related univariate ACIs and a decrease in low temperature stress related univariate ACIs. The average occurrence of the multivariate ACI SPI_m & HS30 is expected to increase, while multivariate ACIs including low temperature stress is likely to decrease until mid-century. For the ACI HPE, which represents potential waterlogging, the range of the climate model ensemble shows that it is uncertain whether the average number of HPE is expected to change. Thus, the second hypothesis can be accepted for all ACIs except for the ACI HPE, for which the second hypothesis is rejected due to the uncertainties.

Regarding the variability of ACIs, the focus lied on the temporal variability. The temporal climate variability was investigated by analysing the temporal standard deviation of the yearly number of an ACI. In most cases, an increase in the average occurrence of an ACI was associated with an increase in standard deviation and a decrease in the average occurrence with a decrease in standard deviation. However, regarding the ACI HPE, change signals for the standard deviation are again very small and associated with large uncertainties as illustrated by the range of the climate model ensemble.

To some extent, changes in spatial variability are visible. The change signal for an ACI is often strongest where the respective ACI occurs most frequently during the reference period. For example, the occurrence of heat stress related ACIs increase strongest in low altitudes, while the occurrence of low temperature stress related ACIs mostly decreases the most in high altitudes. This increases the spatial contrast in heat stress related ACI occurrence and reduces to some extent the spatial contrast in the occurrence of the ACIs Frost Day and Frostsum between different regions in Switzerland. With these results, the third hypothesis is accepted for all ACIs except for the ACI HPE. For the ACI HPE, the third hypothesis is rejected due to uncertainties in the results.

This thesis gives a broad overview of the potential climate-related challenges in maize cultivation in mid-century. By including ACIs of different stress categories, it is possible to analyse the impact of different aspects of climate change. With the ACI change signal maps being based on a high-resolution grid of, at the time of this thesis, the most up-to-date climate scenarios for Switzerland (CH2018, 2018), they can provide a basis for recommendations in the adaptation process to mitigate the risks of climate change.

7.2 Future Research

This thesis underlines the expected increase of heat and drought stress and the combination of such for maize cultivation in Switzerland until mid-century. It includes the change of climatological parameters, not however the adaptability of farmers. By using more heat and drought stress resistant maize genotypes, it is possible to mitigate the negative consequences of climate change on maize (Holzkämper and Fuhrer, 2015; Waqas *et al.*, 2021). At the end of 2025, the new climate scenarios

CH2025 for Switzerland will be published (MeteoSwiss, 2024b, no date a). With the new CH2025 data, the evaluation of this thesis should be repeated in order to provide up-to-date climate information for end-users.

Moreover, with the new climate data, it may be useful to investigate the impact of climate change on maize varieties that are more compatible with the expected climate in mid-century, in order to provide farmers with information about the advantages and availability of more appropriate maize genotypes within the next decades. In this way, the adaptability of farmers could be included in climate change impact analysis. This could however also mean, that ACIs with new thresholds are needed, as the used thresholds in this thesis may not be suited for the in mid-century potentially new recommended maize genotypes. Specifically waterlogging is an important, but in comparison to e.g. heat and drought stress a rather poorly investigated stress factor for maize (Rötter *et al.*, 2018). Thus, the expected waterlogging risk for maize cultivation in Switzerland needs to be addressed in more detail in future research.

Furthermore, this thesis provides an overview of how climate change leads to a change in ACI occurrence within a fixed growing season. In a next step, the length of the growing season and the individual phenological phases should be estimated dynamically, based on climatological parameters. A possible way to do so is shown in Holzkämper and Fuhrer (2015). By doing so, the evaluation of the change in ACI occurrence within the respective phenological phase, in which maize is the most susceptible to the respective climatological stress, may be possible. Moreover, with rising temperatures, the phenological development rate of crop is expected to accelerate (Torriani *et al.*, 2007). By focusing on dynamically estimated phenological phase durations, this effect may be taken into account (Holzkämper and Fuhrer, 2015).

8 References

8.1 Literature

AgriAdapt (2019) 'Landwirtschaft und Anpassung. Nachhaltige Anpassung der Europäischen Landwirtschaft an den Klimawandel', p. 68. Available at: <https://agriadapt.eu/documents/?lang=de>.

Akoglu, H. (2018) 'User's guide to correlation coefficients', *Turkish Journal of Emergency Medicine*, 18(3), pp. 91–93. <https://doi.org/10.1016/j.tjem.2018.08.001>.

Anami, S. *et al.* (2009) 'Molecular Improvement of Tropical Maize for Drought Stress Tolerance in Sub-Saharan Africa', *Critical Reviews in Plant Sciences*, 28(1–2), pp. 16–35. <https://doi.org/10.1080/07352680802665305>.

Arnell, N. W. and Freeman, A. (2021) 'The effect of climate change on agro-climatic indicators in the UK', *Climatic Change*, 165(40). <https://doi.org/10.1007/s10584-021-03054-8>.

Beguéría, S. and Vicente-Serrano, S. M. (2023) *SPEI: Calculation of the Standardized Precipitation-Evapotranspiration Index*. Available at: <https://cran.r-project.org/package=SPEI>.

Bolker, B. B. (13:55, 30 November 2012) '<http://www.math.mcmaster.ca/bolker/R/misc/legendx.R>' [Comment on the online forum post 'increasing the size of the coloured squares on histogram legends in R'], *Stack Overflow*. Available at: <https://stackoverflow.com/questions/13644149/increasing-the-size-of-the-coloured-squares-on-histogram-legends-in-r> (Accessed: 11 April 2024).

Bundesamt für Landwirtschaft BLW (2024) *Bodenrecht*. Available at: <https://www.blw.admin.ch/blw/de/home/instrumente/boden--und-pachtrecht/bodenrecht.html> (Accessed: 25 April 2024).

Bundesamt für Statistik (2022) *Landwirtschaft und Ernährung, Taschenstatistik 2022*. BFS, Neuchâtel 2022. Available at: <https://www.bfs.admin.ch/bfs/de/home/aktuell/neue-veroeffentlichungen.assetdetail.22906536.html>.

Buzzi, F. *et al.* (2021) 'Temperatursummen-Karten für die Sortenwahl im Maisanbau', *Agrarforschung Schweiz*, 12, pp. 1–8. <https://doi.org/10.34776/afs12-1>.

CH2018 (2018) *CH2018 - Climate Scenarios for Switzerland, Technical Report*. National Centre for Climate Services, Zurich.

CH2018 Project Team (2018) *CH2018 - Climate Scenarios for Switzerland*. National Centre for Climate Services. <https://doi.org/10.18751/Climate/Scenarios/CH2018/1.0>.

Copernicus European Drought Observatory (EDO) (2020) *Standardized Precipitation Index (SPI)*. Available at: <https://edo.jrc.ec.europa.eu/> (Accessed: 3 January 2024).

Dierauer, H. and Gelencsér, T. (2019) *Biomais, Merkblatt*. FiBL. Available at: www.fibl.org. (Accessed: 1 June 2023).

Eder, J., Ziegler, A. and Eiblmeier, P. (no date) *Hinweise zum Mais-Reifeproggnosemodell nach AGPM*. Available at: <https://web.archive.org/web/20130318031104/http://www.lfl.bayern.de/ipz/mais/08509/> (Accessed: 9 January 2024).

Eisenring, S., Holzkämper, A. and Calanca, P. (2021) *Berechnung der Bewässerungsbedürfnisse unter aktuellen und zukünftigen Bedingungen in der Schweiz*, *Agroscope Science*. Agroscope. <https://doi.org/10.34776/as107g>.

Eitzinger, J. *et al.* (2012) 'REVIEW AND ASSESSMENT OF AGROCLIMATIC INDICES AND SIMULATION MODELS IN EUROPE', in Orlandini, Simone and Nejedlik, P. (eds) *Climate Change Impacts on Agriculture in Europe: Final Report of COST Action 734 'Impact of climate change and variability on European agriculture'*. Firenze: Firenze University Press, pp. 1–45. <https://doi.org/10.36253/978-88-6655-207-9>.

Elmore, R. W. (2012) *Stress, Anthesis - Silk Interval and Corn Yield Potential*. Available at: <https://crops.extension.iastate.edu/cropnews/2012/07/stress-anthesis-silk-interval-and-corn-yield-potential> (Accessed: 15 January 2024).

Federal Office of Topography swisstopo (2024) 'swissBOUNDARIES3D'. Available at: <https://www.swisstopo.admin.ch/de/landschaftsmodell-swissboundaries3d>.

Fonseca, A. E. *et al.* (2003) 'Tassel Morphology as an Indicator of Potential Pollen Production in Maize', *Crop Management*, 2(1). <https://doi.org/10.1094/CM-2003-0804-01-RS>.

Foyer, C. H. *et al.* (2002) 'Regulation of photosynthesis and antioxidant metabolism in maize leaves at optimal and chilling temperatures: review', *Plant Physiology and Biochemistry*, 40, pp. 659–668. Available at: www.elsevier.com/locate/plaphy (Accessed: 8 January 2024).

Githui, F. *et al.* (2022) 'Modelling Waterlogging Impacts on Crop Growth: A Review of Aeration Stress Definition in Crop Models and Sensitivity Analysis of APSIM', *International Journal of Plant Biology*, pp. 180–200. <https://doi.org/10.3390/ijpb13030017>.

Grömping, U. (2006) 'Relative importance for linear regression in R: The package relaimpo', *Journal of Statistical Software*, 17(1), pp. 1–27. <https://doi.org/10.18637/jss.v017.i01>.

Gudmundsson, L. and Stagge, J. H. (2016) 'SCI: Standardized Climate Indices such as SPI, SRI or SPEI'. R package version 1.0-2. Available at: <https://rdr.io/cran/SCI/man/SCI-package.html> (Accessed: 24 September 2023).

Guo, Y. *et al.* (2023) 'Quantifying hazard of drought and heat compound extreme events during maize (*Zea mays* L.) growing season using Magnitude Index and Copula', *Weather and Climate Extremes*, 40. <https://doi.org/10.1016/J.WACE.2023.100566>.

Hawkins, E. *et al.* (2013) 'Increasing influence of heat stress on French maize yields from the 1960s to the 2030s.', *Global change biology*, 19(3), pp. 937–947. <https://doi.org/10.1111/gcb.12069>.

Hiltbrunner, J. *et al.* (2023) 'Liste der empfohlenen Maissorten für die Ernte 2023', *Agroscope Transfer*, 471, pp. 1–6.

Holzkämper, A. *et al.* (2015) 'Spatial and temporal trends in agro-climatic limitations to production potentials for grain maize and winter wheat in Switzerland', *Regional Environmental Change*, 15, pp. 109–122. <https://doi.org/10.1007/s10113-014-0627-7>.

Holzkämper, A. (2020) 'Varietal adaptations matter for agricultural water use – a simulation study on grain maize in Western Switzerland', *Agricultural Water Management*, 237. <https://doi.org/10.1016/J.AGWAT.2020.106202>.

Holzkämper, A., Calanca, P. and Fuhrer, J. (2013) 'Identifying climatic limitations to grain maize yield potentials using a suitability evaluation approach', *Agricultural and Forest Meteorology*, 168, pp. 149–159. <https://doi.org/10.1016/j.agrformet.2012.09.004>.

- Holzkämper, A. and Fuhrer, J. (2015) 'Wie sich der Klimawandel auf den Maisanbau in der Schweiz auswirkt', *Agrarforschung Schweiz*, 6(10), pp. 440–447.
- Hu, J. *et al.* (2023) 'The effects of high temperature, drought, and their combined stresses on the photosynthesis and senescence of summer maize', *Agricultural Water Management*, 289, p. 108525. <https://doi.org/10.1016/j.agwat.2023.108525>.
- Huang, C. *et al.* (2022) 'Effects of waterlogging at different stages and durations on maize growth and grain yields', *Agricultural Water Management*, 261, p. 107334. <https://doi.org/10.1016/j.agwat.2021.107334>.
- Hussain, H. A. *et al.* (2018) 'Chilling and Drought Stresses in Crop Plants: Implications, Cross Talk, and Potential Management Opportunities'. <https://doi.org/10.3389/fpls.2018.00393>.
- Hussain, H. A. *et al.* (2020) 'Maize Tolerance against Drought and Chilling Stresses Varied with Root Morphology and Antioxidative Defense System', *Plants*, 9(6), pp. 1–19. <https://doi.org/10.3390/PLANTS9060720>.
- IPCC (2021) 'Summary for policymakers', in MassonDelmotte, V. *et al.* (eds) *Climate Change 2021: The Physical Science Basis. Contribution of Working Group I to the Sixth Assessment Report of the Intergovernmental Panel on Climate Change*. Cambridge University Press, Cambridge, United Kingdom and New York, NY, USA, pp. 3–32. <https://doi.org/10.1017/9781009157896.001>.
- James, D. and Hornik, K. (2023) 'chron: Chronological Objects which Can Handle Dates and Times'. R package version 2.3-61. Available at: <https://cran.r-project.org/package=chron>.
- Kaur, P. *et al.* (2023) 'Corn Silk as an Agricultural Waste: A Comprehensive Review on Its Nutritional Composition and Bioactive Potential', *Waste and Biomass Valorization*, 14(5), pp. 1413–1432. <https://doi.org/10.1007/s12649-022-02016-0>.
- Kotlarski, S. and Rajczak, J. (2018) *CH2018 - Climate Scenarios for Switzerland, Documentation of the localized CH2018 datasets, Transient daily time series at the local scale: DAILY-LOCAL, DAILY-GRIDDED*.
- Kozłowski, T. T. (1997) 'Responses of woody plants to flooding and salinity', *Tree Physiology*, 17(7), p. 490. <https://doi.org/10.1093/treephys/17.7.490>.
- Lobell, D. B. and Field, C. B. (2007) 'Global scale climate–crop yield relationships and the impacts of recent warming', *Environmental Research Letters*, 2:014002. <https://doi.org/10.1088/1748-9326/2/1/014002>.
- Mathieu, J. A. and Aires, F. (2018) 'Assessment of the agro-climatic indices to improve crop yield forecasting', *Agricultural and Forest Meteorology*, 253–254, pp. 15–30. <https://doi.org/10.1016/j.agrformet.2018.01.031>.
- McKee, T. B., Doesken, N. J. and Kleist, J. (1993) *The relationship of drought frequency and duration to time scales, Eight Conference on Applied Climatology, 17-22 January 1993*. Anaheim, California.
- McMaster, G. S. and Wilhelm, W. W. (1997) 'Growing degree-days: one equation, two interpretations', *Agricultural and Forest Meteorology*, 87(4), pp. 291–300. [https://doi.org/10.1016/S0168-1923\(97\)00027-0](https://doi.org/10.1016/S0168-1923(97)00027-0).
- Meier, M., Fuhrer, J. and Holzkämper, A. (2018) 'Changing risk of spring frost damage in grapevines due to climate change? A case study in the Swiss Rhone Valley', *International Journal of Biometeorology*, 62(6), pp. 991–1002. <https://doi.org/10.1007/s00484-018-1501-y>.

MeteoSwiss (2024a) 'Climate normals 1991-2020: Frost days (minimum lower than 0 degrees C)'. Available at: <https://www.meteoschweiz.admin.ch/service-und-publikationen/applikationen/ext/climate-normtables.html>.

MeteoSwiss (2024b) *MeteoSchweiz bereitet die neuen Klimaszenarien vor, MeteoSchweiz-Blog | 22. März 2024*. Available at: <https://www.meteoschweiz.admin.ch/ueber-uns/meteoschweiz-blog/de/2024/03/meteoschweiz-klimaszenarien-vorbereitung-ch2025.html> (Accessed: 1 April 2024).

MeteoSwiss (no date a) *Klima CH2025*. Available at: <https://www.meteoschweiz.admin.ch/ueber-uns/forschung-und-zusammenarbeit/projekte/2023/klima-ch2025.html> (Accessed: 1 April 2024).

MeteoSwiss (no date b) *Phenology*. Available at: <https://www.meteoswiss.admin.ch/weather/weather-and-climate-from-a-to-z/phenology.html> (Accessed: 29 April 2024).

MeteoSwiss (no date c) *Rain*. Available at: <https://www.meteoswiss.admin.ch/weather/hazards/explanation-of-the-danger-levels/rain.html> (Accessed: 16 January 2024).

MeteoSwiss and Federal Department of Home Affairs (2015) *Documentation of MeteoSwiss Grid-Data Products, Local Time Series (LTS)*. Available at: <https://www.meteoswiss.admin.ch/climate/the-climate-of-switzerland/spatial-climate-analyses.html>.

MeteoSwiss and Federal Department of Home Affairs (2021a) *Documentation of MeteoSwiss Grid-Data Products, Daily Mean, Minimum and Maximum Temperature: TabsD, TminD, TmaxD*. Available at: <https://www.meteoswiss.admin.ch/climate/the-climate-of-switzerland/spatial-climate-analyses.html>.

MeteoSwiss and Federal Department of Home Affairs (2021b) 'Documentation of MeteoSwiss Grid-Data Products, Daily Precipitation (final analysis): RhiresD'. Available at: <https://www.meteoswiss.admin.ch/climate/the-climate-of-switzerland/spatial-climate-analyses.html> (Accessed: 21 December 2023).

MeteoSwiss and Federal Department of Home Affairs (2021c) *MeteoSwiss Spatial Climate Analyses: Documentation of Datasets for Users*. Available at: <https://www.meteoswiss.admin.ch/climate/the-climate-of-switzerland/spatial-climate-analyses.html>.

Meuli, K. (2020) *Wasser clever nutzen, die umwelt*. Bundesamt für Umwelt BAFU. Available at: <https://www.bafu.admin.ch/bafu/de/home/themen/wasser/dossiers/magazin2020-4-dossier.html>.

Mittler, R. (2006) 'Abiotic stress, the field environment and stress combination', *Trends in Plant Science*, 11(1), pp. 15–19. <https://doi.org/10.1016/j.tplants.2005.11.002>.

NCCS (2021) *How are the impacts of climate change investigated?* Available at: <https://www.nccs.admin.ch/nccs/en/home/climate-change-and-impacts/climate-basics/how-are-the-impacts-of-climate-change-investigated-.html> (Accessed: 5 April 2024).

NCCS (2023) *NCCS-Impacts programme*. Available at: <https://www.nccs.admin.ch/impacts-en> (Accessed: 18 October 2023).

NCCS (2024) *Project 'Ecosystem services'*. Available at: <https://www.nccs.admin.ch/nccs/en/home/climate-change-and-impacts/nccs-impacts/oekosystemleistungen.html> (Accessed: 19 April 2024).

Nobakht, M. et al. (2019) *Agroclimatic indicators from 1951 to 2099 derived from climate projections, Copernicus Climate Change Service (C3S) Climate Data Store (CDS)*. <https://doi.org/10.24381/cds.dad6e055>.

- Nobakht, M. *et al.* (2024) *Agroclimatic Indicators: Product User Guide and Specification (PUGS)*. Available at: <https://confluence.ecmwf.int/pages/viewpage.action?pageId=278550972#heading-Relatedarticles> (Accessed: 19 April 2024).
- Nychka, D. *et al.* (2021) 'fields: Tools for spatial data'. R package version 15.2. Available at: <https://github.com/dnychka/fieldsRPackage>.
- Olesen, J. E. and Bindi, M. (2002) 'Consequences of climate change for European agricultural productivity, land use and policy', *European Journal of Agronomy*, 16(4), pp. 239–262. [https://doi.org/10.1016/S1161-0301\(02\)00004-7](https://doi.org/10.1016/S1161-0301(02)00004-7).
- OpenAI (no date) *ChatGPT-3.5*. Available at: <https://chatx.de/> (Accessed: 11 April 2024).
- Parent, B. *et al.* (2018) 'Maize yields over Europe may increase in spite of climate change, with an appropriate use of the genetic variability of flowering time', 115(42), pp. 10642–10647. <https://doi.org/10.1073/pnas.1720716115>.
- Pasley, H. *et al.* (2022) 'How to build a crop model. A review', *Agronomy for Sustainable Development*, 43(1). <https://doi.org/10.1007/s13593-022-00854-9>.
- Pierce, D. (2023) 'ncdf4: Interface to Unidata netCDF (Version 4 or Earlier) Format Data Files'. R package version 1.21. Available at: <https://cran.r-project.org/package=ncdf4>.
- Plate, T. and Heiberger, R. (2016) 'abind: Combine Multidimensional Arrays'. R package version 1.4-5. Available at: <https://cran.r-project.org/package=abind>.
- R Core Team (2023) 'R: A Language and Environment for Statistical Computing'. R Foundation for Statistical Computing, Vienna, Austria. Available at: <https://www.r-project.org/>.
- Reidsma, P. *et al.* (2010) 'Adaptation to climate change and climate variability in European agriculture: The importance of farm level responses', *European Journal of Agronomy*, 32(1), pp. 91–102. <https://doi.org/10.1016/j.eja.2009.06.003>.
- Ren, B. *et al.* (2016) 'Effects of Duration of Waterlogging at Different Growth Stages on Grain Growth of Summer Maize (*Zea mays* L.) Under Field Conditions', *Journal of Agronomy and Crop Science*, 202(6), pp. 564–575. <https://doi.org/10.1111/JAC.12183>.
- Rossini, M. A., Maddonni, G. A. and Otegui, M. E. (2016) 'Multiple abiotic stresses on maize grain yield determination: Additive vs multiplicative effects', *Field Crops Research*, 198, pp. 280–289. <https://doi.org/10.1016/J.FCR.2016.07.004>.
- Rötter, R. P. *et al.* (2018) 'Linking modelling and experimentation to better capture crop impacts of agroclimatic extremes—A review', *Field Crops Research*, 221, pp. 142–156. <https://doi.org/10.1016/j.fcr.2018.02.023>.
- Sánchez, B., Rasmussen, A. and Porter, J. R. (2014) 'Temperatures and the growth and development of maize and rice: a review', *Global Change Biology*, 20(2), pp. 408–417. <https://doi.org/10.1111/GCB.12389>.
- Scherrer, S. C. *et al.* (2022) 'Trends and drivers of recent summer drying in Switzerland', *Environmental Research Communications*, 4(2). <https://doi.org/10.1088/2515-7620/ac4fb9>.
- Schweizer Bauernverband (2021) 'Potential ausgewählter Ackerkulturen in der Schweiz'. Available at: <https://www.sbv-usp.ch/de/grosses-potential-fuer-den-schweizer-ackerbau>.
- Seneviratne, S. I. *et al.* (2010) 'Investigating soil moisture–climate interactions in a changing climate: A review', *Earth-Science Reviews*, 99(3), pp. 125–161. <https://doi.org/10.1016/j.earscirev.2010.02.004>.

- Shabbir, R. *et al.* (2022) 'Combined Abiotic Stresses: Challenges and Potential for Crop Improvement', *Agronomy*, 12(11). <https://doi.org/10.3390/agronomy12112795>.
- Smit, B. and Skinner, M. (2002) 'Adaptation options in agriculture to climate change: a topology. Mitig Adapt Strateg Glob Change 7:85-114', *Mitigation and Adaptation Strategies for Global Change*, 7, pp. 85–114. <https://doi.org/10.1023/A:1015862228270>.
- Southworth, J. *et al.* (2000) 'Consequences of future climate change and changing climate variability on maize yields in the midwestern United States', *Agriculture, Ecosystems and Environment*, 82(1–3), pp. 139–158. [https://doi.org/10.1016/S0167-8809\(00\)00223-1](https://doi.org/10.1016/S0167-8809(00)00223-1).
- Stagge, J. H. *et al.* (2015) 'Candidate Distributions for Climatological Drought Indices (SPI and SPEI)', *International Journal of Climatology*, 35(13), pp. 4027–4040. <https://doi.org/10.1002/JOC.4267>.
- Stagge, J. H. *et al.* (2016) 'Response to comment on "Candidate Distributions for Climatological Drought Indices (SPI and SPEI)"', *International Journal of Climatology*, 36(4), pp. 2132–2138. <https://doi.org/10.1002/JOC.4564>.
- Stephenson, A. G. (2002) 'evd: Extreme Value Distributions', *R News*, 2(2). Available at: <https://cran.r-project.org/doc/Rnews/>.
- Strickhof (2023) *Merkblatt Pflanzenbau - Mais*. Available at: <https://www.strickhof.ch/publikationen/merkblatt-mais/> (Accessed: 1 June 2023).
- Suzuki, N. *et al.* (2014) 'Abiotic and biotic stress combinations', *New Phytologist*, 203(1), pp. 32–43. <https://doi.org/10.1111/NPH.12797>.
- Tian, L. *et al.* (2019) 'Effects of waterlogging stress at different growth stages on the photosynthetic characteristics and grain yield of spring maize (*Zea mays* L.) Under field conditions', *Agricultural Water Management*, 218, pp. 250–258. <https://doi.org/10.1016/j.agwat.2019.03.054>.
- Torriani, D. S. *et al.* (2007) 'Potential effects of changes in mean climate and climate variability on the yield of winter and spring crops in Switzerland', *Climate Research*, 34(1), pp. 59–69. <https://doi.org/10.3354/CR034059>.
- Tschurr, F. *et al.* (2020) 'Climate scenarios and agricultural indices: A case study for Switzerland', *Atmosphere*, 11(5), pp. 1–23. <https://doi.org/10.3390/atmos11050535>.
- Waqas, M. A. *et al.* (2021) 'Thermal stresses in maize: Effects and management strategies', *Plants*, 10(2), pp. 1–23. <https://doi.org/10.3390/plants10020293>.
- Webber, H. *et al.* (2022) 'Framework to guide modeling single and multiple abiotic stresses in arable crops', *Agriculture, Ecosystems and Environment*, 340. <https://doi.org/10.1016/J.AGEE.2022.108179>.
- Wickham, H. (2016) 'ggplot2: Elegant Graphics for Data Analysis'. Springer-Verlag New York.
- Wickham, H. and Bryan, J. (2023) 'readxl: Read Excel Files'. R package version 1.4.3. Available at: <https://cran.r-project.org/package=readxl>.
- World Meteorological Organization (2012) *Standardized Precipitation Index User Guide*, WMO. Edited by M. Svoboda, M. Hayes, and D. A. Wood. Geneva. Available at: http://library.wmo.int/opac/index.php?lvl=notice_display&id=13682 (Accessed: 19 March 2024).
- Yanar, Y., Lipps, P. E. and Deep, I. W. (1997) 'Effect of Soil Saturation Duration and Soil Water Content on Root Rot of Maize Caused by *Pythium arrhenomanes*', *Plant Disease*, 81(5), pp. 475–480. <https://doi.org/10.1094/PDIS.1997.81.5.475>.

- Yin, X. *et al.* (1995) 'A nonlinear model for crop development as a function of temperature', *Agricultural and Forest Meteorology*, 77(1–2), pp. 1–16. [https://doi.org/10.1016/0168-1923\(95\)02236-Q](https://doi.org/10.1016/0168-1923(95)02236-Q).
- Zeileis, A. *et al.* (2020) 'colorspace: A Toolbox for Manipulating and Assessing Colors and Palettes', *Journal of Statistical Software*, 96(1), pp. 1–49. <https://doi.org/10.18637/jss.v096.i01>.
- Zhang, H. *et al.* (2014) 'Transcriptomes and Proteomes Define Gene Expression Progression in Pre-meiotic Maize Anthers', *G3 Genes Genomes Genetics*, 4, pp. 993–1010. <https://doi.org/10.1534/g3.113.009738>.
- Zhang, Y. and Li, Z. (2020) 'Uncertainty Analysis of Standardized Precipitation Index Due to the Effects of Probability Distributions and Parameter Errors', *Frontiers in Earth Science*, 8(76). <https://doi.org/10.3389/feart.2020.00076>.
- Zhao, Y. *et al.* (2023) 'Dynamic vulnerability assessment of maize under low temperature and drought concurrent stress in Songliao Plain', *Agricultural Water Management*, 286(Article 108400). <https://doi.org/10.1016/j.agwat.2023.108400>.
- Zhou, X. *et al.* (2022) 'Recent Advances in the Analysis of Cold Tolerance in Maize.', *Frontiers in plant science*, 13. <https://doi.org/10.3389/fpls.2022.866034>.
- Zscheischler, J. *et al.* (1984) *Handbuch Mais: Anbau - Verwertung - Fütterung*. 3. DLG-Verlag Frankfurt (Main), BLV Verlagsgesellschaft München, Landwirtschaftsverlag Münster-Hiltrup, Österreichischer Agrarverlag Wien, Verbandsdruckerei/Wirz Bern.

8.2 Used illustrations in Figures

Pixabay (2013): <https://pixabay.com/de/vectors/mais-landwirtschaft-biologie-155126/> (Accessed: 25 April 2024)

Pixabay (2014): <https://pixabay.com/de/vectors/mais-gem%C3%BCse-ernte-getreide-306886/> (Accessed: 25 April 2024)

Appendices

A Supplemental results of ACI validation with yield data

A.1 Correlation between maize yield and individual ACIs

Table 6: Spearman's rank correlation ρ between ACI occurrence and maize yield and the corresponding p-value for the municipalities Aristau, Dietwil and Islisberg. For each municipality, the number of years with available maize yield data is listed.

ACI	Aristau (18 yrs.)		Dietwil (20 yrs.)		Islisberg (17 yrs.)	
	ρ	p-value	ρ	p-value	ρ	p-value
HS30	0.15	0.56	0.19	0.41	0.01	0.96
HS35	-0.11	0.68	0.14	0.56	-0.30	0.24
HS35sum	-0.11	0.68	0.14	0.56	-0.32	0.22
Frost Day	0.00	1.00	–	–	-0.13	0.63
Frostsum	0.00	1.00	–	–	-0.13	0.63
LT6	0.04	0.88	-0.28	0.24	-0.22	0.40
HPE	0.32	0.19	-0.41	0.07	-0.08	0.75
SPI _m	-0.22	0.37	0.57	0.01	0.31	0.23
SPI _e	0.14	0.58	0.00	1.00	0.38	0.13
SPI _m & HS30	-0.49	0.04	0.33	0.15	0.15	0.56
SPI _e & HS35	–	–	–	–	–	–
HPE & HS30	–	–	–	–	–	–
HPE & HS35	–	–	–	–	–	–
SPI _m & Frost Day	0.00	1.00	–	–	-0.13	0.63
SPI _e & Frost Day	–	–	–	–	–	–
HPE & Frost Day	–	–	–	–	–	–

Table 7: Spearman's rank correlation ρ between ACI occurrence and maize yield and the corresponding p-value for the municipalities Moehlin, Zetzwil and Hohenrain. For each municipality, the nr. of years with available maize yield data is listed.

Spearman's rank correlation coefficient						
ACI	Moehlin (19 yrs.)		Zetzwil (19 yrs.)		Hohenrain (18 yrs.)	
	ρ	p-value	ρ	p-value	ρ	p-value
HS30	-0.23	0.34	-0.18	0.45	0.04	0.87
HS35	-0.11	0.65	-0.32	0.19	-0.40	0.10
HS35sum	-0.11	0.65	-0.32	0.19	-0.40	0.10
Frost Day	-	-	0.02	0.93	0.30	0.22
Frostsum	-	-	0.02	0.93	0.30	0.22
LT6	0.14	0.56	0.20	0.42	0.18	0.47
HPE	-0.19	0.44	-0.24	0.32	-0.09	0.73
SPI _m	0.15	0.53	0.25	0.30	-0.27	0.28
SPI _e	-0.03	0.90	0.15	0.55	-0.16	0.52
SPI _m & HS30	-0.24	0.33	0.00	0.99	-0.21	0.41
SPI _e & HS35	-	-	-	-	-	-
HPE & HS30	-	-	-	-	-	-
HPE & HS35	-	-	-	-	-	-
SPI _m & Frost Day	-	-	0.02	0.93	0.30	0.22
SPI _e & Frost Day	-	-	-	-	-	-
HPE & Frost Day	-	-	-	-	-	-

Table 8: Spearman's rank correlation ρ between ACI occurrence and maize yield and the corresponding p-value for the municipalities Ramsen, Schlatt and Thundorf. For each municipality, the nr. of years with available maize yield data is listed.

Spearman's rank correlation coefficient						
ACI	Ramsen (19 yrs.)		Schlatt (18 yrs.)		Thundorf (17 yrs.)	
	ρ	p-value	ρ	p-value	ρ	p-value
HS30	-0.23	0.33	-0.41	0.09	-0.11	0.68
HS35	-0.42	0.07	-0.57	0.01	-	-
HS35sum	-0.37	0.12	-0.57	0.01	-	-
Frost Day	-	-	-0.21	0.40	-0.05	0.85
Frostsum	-	-	-0.21	0.40	-0.05	0.85
LT6	0.26	0.28	-0.09	0.72	0.26	0.31
HPE	0.09	0.73	0.07	0.79	0.21	0.42
SPI _m	-0.14	0.57	0.17	0.49	0.03	0.91
SPI _e	-0.16	0.51	0.28	0.27	-0.10	0.70
SPI _m & HS30	-0.16	0.52	-0.01	0.96	-0.41	0.10
SPI _e & HS35	-	-	-	-	-	-
HPE & HS30	-	-	-	-	-	-
HPE & HS35	-	-	-	-	-	-
SPI _m & Frost Day	-	-	-	-	-0.05	0.85
SPI _e & Frost Day	-	-	-	-	-	-
HPE & Frost Day	-	-	-	-	-	-

Table 9: Spearman's rank correlation ρ between ACI occurrence and maize yield and the corresponding p-value for the municipalities Yvorne, Schwerzenbach and Thalheim an der Thur. For each municipality, the nr. of years with available maize yield data is listed.

Spearman's rank correlation coefficient (r_s)						
ACI	Yvorne (19 yrs.)		Schwerzenbach (17 yrs.)		Thalheim an der Thur (17 yrs.)	
	ρ	p-value	ρ	p-value	ρ	p-value
HS30	-0.01	0.96	-0.14	0.60	-0.61	0.01
HS35	-	-	-0.11	0.68	-0.52	0.03
HS35sum	-	-	-0.10	0.69	-0.52	0.03
Frost Day	0.43	0.07	-	-	-0.20	0.43
Frostsum	0.43	0.06	-	-	-0.20	0.43
LT6	0.38	0.11	-0.55	0.02	-0.25	0.34
HPE	-0.19	0.44	-0.12	0.65	0.39	0.12
SPI _m	-0.14	0.57	0.25	0.32	-0.28	0.27
SPI _e	-0.29	0.22	0.09	0.72	-0.16	0.55
SPI _m & HS30	-0.36	0.14	0.02	0.94	-0.15	0.56
SPI _e & HS35	-	-	-	-	-	-
HPE & HS30	-	-	-	-	-	-
HPE & HS35	-	-	-	-	-	-
SPI _m & Frost Day	0.36	0.13	-	-	-0.20	0.43
SPI _e & Frost Day	-	-	-	-	-	-
HPE & Frost Day	-	-	-	-	-	-

A.2 Multiple linear regression models

Table 10: Output of the multiple linear regression model for maize yield and all univariate ACIs and the corresponding p-value for individual municipalities. For each municipality, the number of years with available maize yield data is listed.

ACI	R ²	Adjusted R ²	p-value	Nr. of yrs. with yield data
Aristau	0.37	-0.19	0.71	18
Dietwil	0.34	0.04	0.4	20
Islisberg	0.4	-0.2	0.7	17
Moehlin	0.62	0.37	0.08	19
Zetzwil	0.46	0.03	0.45	19
Hohenrain	0.35	-0.1	0.62	18
Ramsen	0.25	-0.24	0.8	19
Schlatt	0.68	0.4	0.1	18
Thundorf	0.26	-0.19	0.74	17
Yvorne	0.53	0.23	0.19	19
Schwerzenbach	0.61	0.31	0.16	17
Thalheim an der Thur	0.5	-0.01	0.51	17

A.3 Relative importance models

Table 11: Relative importance of each individual ACI listed below for maize yield variation in Aristau (nr. of years with maize yield data = 18 years). The metrics are normalised sum to 100%. The occurrence of the ACIs not included in this list was too low for the ACI to be included in this estimation. The output of the relative importance model shows the portion of maize yield variation explained by the listed univariate ACIs.

Aristau			
ACI	Relative importance [% of R²]		
LT6	0.05		
SPIIm	0.41		
HPE	0.04		
HS30	0.32		
HS35	0.10		
HS35sum	0.09		
	R²	Adjusted R²	p-value
Relative importance model	0.34	-0.02	0.5

Table 12: Relative importance of each individual ACI listed below for maize yield variation in Dietwil (nr. of years with maize yield data = 20 years). The metrics are normalised sum to 100%. The occurrence of the ACIs not included in this list was too low for the ACI to be included in this estimation. The output of the relative importance model shows the portion of maize yield variation explained by the listed univariate ACIs.

Dietwil			
ACI	Relative importance [% of R²]		
LT6	0.11		
SPIIm	0.25		
HPE	0.60		
HS30	0.05		
	R²	Adjusted R²	p-value
Relative importance model	0.24	0.04	0.35

Table 13: Relative importance of each individual ACI listed below for maize yield variation in Islisberg (nr. of years with maize yield data = 17 years). The metrics are normalised sum to 100%. The occurrence of the ACIs not included in this list was too low for the ACI to be included in this estimation. The output of the relative importance model shows the portion of maize yield variation explained by the listed univariate ACIs.

Islisberg			
ACI	Relative importance [% of R²]		
LT6	0.03		
SPI _m	0.26		
SPI _e	0.30		
HPE	0.09		
HS30	0.03		
HS35	0.08		
HS35sum	0.21		
	R²	Adjusted R²	p-value
Relative importance model	0.32	-0.2	0.73

Table 14: Relative importance of each individual ACI listed below for maize yield variation in Moehlin (nr. of years with maize yield data = 19 years). The metrics are normalised sum to 100%. The occurrence of the ACIs not included in this list was too low for the ACI to be included in this estimation. The output of the relative importance model shows the portion of maize yield variation explained by the listed univariate ACIs.

Moehlin			
ACI	Relative importance [% of R²]		
LT6	0.04		
SPI _m	0.14		
SPI _e	0.10		
HPE	0.08		
HS30	0.17		
HS35	0.20		
HS35sum	0.27		
	R²	Adjusted R²	p-value
Relative importance model	0.62	0.37	0.08

Table 15: Relative importance of each individual ACI listed below for maize yield variation in Zetzwil (nr. of years with maize yield data = 19 years). The metrics are normalised sum to 100%. The occurrence of the ACIs not included in this list was too low for the ACI to be included in this estimation. The output of the relative importance model shows the portion of maize yield variation explained by the listed univariate ACIs.

Zetzwil			
ACI	Relative importance [% of R²]		
LT6	0.33		
SPIm	0.13		
SPIe	0.05		
HPE	0.09		
HS30	0.22		
HS35	0.09		
HS35sum	0.09		
	R²	Adjusted R²	p-value
Relative importance model	0.46	0.12	0.32

Table 16: Relative importance of each individual ACI listed below for maize yield variation in Hohenrain (nr. of years with maize yield data = 18 years). The metrics are normalised sum to 100%. The occurrence of the ACIs not included in this list was too low for the ACI to be included in this estimation. The output of the relative importance model shows the portion of maize yield variation explained by the listed univariate ACIs.

Hohenrain			
ACI	Relative importance [% of R²]		
LT6	0.11		
SPIm	0.44		
HPE	0.25		
HS30	0.19		
	R²	Adjusted R²	p-value
Relative importance model	0.1	-0.18	0.84

Table 17: Relative importance of each individual ACI listed below for maize yield variation in Ramsen (nr. of years with maize yield data = 19 years). The metrics are normalised sum to 100%. The occurrence of the ACIs not included in this list was too low for the ACI to be included in this estimation. The output of the relative importance model shows the portion of maize yield variation explained by the listed univariate ACIs.

Ramsen			
ACI	Relative importance [% of R²]		
LT6	0.11		
SPIm	0.29		
SPIe	0.11		
HS30	0.06		
HS35	0.34		
HS35sum	0.09		
	R²	Adjusted R²	p-value
Relative importance model	0.24	-0.14	0.7

Table 18: Relative importance of each individual ACI listed below for maize yield variation in Schlatt (nr. of years with maize yield data = 18 years). The metrics are normalised sum to 100%. The occurrence of the ACIs not included in this list was too low for the ACI to be included in this estimation. The output of the relative importance model shows the portion of maize yield variation explained by the listed univariate ACIs.

Schlatt			
ACI	Relative importance [% of R²]		
LT6	0.17		
SPI _m	0.28		
SPI _e	0.32		
HPE	0.02		
HS30	0.06		
HS35	0.09		
HS35sum	0.05		
	R²	Adjusted R²	p-value
Relative importance model	0.66	0.43	0.07

Table 19: Relative importance of each individual ACI listed below for maize yield variation in Thundorf (nr. of years with maize yield data = 17 years). The metrics are normalised sum to 100%. The occurrence of the ACIs not included in this list was too low for the ACI to be included in this estimation. The output of the relative importance model shows the portion of maize yield variation explained by the listed univariate ACIs.

Thundorf			
ACI	Relative importance [% of R²]		
LT	0.17		
SPI _m	0.11		
SPI _e	0.04		
HPE	0.33		
HS30	0.35		
	R²	Adjusted R²	p-value
Relative importance model	0.26	-0.08	0.6

Table 20: Relative importance of each individual ACI listed below for maize yield variation in Yvorne (nr. of years with maize yield data = 17 years). The metrics are normalised sum to 100%. The occurrence of the ACIs not included in this list was too low for the ACI to be included in this estimation. The output of the relative importance model shows the portion of maize yield variation explained by the listed univariate ACIs.

Yvorne			
ACI	Relative importance [% of R²]		
Frost Day	0.13		
Frostsum	0.22		
LT6	0.14		
SPI _m	0.06		
SPI _e	0.17		
HPE	0.04		
HS30	0.24		
	R²	Adjusted R²	p-value
Relative importance model	0.53	0.23	0.19

Table 21: Relative importance of each individual ACI listed below for maize yield variation in Schwerzenbach (nr. of years with maize yield data = 17 years). The metrics are normalised sum to 100%. The occurrence of the ACIs not included in this list was too low for the ACI to be included in this estimation. The output of the relative importance model shows the portion of maize yield variation explained by the listed univariate ACIs.

Schwerzenbach			
ACI	Relative importance [% of R²]		
LT6	0.54		
SPI _m	0.19		
SPI _e	0.02		
HPE	0.07		
HS30	0.11		
HS35	0.03		
HS35sum	0.04		
	R²	Adjusted R²	p-value
Relative importance model	0.61	0.31	0.16

Table 22: Relative importance of each individual ACI listed below for maize yield variation in Thalheim an der Thur (nr. of years with maize yield data = 17 years). The metrics are normalised sum to 100%. The occurrence of the ACIs not included in this list was too low for the ACI to be included in this estimation. The output of the relative importance model shows the portion of maize yield variation explained by the listed univariate ACIs.

Thalheim an der Thur			
ACI	Relative importance [% of R²]		
LT6	0.10		
SPI _m	0.05		
SPI _e	0.08		
HPE	0.12		
HS30	0.48		
HS35	0.10		
HS35sum	0.07		
	R²	Adjusted R²	p-value
Relative importance model	0.48	0.07	0.4

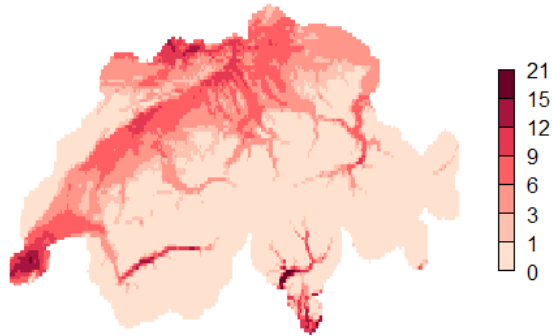
B Enlarged maps showing ACI occurrence and change signals

B.1 Heat stress

Average yearly number of HS30

Observation
1981-2010
5. May - 11. October

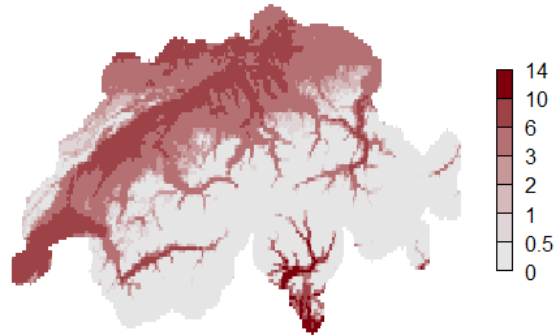
[Days]



Standard deviation of the yearly number of HS30

Observation
1981-2010
5. May - 11. October

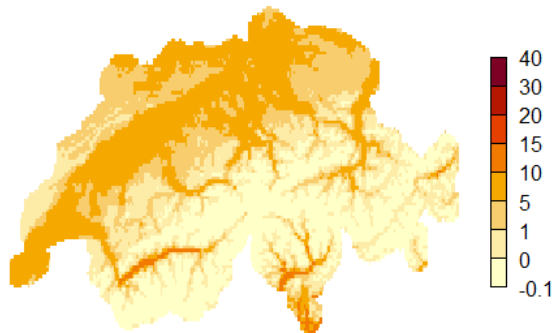
[Days]



Average yearly number of HS30

RCP 2.6: Change signal
2045-2074
5. May - 11. October

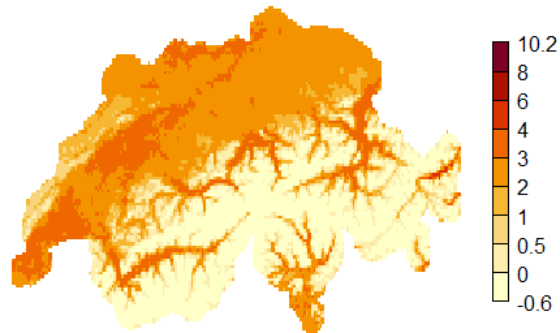
[Days]



Standard deviation of the yearly number of HS30

RCP 2.6: Change signal
2045-2074
5. May - 11. October

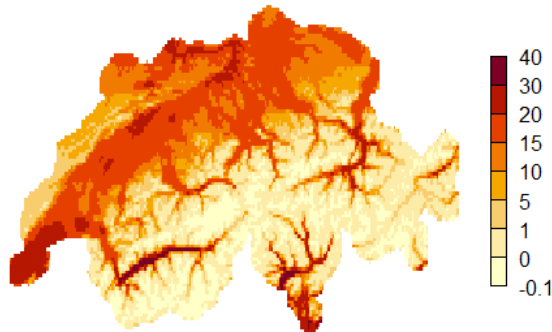
[Days]



Average yearly number of HS30

RCP 8.5: Change signal
2045-2074
5. May - 11. October

[Days]



Standard deviation of the yearly number of HS30

RCP 8.5: Change signal
2045-2074
5. May - 11. October

[Days]

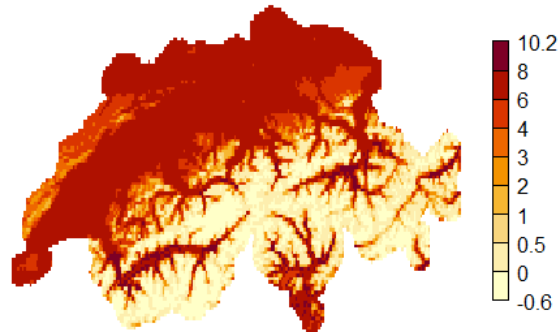
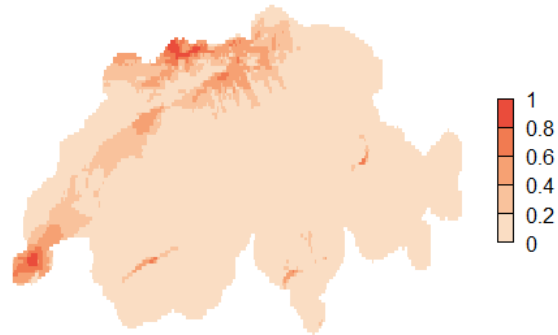


Figure 25: Left column: Average yearly number of HS30 based on observational data during the reference period (top) and based on the RCP 2.6 scenario (middle) and the RCP 8.5 scenario (bottom) during mid-century. Right column: Same as on the left but for the standard deviation of the yearly number of HS30.

Average yearly number of HS35

Observation
1981-2010
5. May - 11. October

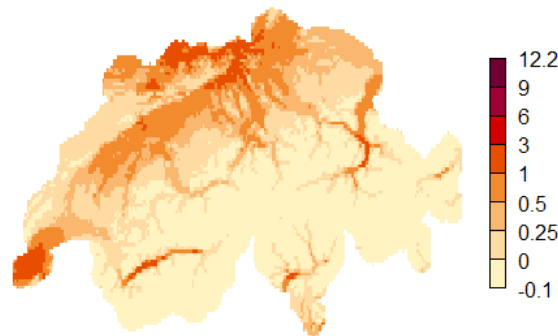
[Days]



Average yearly number of HS35

RCP 2.6: Change signal
2045-2074
5. May - 11. October

[Days]



Average yearly number of HS35

RCP 8.5: Change signal
2045-2074
5. May - 11. October

[Days]

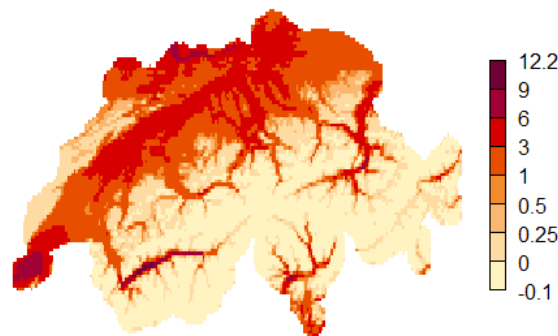
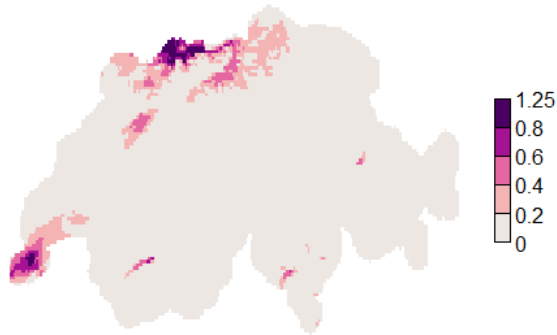


Figure 26: Average yearly number of HS35 based on observational data during the reference period (top) and based on the RCP 2.6 scenario (middle) and the RCP 8.5 scenario (bottom) during mid-century.

Average yearly HS35sum

Observation
1981-2010
5. May - 11. October

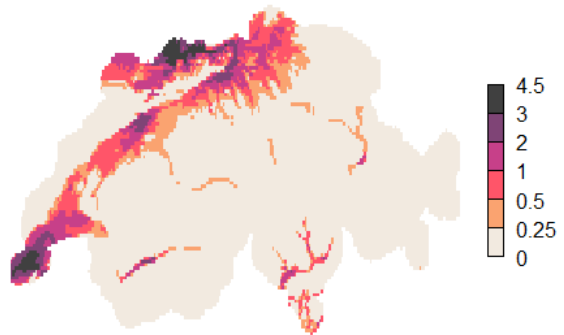
[°C]



Standard deviation of the yearly HS35sum

Observation
1981-2010
5. May - 11. October

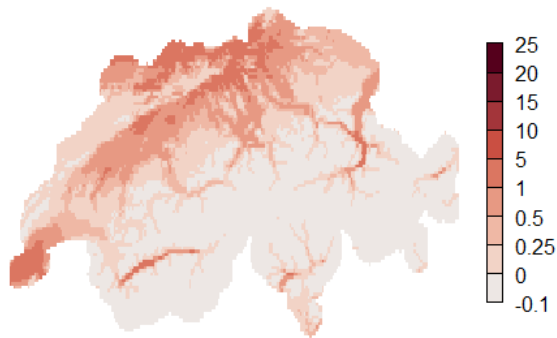
[°C]



Average yearly HS35sum

RCP 2.6: Change signal
2045-2074
5. May - 11. October

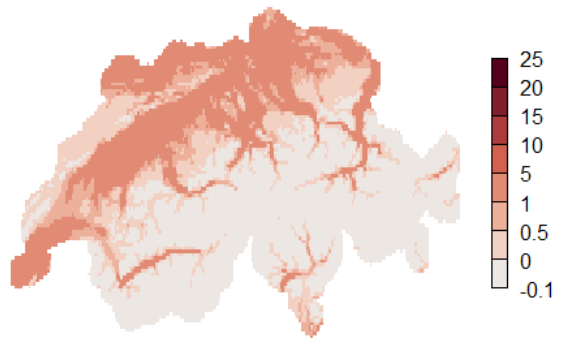
[°C]



Standard deviation of the yearly HS35sum

RCP 2.6: Change signal
2045-2074
5. May - 11. October

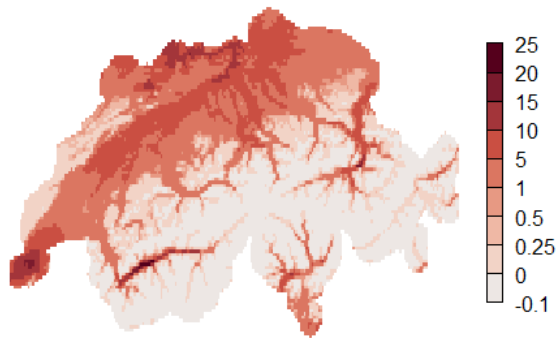
[°C]



Average yearly HS35sum

RCP 2.6: Change signal
2045-2074
5. May - 11. October

[°C]



Standard deviation of the yearly HS35sum

RCP 8.5: Change signal
2045-2074
5. May - 11. October

[°C]

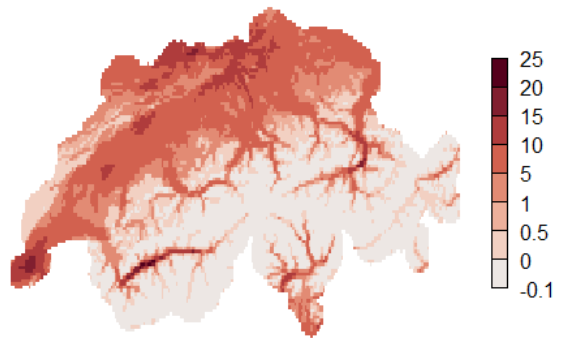


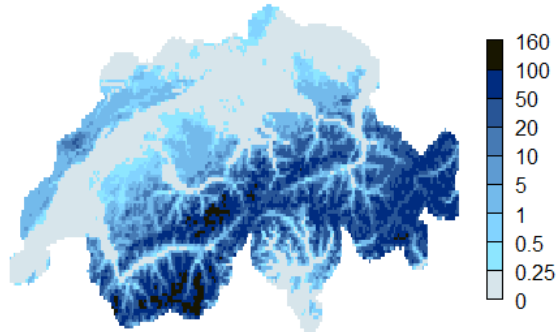
Figure 27: Left column: Average yearly HS35sum based on observational data during the reference period (top) and based on the RCP 2.6 scenario (middle) and the RCP 8.5 scenario (bottom) during mid-century. Right column: Same as on the left but for the standard deviation of the yearly HS35sum.

B.2 Low temperature stress

Average yearly number of Frost Days

Observation
1981-2010
5. May - 11. October

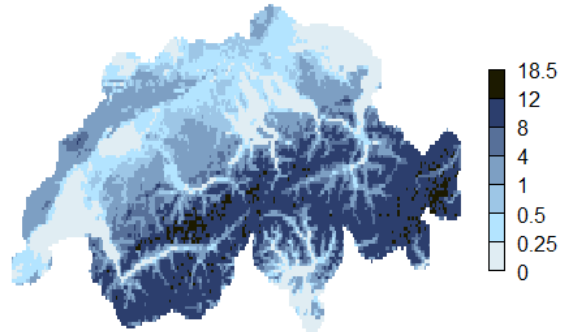
[Days]



Standard deviation of the yearly number of Frost Days

Observation
1981-2010
5. May - 11. October

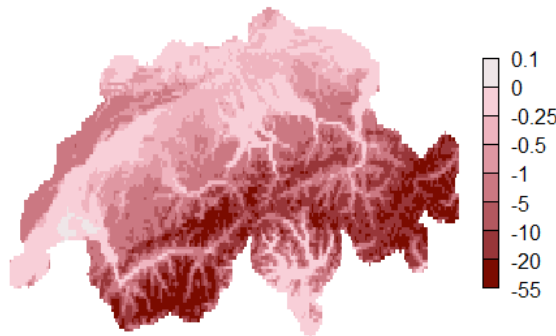
[Days]



Average yearly number of Frost Days

RCP 2.6: Change signal
2045-2074
5. May - 11. October

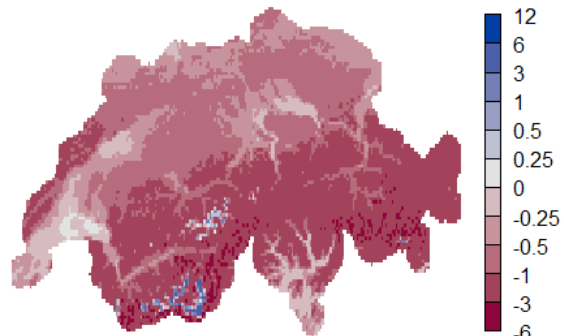
[Days]



Standard deviation of the yearly number of Frost Days

RCP 2.6: Change signal
2045-2074
5. May - 11. October

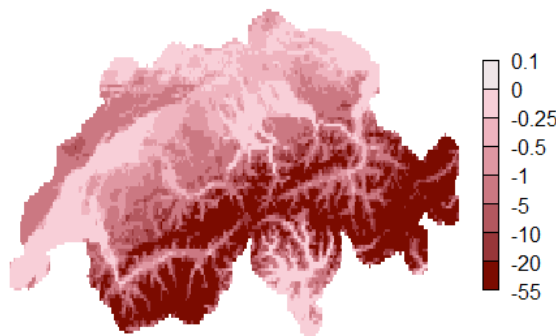
[Days]



Average yearly number of Frost Days

RCP 8.5: Change signal
2045-2074
5. May - 11. October

[Days]



Standard deviation of the yearly number of Frost Days

RCP 8.5: Change signal
2045-2074
5. May - 11. October

[Days]

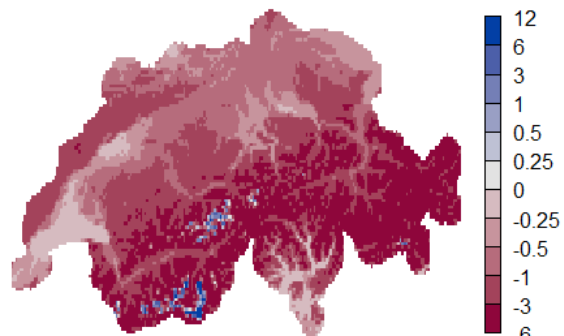
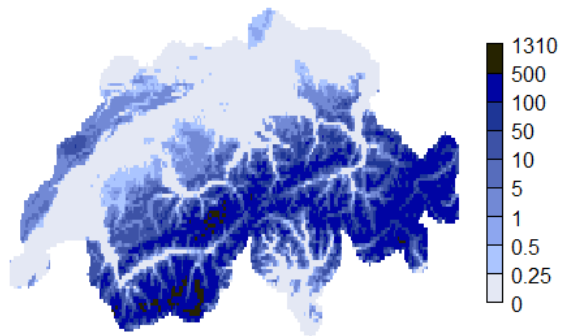


Figure 28: Left column: Average yearly number of Frost Days based on observational data during the reference period (top) and based on the RCP 2.6 scenario (middle) and the RCP 8.5 scenario (bottom) during mid-century. Right column: Same as on the left but for the standard deviation of the yearly number of Frost Days.

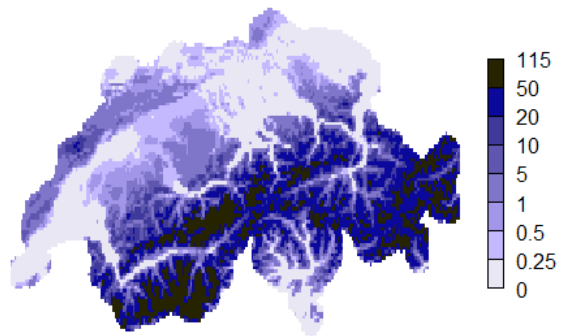
Average yearly Frostsum

Observation
1981-2010
5. May - 11. October



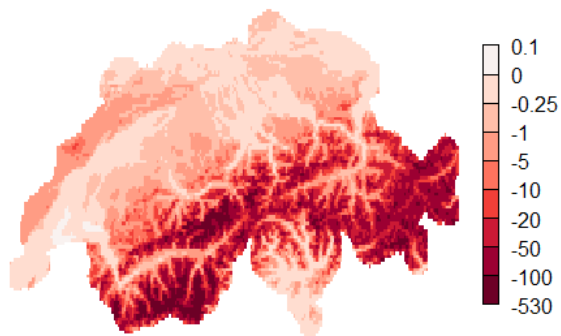
Standard deviation of the yearly Frostsum

Observation
1981-2010
5. May - 11. October



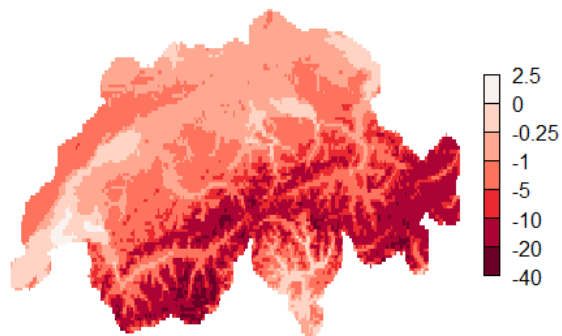
Average yearly Frostsum

RCP 2.6: Change signal
2045-2074
5. May - 11. October



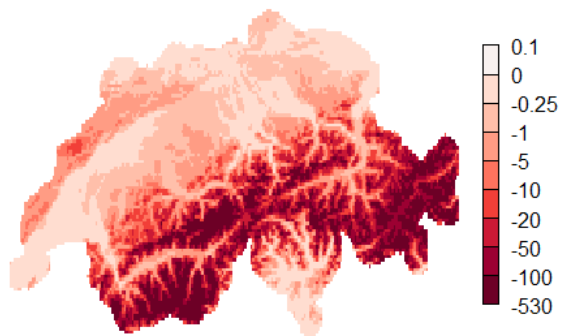
Standard deviation of the yearly Frostsum

RCP 2.6: Change signal
2045-2074
5. May - 11. October



Average yearly Frostsum

RCP 8.5: Change signal
2045-2074
5. May - 11. October



Standard deviation of the yearly Frostsum

RCP 8.5: Change signal
2045-2074
5. May - 11. October

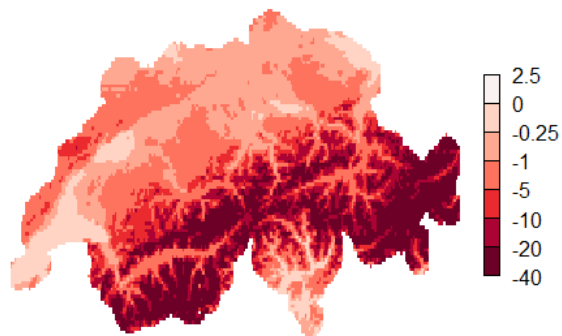


Figure 29: Left column: Average yearly Frostsum based on observational data during the reference period (top) and based on the RCP 2.6 scenario (middle) and the RCP 8.5 scenario (bottom) during mid-century. Right column: Same as on the left but for the standard deviation of the yearly Frostsum.

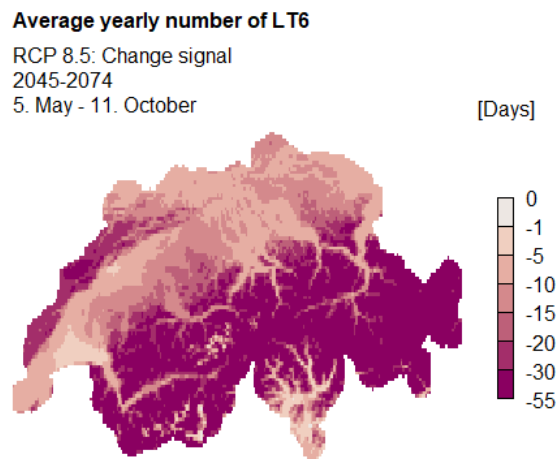
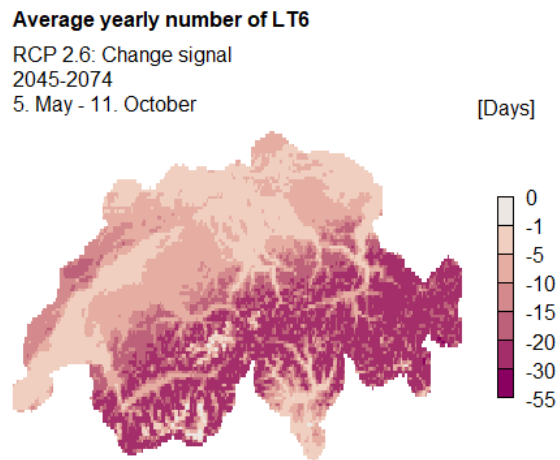
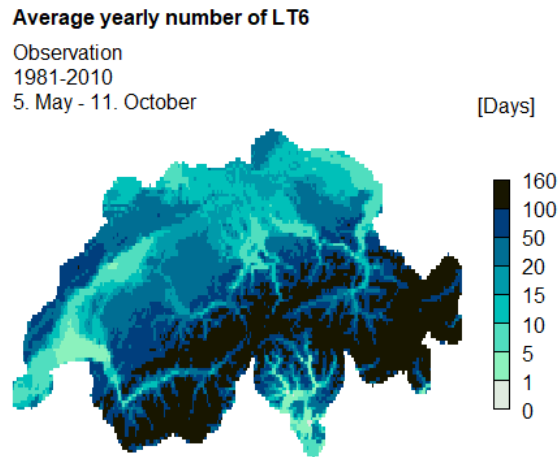


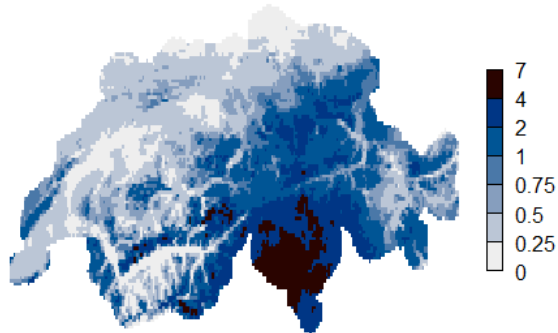
Figure 30: Average yearly number of LT6 based on observational data during the reference period (top) and based on the RCP 2.6 scenario (middle) and the RCP 8.5 scenario (bottom) during mid-century.

B.3 Potential waterlogging

Average yearly number of HPE

Observation
1981-2010
5. May - 11. October

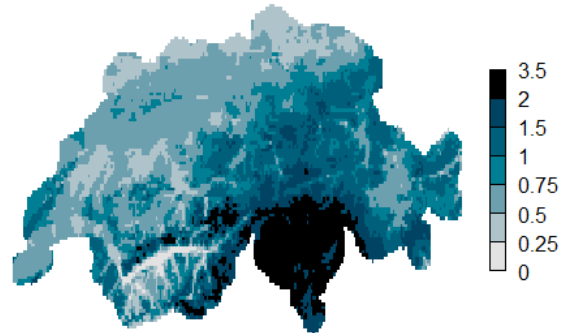
[Days]



Standard deviation of the yearly number of HPE

Observation
1981-2010
5. May - 11. October

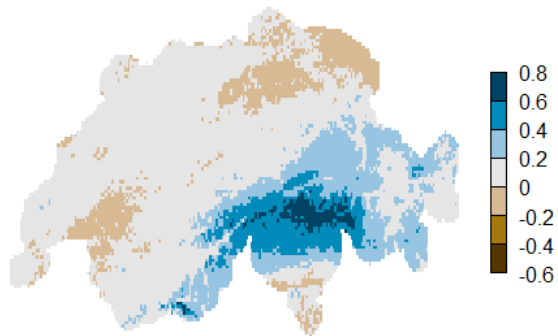
[Days]



Average yearly number of HPE

RCP 2.6: Change signal
2045-2074
5. May - 11. October

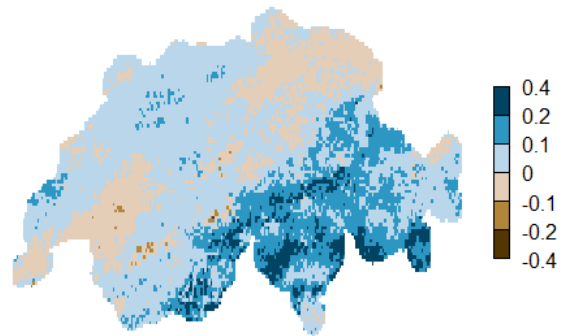
[Days]



Standard deviation of the yearly number of HPE

RCP 2.6: Change signal
2045-2074
5. May - 11. October

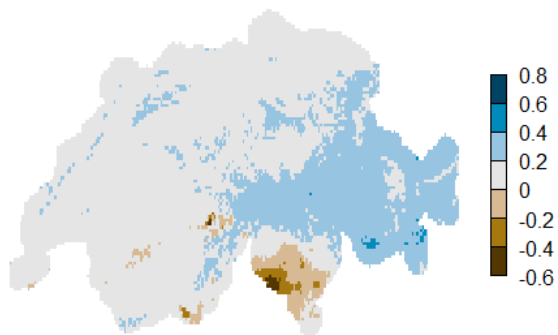
[Days]



Average yearly number of HPE

RCP 8.5: Change signal
2045-2074
5. May - 11. October

[Days]



Standard deviation of the yearly number of HPE

RCP 8.5: Change signal
2045-2074
5. May - 11. October

[Days]

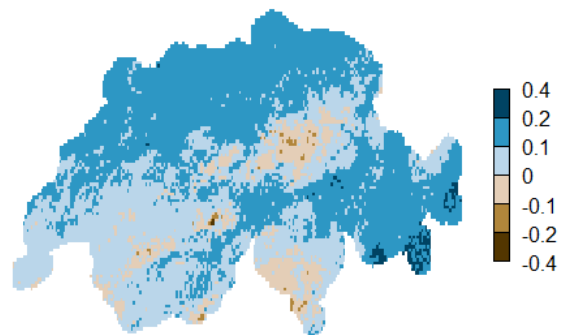


Figure 31: Left column: Average yearly number of HPE based on observational data during the reference period (top) and based on the RCP 2.6 scenario (middle) and the RCP 8.5 scenario (bottom) during mid-century. Right column: Same as on the left but for the standard deviation of the yearly number of HPE.

B.4 Drought

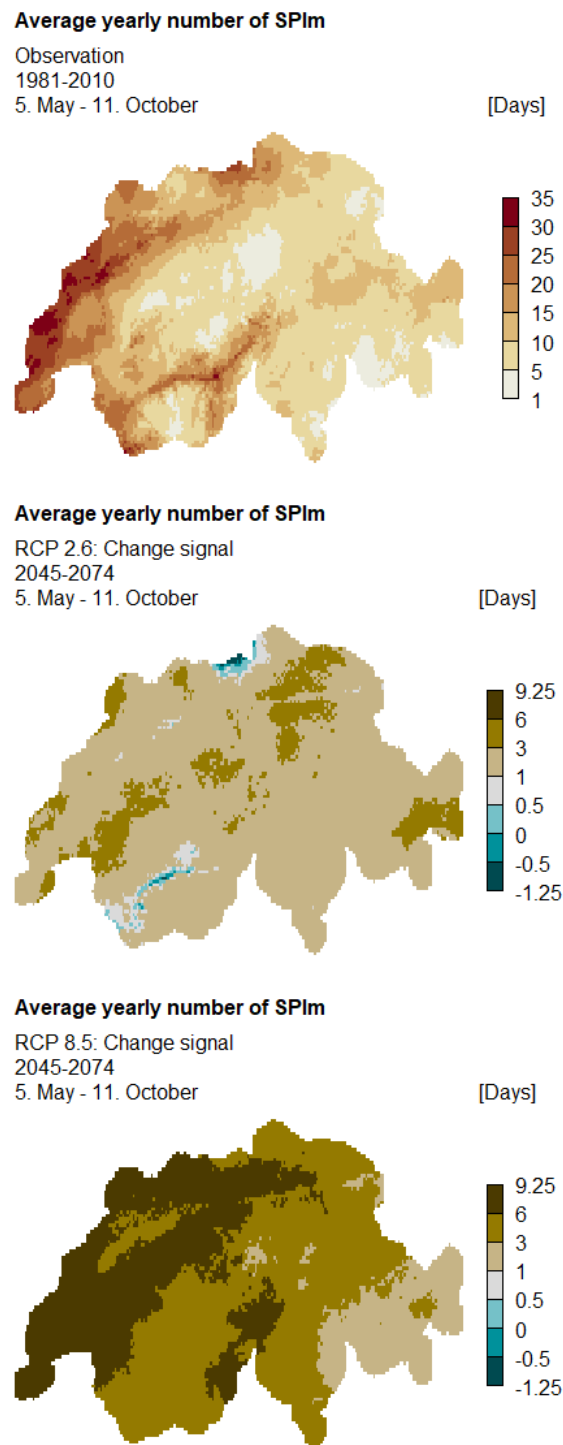


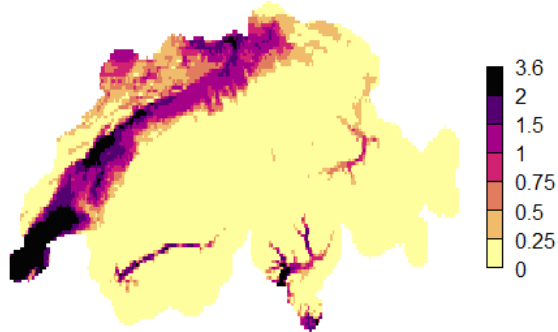
Figure 32: Average yearly number of SPI_m based on observational data during the reference period (top) and based on the RCP 2.6 scenario (middle) and the RCP 8.5 scenario (bottom) during mid-century.

B.5 Concurrent stress

Average yearly number of SPI_m & HS30

Observation
1981-2010
5. May - 11. October

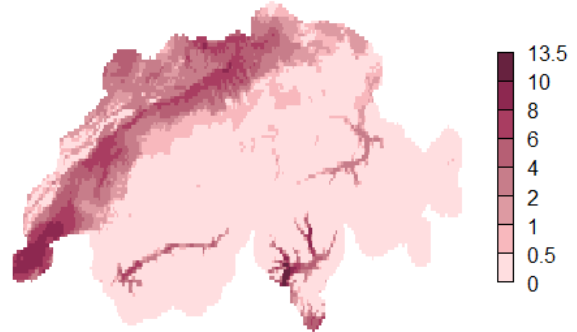
[Days]



Standard deviation of the yearly number of SPI_m & HS30

Observation
1981-2010
5. May - 11. October

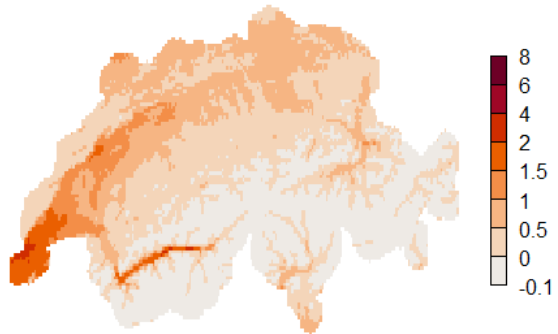
[Days]



Average yearly number of SPI_m & HS30

RCP 2.6: Change signal
2045-2074
5. May - 11. October

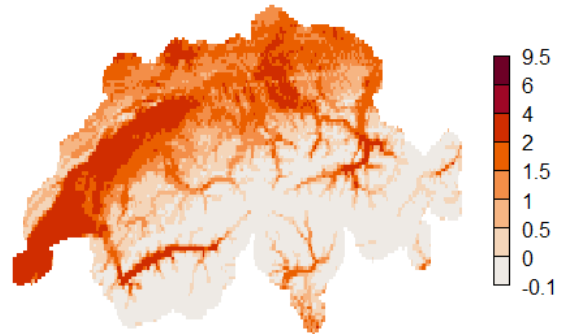
[Days]



Standard deviation of the yearly number of SPI_m & HS30

RCP 2.6: Change signal
2045-2074
5. May - 11. October

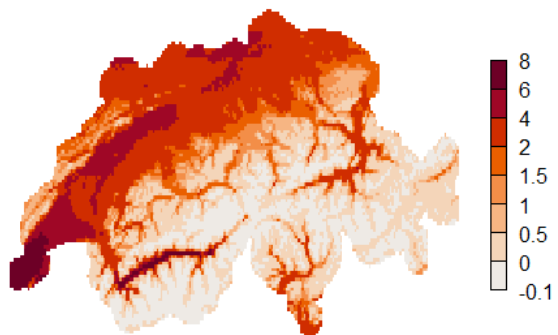
[Days]



Average yearly number of SPI_m & HS30

RCP 8.5: Change signal
2045-2074
5. May - 11. October

[Days]



Standard deviation of the yearly number of SPI_m & HS30

RCP 8.5: Change signal
2045-2074
5. May - 11. October

[Days]

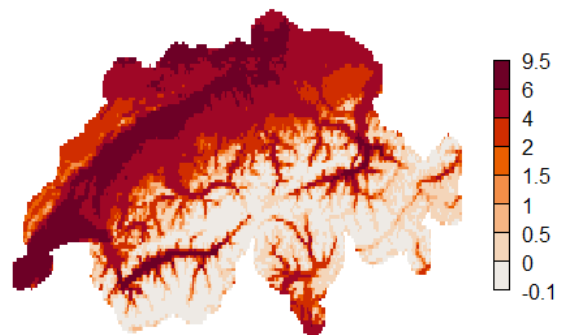
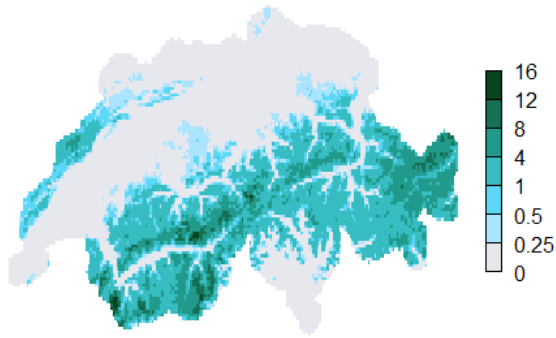


Figure 33: Left column: Average yearly number of SPI_m & HS30 based on observational data during the reference period (top) and based on the RCP 2.6 scenario (middle) and the RCP 8.5 scenario (bottom) during mid-century. Right column: Same as on the left but for the standard deviation of the yearly number of SPI_m & HS30.

Average yearly number of SPIm & Frost Days

Observation
1981-2010
5. May - 11. October

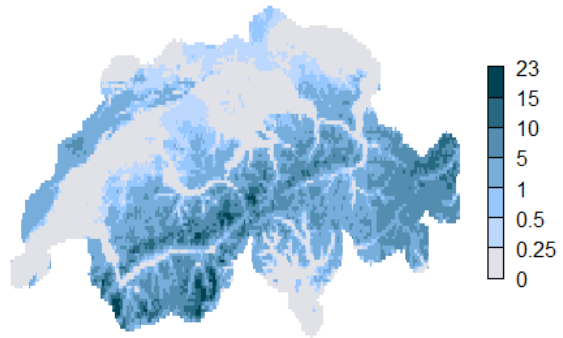
[Days]



Standard deviation of the yearly number of SPIm & Frost Days

Observation
1981-2010
5. May - 11. October

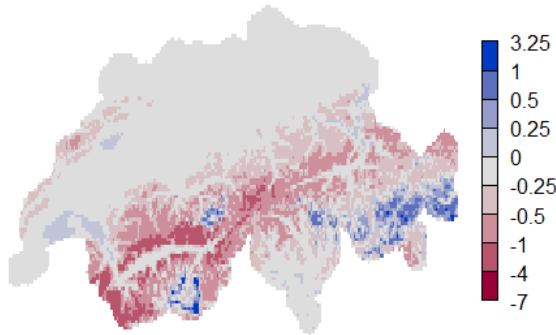
[Days]



Average yearly number of SPIm & Frost Days

RCP 2.6: Change signal
2045-2074
5. May - 11. October

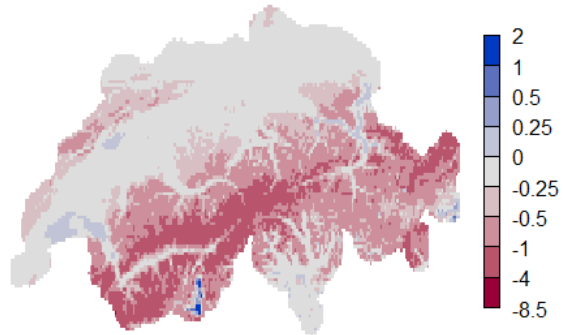
[Days]



Standard deviation of the yearly number of SPIm & Frost Days

RCP 2.6: Change signal
2045-2074
5. May - 11. October

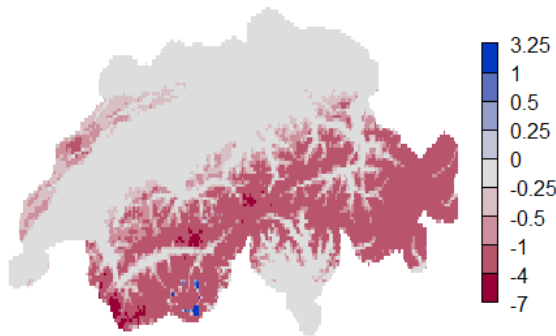
[Days]



Average yearly number of SPIm & Frost Days

RCP 8.5: Change signal
2045-2074
5. May - 11. October

[Days]



Standard deviation of the yearly number of SPIm & Frost Days

RCP 8.5: Change signal
2045-2074
5. May - 11. October

[Days]

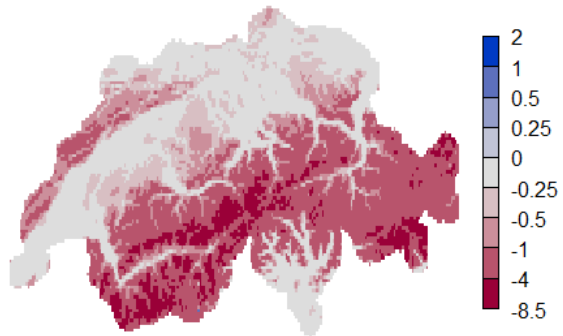
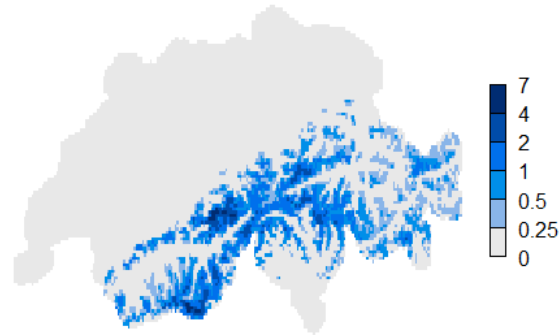


Figure 34: Left column: Average yearly number of SPIm & Frost Days based on observational data during the reference period (top) and based on the RCP 2.6 scenario (middle) and the RCP 8.5 scenario (bottom) during mid-century. Right column: Same as on the left but for the standard deviation of the yearly number of SPIm & Frost Days.

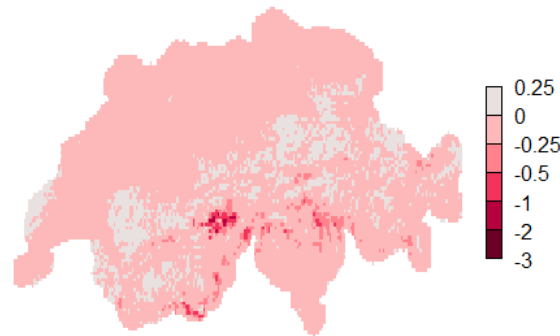
Average yearly number of HPE & Frost Days

Observation
1981-2010
5. May - 11. October [Days]



Average yearly number of HPE & Frost Days

RCP 2.6: Change signal
2045-2074
5. May - 11. October [Days]



Average yearly number of HPE & Frost Days

RCP 8.5: Change signal
2045-2074
5. May - 11. October [Days]

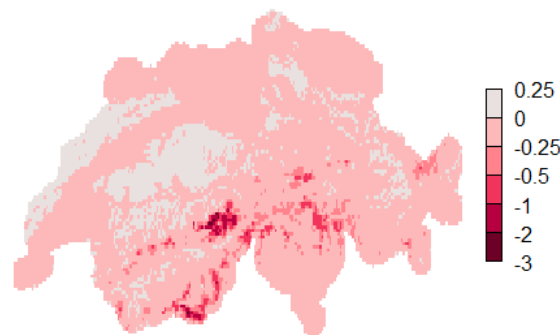


Figure 35: Average yearly number of HPE & Frost Days based on observational data during the reference period (top) and based on the RCP 2.6 scenario (middle) and the RCP 8.5 scenario (bottom) during mid-century.

C Used R packages

All programming for this thesis was conducted in R studio (R Core Team, 2023), using OpenAI's GPT-3.5 (OpenAI, no date) to help with the programming. In the following, the R packages are listed that have been used besides the packages included in R Studio.

C.1 Packages to work with NetCDF data or excel files

'chron' (James and Hornik, 2023)

'ncdf4' (Pierce, 2023)

'readxl' (Wickham and Bryan, 2023)

C.2 Packages used for data analysis and manipulation

'ggplot2' (Wickham, 2016)

'abind' (Plate and Heiberger, 2016)

'relaimpo' (Grömping, 2006)

C.3 Packages used for the calculation of the SPI

'SCI' (Stagge *et al.*, 2015, 2016; Gudmundsson and Stagge, 2016)

'SPEI' (Beguería and Vicente-Serrano, 2023)

'evd' (Stephenson, 2002)

C.4 Packages for plotting

'fields' (Nychka *et al.*, 2021)

'colorspace' (Zeileis *et al.*, 2020)

Source hack of the 'legend' function in R studio:


<http://www.math.mcmaster.ca/bolker/R/misc/legendx.R> (Bolker, 13:55, 30 November 2012)

Personal declaration

I hereby declare that the submitted thesis is the result of my own, independent work. All external sources are explicitly acknowledged in the thesis.

Signed:

Date:



29.04.2024
